Coding the Presence of Visual Objects in a

Recurrent Neural Network of Visual Cortex

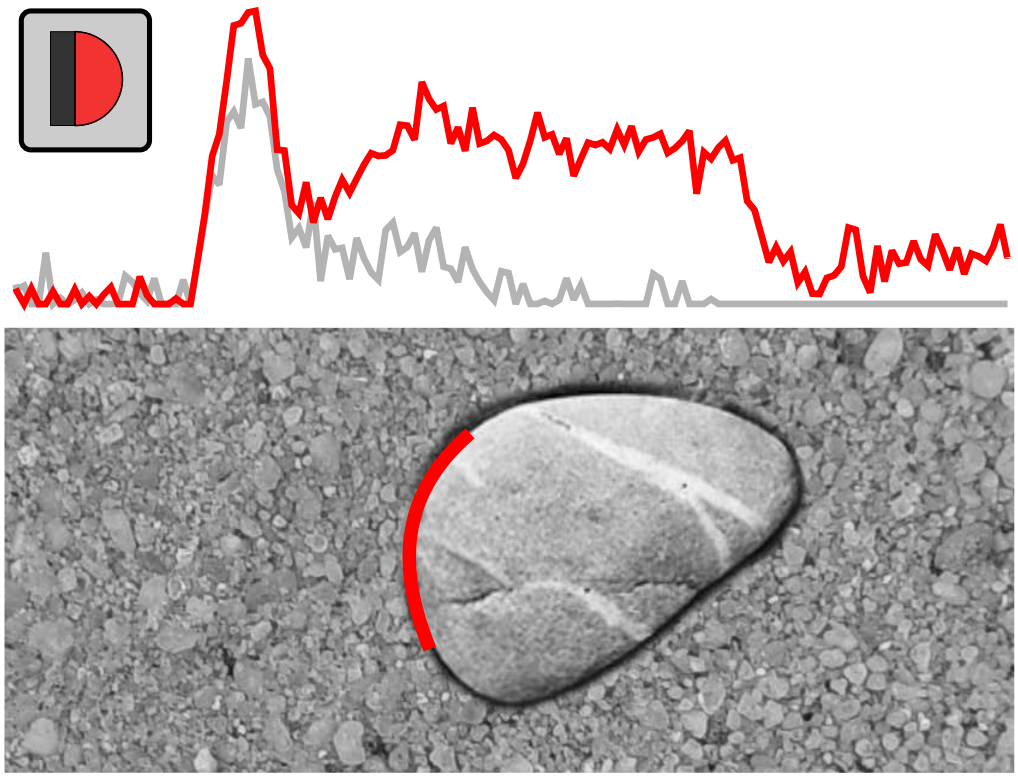

Timm Zwickel

Coding the Presence of Visual Objects in a Recurrent Neural Network of Visual Cortex

Dissertation

zur Erlangung des Doktorgrades
der Naturwissenschaften
(Dr. rer. nat.)

dem Fachbereich Physik
der Philipps-Universität Marburg
vorgelegt von

Timm Zwickel

Marburg/Lahn, Juni 2006

Vom Fachbereich Physik der Philipps-Universität Marburg als Dissertation angenommen am 12.07.2006

Erstgutachter: Prof. Dr. Reinhard Eckhorn

Zweitgutachter: Prof. Dr. Heiko Neumann

Tag der mündlichen Prüfung: 13.07.2006

To Julia

Truth is I thought it mattered,
I though that music mattered,
But does it bollocks,
Not compared to our people matter.

Chumbawamba

Contents

Zusammenfassung

Bevor wir in der Lage sind Sehobjekte zu erkennen, müssen wir diese von ihrem Hintergrund trennen. Dies bedarf eines schnellen Mechanismus, der feststellt ob und an welchem Ort ein Objekt vorliegt - unabhängig davon um was für ein Objekt es sich handelt.

Vor wenigen Jahren wurden Kantenzugehörigkeitsneurone (*border-ownership neurons*) im Sehkortex wacher Affen gefunden (Zhou et al., 2000), die wahrscheinlich eine Rolle in obig erwähnter Aufgabe spielen. Kantenzugehörigkeitsneurone antworten mit erhöhter Feuerrate, wenn sie die Kante eines Objekts kodieren, das sich von der Kante aus zu einer bestimmten, der vom Neuron bevorzugten, Seite erstreckt. Im Gegensatz dazu feuert das Neuron mit reduzierter Aktivität, wenn die kodierte Kante Teil eines Objektes ist, welches sich zur anderen, nicht bevorzugten Seite erstreckt. Diese Selektivität für die Lage eines Stimulusobjekts bezüglich einer Kante wird Kantenzugehörigkeit (*border ownership*) genannt. Zhou et al. (2000) fanden in den Arealen V1, V2 und V4 des Sehkortex Kantenzugehörigkeitsneurone, die auf orientierte Kontrastkanten und Linien antworteten.

Um den oben beschriebenen schnellen Mechanismus zu erklären, habe ich ein Neuronales Netzwerkmodell entwickelt, das das Vorhandensein von Stimulusobjekten detektiert. Mein Modell bestent aus den folgenden Arealen:

- Areal-1: Kodierung orientierter Kanten
- Areal-2: Kodierung von Kurvenverläufen
- Areal-3: Detektion des Vorhandenseins von Stimulusobjekten

Vorwärtsverschaltungen und laterale Verbindungen unterstützen in meinem Modell die Kodierung von Gestalteigenschaften wie z.B. Ähnlichkeit, guter Verlauf und Konvexität. Die Modellneurone des Areals 3 feuern, wenn ein Objekt im Stimulus vorliegt und kodieren dessen Position unabhängig von der Form des Objekts.

Rückkopplungen von Areal-3 auf Areal-1 unterstützen Orientierungsdetektoren, die die Kontur eines möglichen Objekts kodieren. Diese Rückkopplungen verursachen in unserem Modell den experimentell beobachteten Kantenzugehörigkeitseffekt. Rückkopplung von Kantenzugehörigkeit wirkt direkt auf Neurone, die die konvexen Stellen der Kontur eines Objekts kodieren. Neurone, die konkave Teile der Kontur kodieren, erreicht die Rückkopplung indirekt über laterale Verbindungen innerhalb des Kantenzugehörigkeits-Areals.

Meine Simulationen zeigen, dass Kantenzugehörigkeits-Rückkopplungen mit Hebb'schem Lernen gelernt werden können. Dies ist eine Bestätigung meiner Netzwerkarchitektur.

Mein Netzwerk ist ein umfassendes Modell, das mehrere Aspekte der Objektdetektion und -kodierung beinhaltet. Hiermit lassen sich die experimentellen Beobachtungen von Kantenzugehörigkeit reproduzieren. Desweiteren arbeiten die Mechanismen unseres Modells schnell und sie verbessern signifikant die Figur-Hintergrund-Trennung, die benötigt wird, um in nachfolgenden Schritten Objekterkennung leisten zu können.

Abstract

Before we can recognize a visual object our visual system has to segregate it from its background. This requires a fast mechanism for establishing the presence and location of objects independent of their identity.

Recently, *border-ownership* neurons were recorded in monkey visual cortex which might be involved in this task (Zhou et al., 2000). Border-ownership neurons respond with increased rates when an object surface extends to one specific side of the contour they encode. Conversely, the rate decreases when the contour belongs to an object extending to the other side. This selectivity for object position relative to a contour is called border-ownership. Zhou et al. (2000) found border-ownership neurons that encode oriented contrast edges or lines in areas V1, V2, and V4 of visual cortex in awake monkeys.

In order to explain the basic mechanisms required for fast coding of object presence I developed a neural network model of visual cortex consisting of these three areas:

- Area 1: encoding orientation contours
- Area 2: encoding curvatures
- Area 3: detecting the presence of stimulus objects

In my model feed-forward and lateral connections support coding of Gestalt properties including similarity, good continuation and convexity. Model neurons of the highest area (Area-3) respond to the presence of an object and encode its position, invariant of its form.

Feedback connections from Area-3 to Area-1 facilitate orientation detectors activated by contours belonging to potential objects, and thus generate the experimentally observed border-ownership property. Border-ownership feedback is transmitted directly to neurons encoding convex contours of an object and indirectly via lateral connections into concavities.

My simulations show that the border-ownership connections of my model can be learned with Hebbian learning. This confirms my networks architecture.

In conclusion, my network is an encompassing model bringing together several aspects of object detection and coding. The model reproduces the experimental observations of border-ownership by Zhou et al. (2000). Further, border-ownership feedback control acts fast and significantly improves the figure-ground segregation required for the consecutive task of object recognition.

Chapter 1

Introduction

Parts of this chapter and of Chapters 3, 4 and 8 are accepted for publication in the journal "Biosystems", 2006, special edition "Neural Coding".

1.1 Object Coding in Visual Cortex

In order to recognise an object, we need to separate it from its background. This separation implies grouping together the features of the object. Knowing which features belong to the object would greatly support separating them from the background. We[I] suggest a model of how higher visual processes aid early figure ground segregation to achieve just that.

1.1.1 Dorsal and Ventral Pathways and Feedback

Cortical visual processing is often divided into two major pathways. The dorsal (*Where?*) pathway is thought to extract information about object presence, position and size from visual stimuli. In contrast, the ventral (*What?*) pathway is more concerned with the encoding of form and identity of objects. The pathways differ with respect to their input. The dorsal pathway receives magno-cellular input with short delay, the ventral pathway receives both fast magno- and slow parvo-cellular input (see e.g., Schmolesky et al., 1998; Lamme and Roelfsema, 2000; Bullier, 2001). Dorsal pathway neurons have been

[I]The research presented in this dissertation was done by me, the author, i.e. I developed the computer models, ran the simulations and evaluated the results. Nonetheless, I have chosen to write this publication in the first person plural (*we*) since this work was only possible through the continuous collaboration with my colleagues in the NeuroPhysics group. Parts of this dissertation were previously jointly published with them.

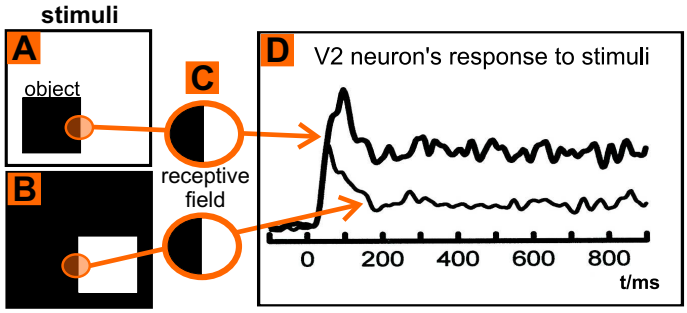

Figure 1.1: Averaged activity of a border-ownership neuron preferring objects stretching from its classical receptive field (**cRF**) to the left recorded in awake monkey. Modified from Zhou and coworkers (2000).

assumed to encode presence of objects and their position in visual scenes independent of their form (*identity*) (Bullier, 2001; Goodale and Milner, 1992). As has been previously discussed (Vidyasagar, 1999; Bullier, 2001), we suggest that there is feedback from higher area dorsal neurons, which detect an object's presence and location, to neurons in lower primary visual cortex (V1) encoding the object's contour and surface. Short-latency magnocellular input to the dorsal pathway and fast feed-forward (Thorpe et al., 1996) and feedback connections (Hupe et al., 2001) would allow feedback to coincide with the longer-latency input from the retina to area V1 of the parvocellular pathway. Such a mechanism could provide neurons in early areas with information about the probability of object presence in the current stimulus, including object size and position, invariant of form. In addition, it would aid figure-ground segregation in V1 and ventral stream areas receiving input from V1.

1.1.2 Border-Ownership

One important step in segregating object from ground is to identify the contour of the object. From the perception of bistable pictures (Rubin, 1921) we know that an object's contour is perceived as part of the object. Recently, Zhou et al. (2000) studied neurons encoding oriented contrast edges or lines in areas V1, V2, and V4 of visual cortex in awake monkeys. A large percentage of those neurons responded with increased rates when an object surface extended to one specific side of the contour. Conversely, the rate decreased when the contour belonged to an object extending to the other side. This selectivity for object position relative to a contour was termed *border-ownership* (**BO**). Figure 1.1 shows two stimuli (A,B) in which the same con-

tour belongs to different objects. Note that the local stimulus properties, including orientation and contrast (Figure 1.1C), are identical. Nonetheless, the activity is higher for stimulus A than for stimulus B (Figure 1.1D). Zhou et al. (2000) found that the difference between responses to preferred and non-preferred object sides emerged already before the peak of the onset response (Figure 1.1D) and was only weakly dependent on object size. Even when stimuli with misleading local cues were presented (e.g., at the inner side of a C-shaped stimulus) the neurons responded according to their preference with respect to object side.

Several mechanisms have been suggested to explain the BO effect (Kikuchi and Akashi, 2001; Nishimura and Sakai, 2004; Li, 2005), all focussed on area V2. However, BO neurons have been found even in primary visual cortex. Since BO neurons were mostly found in areas V2 and V4 ($> 50\%$) (Zhou et al., 2000) and only few in V1 (18%), above models focussed on V2. BO properties in V1 were assumed to receive fast feedback connections from V2 (Girard et al., 2001). Models by Li (2005), Kikuchi and Akashi (2001) and Nishimura and Sakai (2004) assumed that BO properties arise by feed-forward connections to, and lateral connections in, V2. Li (2005) discussed that feedback of attention from higher areas could influence lateral processes coding BO. Li also suggested that this could be achieved by modulation of neurons encoding an object's contour. Thus, switches in perception, as in the example of Rubin's vase (Rubin, 1921), could be explained by feedback only to the contour of one of two objects sharing a contour. There have been two approaches explaining BO by intra-areal connectivity: (1) cascades of activation running along the object's contour (Kikuchi and Akashi, 2001; Li, 2005) and (2) long-range connections between neurons encoding opposite contours of the object (Nishimura and Sakai, 2004). Our model differs from those approaches in that we explain BO by feedback from higher areas of the dorsal visual pathway.

1.1.3 Feedback Models

Besides many feed-forward models of the visual system mainly dealing with object recognition (e.g., Riesenhuber and Poggio, 1999), there are a number of models, suggesting recurrent feedback networks for improving figure-ground segregation. One locally limited model suggested feedback from inhibitory interneurons to reduce mainly uncorrelated noise, since neurons encoding an object facilitate each other by lateral connections (Eckhorn et al., 1992). A

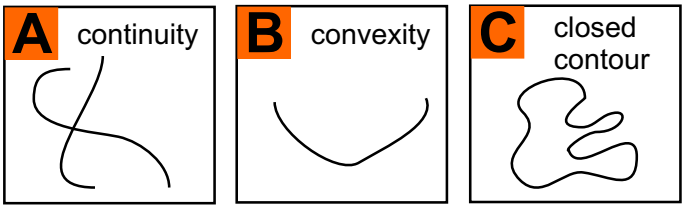

Figure 1.2: Examples of Gestalt laws. Gestalt laws describe properties common to objects occurring in natural stimuli. They aid the grouping of stimuli to objects and allow the detection of the presence of objects. Gestalt laws are implicitly encoded in the structure of the visual system.

frequently implemented feedback mechanism uses integration over greater lateral distances due to the larger classical receptive fields (**cRF**[II]) in higher visual areas and feedback from these areas to aid figure-ground segregation in lower areas (Gove et al., 1995; Weitzel et al., 1997; Neumann and Sepp, 1999; Bayerl and Neumann, 2004).

1.1.4 Gestalt Rules

Object perception adheres to certain empirical rules which have been formalised in Gestalt theory (Wertheimer, 1923). *Gestalt laws* (Figure 1.2) describe which local visual features support perceptual grouping. We (as others, e.g., Wörgötter et al., 2004) assume that Gestalt properties are manifest in the wiring and therefore we included three Gestalt laws on the network level in order to aid object coding.

To investigate the possible mechanisms underlying border-ownership properties, we have developed a neural network model of the primate visual system. In this model we show how early area neurons can exhibit different border-ownership properties despite identical cRFs. For that purpose we modelled basic properties of the dorsal and parts of the ventral stream of the visual system necessary for coding object presence. Feedback from the highest area of the dorsal pathway provides lower area neurons with information that enables them to encode BO properties and thus, enhance figure-ground segregation.

[II]The *classical receptive field* (cRF) of a neuron is the area of visual space in which a stimulus presentation leads to a response of this neuron.

1.2 Chapter Overview

Here we give a brief overview over the content of each chapter.

Model Neuron and Basic Circuitry

Chapter 2: The model neuron used throughout our networks is described. Characteristic modes of operation are demonstrated for a single neuron and an excitatory-inhibitory neuron pair. Saturation properties and dependence on decay time constant are shown for the linking synapse. Effects of divisive inhibition are discussed.

Model Architecture

Chapter 3: The architecture of our model is introduced: The network areas, cRF properties and inter- and intra-areal connections. The network parameters are physiologically motivated. Further, the stimulus input and its filtering is described.

Results of the Main Border-Ownership Model

Chapter 4: We describe the behaviour of the network responding to the presentation of a range of stimuli in order to demonstrate object presence detection (in Area-3) and the effect of BO-feedback (in Area-1b). Further, the object detection performance of the model in scenes with noisy input is analysed.

Chapter 5: Lateral conduction delays are added to the previous border-ownership model. This allows better comparison with other models. The model with delays predicts later BO property differentiation in concave than in convex parts of a stimulus object's contour.

Closed Feedback-Loop

Chapter 6: We investigate the effect of adding feedback connections from Area-3 to Area-1a on the model's performance. We show that with this closed loop, figure-ground segregation in Area-1a is improved.

Learning Feedback

Chapter 7: The connection architecture of our model is supported by showing that feedback connections can be learned with a biologically plausible learning rule. We used a Hebbian learning rule. In a simple network we show the main principles necessary for learning feedback modulation. Finally, we demonstrate, that our network model learns connections which are similar to the hand wired connections which we used in previous chapters.

Discussion

Chapter 8: Our model reproduces basic properties of object-presence coding in the dorsal visual pathway. We demonstrate how feedback from a higher level visual area can specifically facilitate activity of neurons at lower stages of the processing hierarchy. This modulation can indicate border-ownership and improve figure-ground segregation.

We compare the properties of our model with electrophysiological results of Zhou et al. (2000). We show how our results relate to other physiological and psychophysical findings and discuss, what our model predicts and which cortical areas could correspond to the modules of our model. Further, we compare our model with

other models on BO and discuss implications of BO coding to figure-ground segregation.

Conclusions

Chapter 9: We recapitulate key results of our model and discuss future perspectives.

Chapter 2

Methods

Outline

The model neuron used throughout our networks is described. Characteristic modes of operation are demonstrated for a single neuron and an excitatory-inhibitory neuron pair. Saturation properties and dependence on decay time constant are shown for the linking synapse. Effects of divisive inhibition are discussed.

2.1 Conceptual Modelling of Functional Mechanisms

The goal of our network is to model basic functional mechanisms of the visual cortex. To achieve this goal drastic abstractions have to be taken from what is known about the brains anatomy and physiology. This is due to two main reasons:

1. A model has to abstract from what is describes, because a one-to-one copy of the entity modelled would not yield any new insight that is not available from the entity itself. Since many basic mechanisms of the functional organisation of visual cortex are still unknown, models suggesting basic mechanisms are needed to further understanding.

2. In order to model several thousands of neurons with numeric simulations, the neuron building blocks have to be simple enough so that the model can be computed by the available computing resources.

Thus, our aim is not to develop a comprehensive model of visual cortex but rather try to demonstrate basic functional mechanisms in an abstracted model.

2.2 Model Neuron Definition

The basic building block of our model is a modified version of the Marburg Model Neuron (Eckhorn et al., 1990). We changed the neuron type from a spike encoder to a graded response neuron with a threshold. Graded response models assume that the activity of a neuron can be expressed by its *firing rate*, which we measure in *spikes per second*.

The model neuron receives excitatory (*feeding*) $F(t)$, inhibitory $I(t)$ and modulatory (*linking*) $L(t)$ input. In each discrete time step, new input is added to the input value of this previous time step, which, before, is exponentially decreased. The excitatory input $F_i(t)$ for neuron i computes to:

$$F_i(t) = \left(\sum_{i,j} w_{i,j} O_j(t-1) \right) + F_i(t-1) e^{-1/\tau_f} \tag{2.1}$$

with the output O_j from Neuron j in the previous timestep, $w_{i,j}$ the coupling strength between neurons j and i, and τ_f the time constant for the decay of activity over time. The computation for the decay of subtractive inhibitory input with two time constants (n=1,2) and of divisive (sometimes referred to as: *shunting*) inhibitory input with one time constant (n=3) is analogous:

$$I_{n,i}(t) = \left(\sum_{i,j} w_{i,j} O_j(t-1) \right) + I_{n,i}(t-1) e^{-1/\tau_{i,n}} \tag{2.2}$$

The modulatory input is additionally bounded above by a saturation function:

$$\begin{aligned} L_i(t) &= \left(\sum_{i,j} w_{i,j} O_j(t-1) \right) \left(L_{max} - L_i(t-1) e^{1/\tau_l} \right) \\ &+ L_i(t-1) e^{-1/\tau_l} \end{aligned} \tag{2.3}$$

with the maximum linking value $L_{max} = 3$. Thus L_i is bounded below and above:

$$L_i(t) \in [0, L_{max}] \tag{2.4}$$

The membrane potential is computed from the above as follows:

$$M_i(t) = \frac{F_i(t)(1 + L_i(t)) - I_{1,i}(t) - \alpha I_{2,i}(t)}{I_{3,i}(t)} + \sigma n(t) \tag{2.5}$$

with $\alpha = \frac{1}{2}$ weighing the slow inhibitory decay half as much as the fast decay. Further, Gaussian-distributed noise $n(t)$ with mean value 0 and standard deviation 1 of the distributed is added. The *linking* modulation is similar to the excitatory modulatory mechanism suggested by Neumann and Sepp (1999). We use two types of transfer functions in our models: A linear response function with slope m and threshold θ:

$$O_i(t) = \begin{cases} m_i(M_i(t) - \theta_i) & \text{if } M_i(t) \geq \theta_i \\ 0 & \text{if } M_i(t) < \theta_i \end{cases} \tag{2.6}$$

Alternatively, the neuron's output is computed with a saturation function beyond threshold θ:

$$O_i(t) = \begin{cases} \frac{\mu_{max}(M_i(t) - \theta_i)}{K + (M_i(t) - \theta_i)} & \text{if } M_i(t) \geq \theta_i \\ 0 & \text{if } M_i(t) < \theta_i \end{cases} \tag{2.7}$$

The saturation function used is a Monod type function with maximum μ_{max} and the half-saturation constant K:

$$y = \frac{\mu_{max} x}{K + x} \tag{2.8}$$

2.3 Model Neuron Dynamics

The dynamics of the model neuron and small neuron assemblies are shown in order to demonstrate the properties of the network's basic building block.

Comparing Neuron Model Activity to Extra-Cellular Recordings

Extra-cellular recordings of neuronal activity yields very noisy data. Extracting the response to a given stimulus from the neuronal activity is a challenging task. It is commonly solved by either recording the activity of several neurons with one electrode and computing

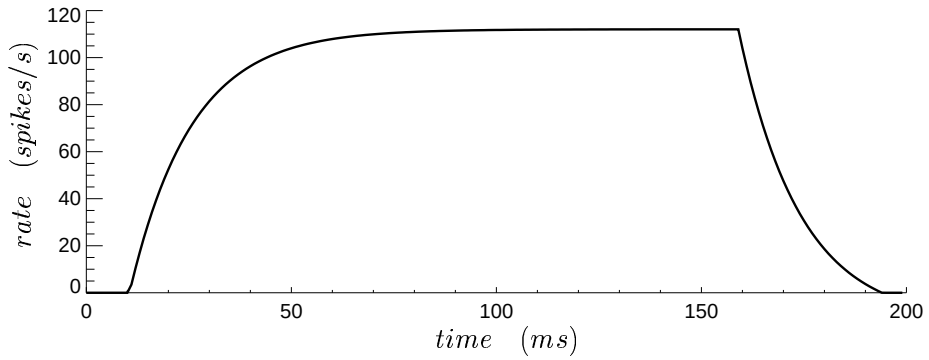

Figure 2.1: Excitatory neuron dynamics. A model neuron stimulated by constant excitatory input (*feeding*) for 150 ms with a stimulus onset at 10 ms.

the *multi unit activity* (MUA[I]) or *local field potential* (LFP[II]). Another approach is to average several responses of one neuron to the same stimulus rendering the neurons average activity over time.

Zhou et al. (2000), whose experimental results we wanted to reproduce with our model, used the latter approach. They averaged over multiple runs and in part over neurons showing the same properties. The activity of our graded response neurons, given in *spikes per second*, is comparable to the average activities computed by Zhou et al. (2000).

Excitatory Neuron

When an excitatory neuron is activated by a steady stimulus the neuron's output increases until a certain rate of saturation. Once the stimulus is switched off, the rate relaxates to 0 spikes/s. In Fig. 2.1 an excitatory neuron's response to a 150 ms lasting stimulus (from 10ms to 160ms) is plotted. The neuron has a feeding time constant τ_f of 15 ms, a threshold $\theta = 6$ and a slope of $m = 2$. After a neuron has been active it takes some time, the relative refractory period, until the membrane potential relaxates to its resting state. During the relative refractory period more input is required to drive the neuron than in its resting state.

2.3.1 Excitatory-Neuron-Inhibitory-Neuron Unit

The brain codes redundantly, i.e. several neurons encode the same or very similar information. Since our model is designed to show basic

[I] raw signals bandpassed at 1-10kHz; full wave rectified; low passed at 140Hz (Frien and Eckhorn, 2000)

[II] low-pass filtering at 1-140Hz (Frien and Eckhorn, 2000)

mechanisms, we abstained from such redundancies. Unlike in the brain, e.g., the cRFs of the neurons of our lowest layer show nearly no overlap. Further, Area-1 neurons only encode 4 orientations.

In order to reproduce the dynamics found in the recordings by Zhou et al. (2000) we model inhibitory effects by complementing each excitatory neuron with an inhibitory neuron. This inhibitory neuron receives excitatory input from the excitatory neuron and in turn inhibits the same excitatory neuron. In visual cortex excitatory and inhibitory neurons are found at a ratio of 4 to 1 (Braitenberg and Schüz, 1991). In our model the ratio is 1 to 1. This ratio does not imply that the mechanism suggested by us requires such a ratio but is due to having no redundancies and requiring at least one excitatory and one inhibitory neuron for every cRF modelled. Since we conceptually model functional mechanisms, we are save to make these abstractions.

Inhibitory Neuron Parameters

Inhibitory input is processed in our model neuron according to equation 2.2 with two input traces with different time constants, one short (τ = 5 ms, ie. $t_{1/2} \approx$ 3.5 ms [III]) and one long (20 ms, ie. $t_{1/2} \approx$ 14 ms), both in the range of $GABA_A$ receptors (see e.g. Rossi and Hamann, 1998).

Graded Response Neurons vs. Spike Coding Neurons

We have chosen to use *graded response neurons* since the mechanisms suggested by us to explain border-ownership coding and other phenomena do not require information about spike times. So a neuron model rendering neuronal firing rate suffices. Hence the more difficult to control *spike coding neurons* were not required.

Neurons with Higher and Lower Tonic Answer

In our model we use neurons with two different characteristics. One type shows a strong transient (*bandpass*) and a weaker tonic (*low pass*) response (Type 1), whereas the other type expresses a tonic activity close to the maximum of the transient answer response (Type 2). In Figure 2.2 the response of an excitatory neuron is plotted to a stimulus with onset at 10 ms lasting for 100 ms. In one simulation (*solid line*) the neuron was inhibited with a weight w of .08 (Type 2), whereas the inhibition strength in the other simulation was w=.3 (*dotted*, Type 1). We used a linear transfer function (Equation 2.6).

2.3.2 Divisive Inhibition

Another type of inhibition used in this model is *divisive* inhibition, see $I_{3,i}$ in equation 2.5. We use divisive inhibition for local normalisation. This is achieved by lateral connections of Gaussian strength with a limited range. In a scene with overall high activity neurons

[III] time constant τ relates to half life $t_{1/2}$ by $t_{1/2} = -ln(\frac{1}{2})\,\tau \approx .693\,\tau$

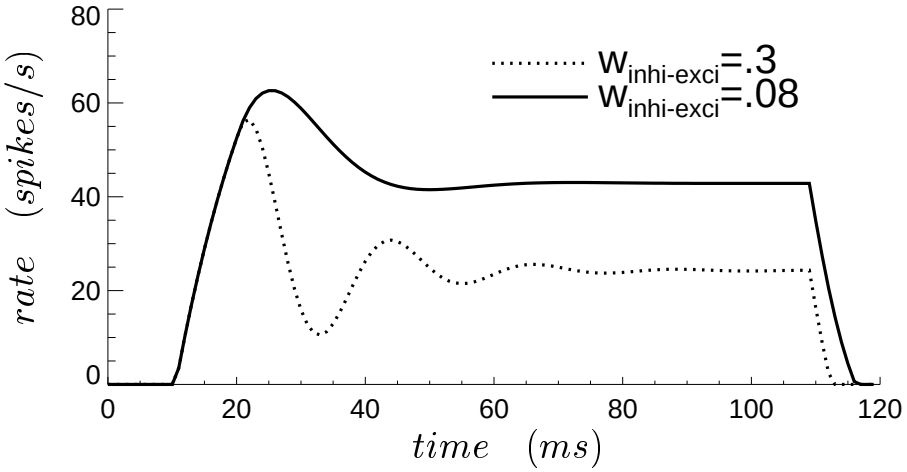

Figure 2.2: Two modes of operation of an excitatory neuron. The response rate of an excitatory neuron stimulated from t =10 ms to t =110 ms varies depending on the strength of inhibition $w_{inhi-exci}$ it receives form the inhibitory neuron it excites. The excitatory neuron had a slope of m=2, a threshold of θ=6, a feeding time constant τ_f=15 and inhibitory time constants $\tau_{i,1}$=5 and $\tau_{i,2}$=17. The inhibitory neuron had the following properties: slope m=2, threshold θ=8, feeding time constant τ_f=13. The weight from excitatory to inhibitory neuron had a strength of w =.04.

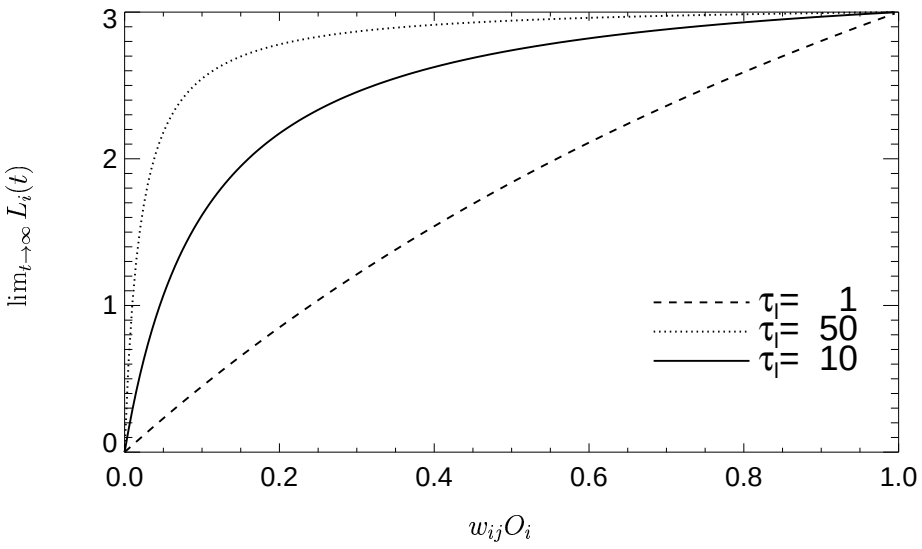

Figure 2.3: Linking strength L_i depends on presynaptic output rate O_j, coupling strength $w_{i,j}$ and time constant τ_l. Linking L_i converges over time ($\lim_{t\to\infty} L_i(t)$) for a given time constant τ_l, showing a saturation function characteristic dependent on input $w_{i,j}O_j$.

hamper each other significantly, resulting in a reduced overall activity. In a regime with low activity there is very little divisive inhibition and thus the rate of the relatively salient stimuli is in the range of the neurons of the former scenario.

2.3.3 Lateral Linking

The effect of linking (Equation 2.3) depends on the output rate O_j of presynaptic neuron j and the coupling strength $w_{i,j}$ to the postsynaptic neuron i.

Due to the factor $L_{max} - L_i(t-1)e^{1/\tau_l}$ in equation 2.3 the linking potential $L_i(t)$ is bounded above to L_{max}. The dynamics of $L_i(t)$ further depends on the postsynaptic decay defined by time constant τ_l.

In Figure 2.3 converged ($\lim_{t\to\infty}$) linking strength L_i is plotted for the scenario of presynaptic activation by just one neuron j for some sample linking time constants τ_l. Due to the upper bound, the membrane potential of a neuron can be increased by linking up to a factor of 4 ($1 + L_{max} = 1 + 3$, see Equation 2.5).

Saturation of linking strength was introduced to limit the effect of linking. This contributes to the stability of our network. When neurons are recurrently connected by linking connections, e.g. two neurons mutually linked to each other laterally, without upper bound and depending on their activity and linking strength, they could increase each other's rate infinitely. By having an upper bound, this is avoided. Physiologically an upper bound for linking strength is plausible: Since the mechanisms in chemical synapses are limited (number of vesicles, number of postsynaptic receptors, magnitude of depolarisation) the strength of a synapse is limited (Markram and Tsodyks, 1996; Chance et al., 1998).

The time constants τ_l=10 and τ_l=50 used in Figure 2.3 are the ones also used throughout our models presented here. The time constant values lie in the range measured by Jensen et al. (1996) for NMDA (N-methyl-D-aspartate) channels. Jensen et al. (1996) found two types of channels both having multiplicative effects, one with time constants in the rage of 15 to 50 ms and one of around approximately 150 ms.

2.4 Feedback Effect Quantification

Figure 4.8 shows results of simulations with and without feedback. With identical stimuli (Figure 4.8.A) for the same neuron (Figure 4.8.B) the difference in activity (Figure 4.8.C) is due to the feedback.

With the *normalised accumulated feedback effect* E_{fb} we quantify the difference in activity between simulations with and without feedback to Area-1b:

$$E_{fb}(t) = \frac{\int_{\tau_1}^{\tau_1+t} A_f(\tau) - A_n(\tau) d\tau}{t \int_{\tau_1}^{\tau_1+t} A_n(\tau) d\tau} \tag{2.9}$$

with time of response onset τ_1, window of integration $\Delta\tau = t$, activity with feedback A_f and without feedback A_n. The effect is normalised to the activity without feedback.

The feedback effect $E_{fb}(t)$ is plotted in 4.8.D. Figures 4.8.E/F show the average activation of a layer of BO neurons with a preferred contour orientation of 90° and BO preference to the left.

Chapter 3

Model Architecture

Outline

The architecture of our model is introduced: The network areas, cRF properties and inter- and intra-areal connections. The network parameters are physiologically motivated. Further, the stimulus input and its fi ltering is described.

3.1 Model Architecture

Our model consists of 4 topologically organised areas (Figure 3.1):

- **Area 1a:** Orientation detection
- **Area 2:** Curvature detection
- **Area 3:** Convex object detection
- **Area 1b:** Orientation detection and border-ownership coding

Via the feed-forward path (Area-1a $\Rightarrow$ Area-2 $\Rightarrow$ Area-3) Area-3 codes object presence and position. Feedback from Area-3 to Area-1b allows border-ownership coding in Area-1b.

In the entire network we use three basic principles for connecting neurons:

- forward convergence (orientation $\Rightarrow$ curvature $\Rightarrow$ convex object)
- lateral inhibition between neurons encoding contradicting stimuli (e.g. different orientation at the same position)

Neuron	excitatory	inhibitory
transfer function slope m	2 (A1,A3)	2
saturation maximum μ_{max}	30 (A2)	
half-saturation constant K	3 (A2)	
threshold $\theta / \frac{spikes}{s}$	6 (A1,A2) 47 (A3)	10 (A1,A3) 20 (A2)
τ_e / ms (excitatory)	5 (A1) 30 (A2,A3)	13 (A1) 7 (A2,A3)
τ_l / ms (linking/facilitatory)	50	10 (A1) 50 (A2,A3)
τ_1 / ms (subtractive inhibitory short)	5	-
τ_2 / ms (subtractive inhibitory long)	17	-
τ_3 / ms (divisive inhibition)	100	-
σ	1.5 (A1) .5 (A2,A3)	.5

Table 3.1: Model parameters. The slopes, thresholds and time constants of neurons in all areas (A1, A2, A3) are listed.

- lateral support between neurons coding correlated stimuli at different retinal positions (implemented with linking connections)

The parameters used in the model can be found in Table 3.1.

3.2 Stimulus Input

Stimuli have a size of 90x90 pixels and are presented for 100 ms. Objects are composed of lines, representing their contours. The stimuli are filtered by 5x5-sized filters with Gabor-shaped luminance sensitivity profiles of 4 different orientations: $0°, 45°, 90°$ and $135°$ (Figure 3.2). After filtering, background brightness is added to the stimulus in order to elicit maintained activity in the network[I]. Further, Gaussian white noise (GWN) σ is added to the membrane potential of every neuron in the network. Together, background brightness and GWN σ elicit an average activity of about 3 spikes per second. Uncorrelated spatiotemporal noise is introduced to the network by adding noise to the neurons' membrane potential (Appendix: Equation 2.5). The result is sampled, yielding a 30x30 pixel input to the network.

3.3 Area-1: Orientation Detection

Area-1 codes the local orientation of luminance contours (Figure 3.1: Area-1a/b). It consists of neurons with cRF properties corresponding

[I]Background brightness was set to 40% of the objects brightness in all experiments unless otherwise noted.

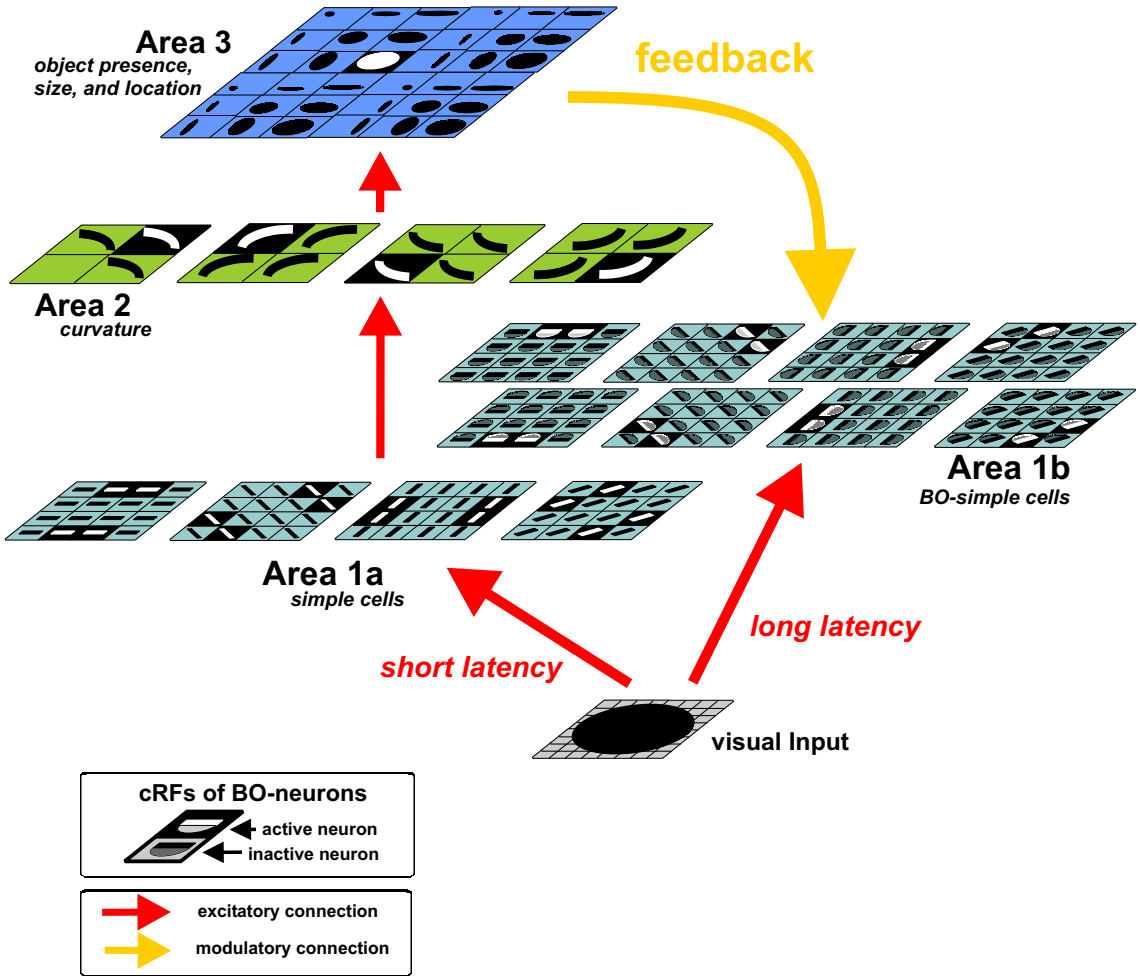

Figure 3.1: Network architecture with antagonistic border-ownership (BO) neurons in area 1b. Through feed-forward convergence, cRF size increases from lower to higher areas in the hierarchy (Area-1a $\Rightarrow$ Area-2 $\Rightarrow$ Area-3). Area-3 provides modulatory feedback to Area-1b. Neurons activated by the exemplary disc stimulus are highlighted in black.

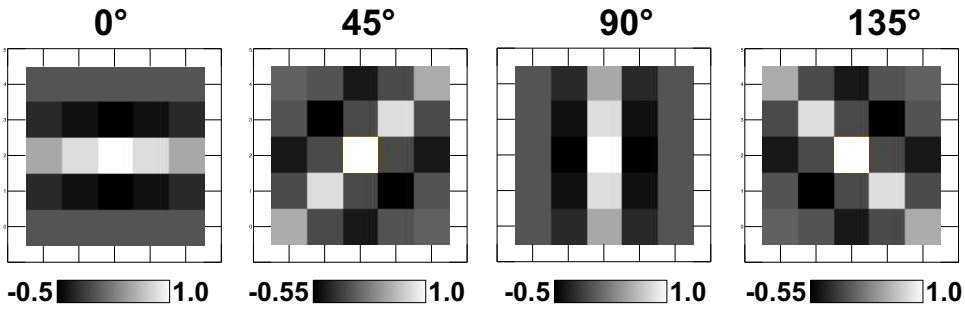

Figure 3.2: Input filters. The orientation selective simple cell properties of the lowest layer are modelled by filtering the input stimuli. As filters we used these 5x5-sized Gabor-shaped luminance sensitivity profiles of 4 different orientations.

to orientation-selective simple cells (Hubel and Wiesel, 1962) encoding a fixed orientation preferences ($0°, 45°, 90°$ or $135°$). Area-1 consists of two subareas, Area-1a and 1b, which are identical, except that in Area-1b there are two neurons with identical cRFs for every 1a-neuron. These pairs of Area-1b neurons receive individual feedback from the highest area of the hierarchy (Area-3). In addition, they inhibit each other (Figure 3.3.D).

Area-1 covers the simulated visual field of 30x30 neurons with non-overlapping cRFs. Area-1 is structured in layers. Neurons encoding the same orientation preference are in one layer, with the exception that BO neurons in Area-1b encoding the same orientation but opposing BO preferences are in separate layers. Every Area-1 layer consists of 30x30 pairs of 1 excitatory and 1 inhibitory neuron. Also in the remaining network every excitatory neuron is accompanied by an inhibitory neuron.

Lateral Connections

Lateral connections in Area-1 fulfill several functions: Local normalisation, sharpening of contrasts and implementation of Gestalt properties. In Figure 3.3 all lateral connections (except divisive inhibition) of an example Area-1a resp. Area-1b neuron (on Figure 3.3 with white background) are shown. In the basic model no delays are implemented. (For simulations with delays see Chapter 5).

Divisive Inhibition

We included surround inhibition in order to enhance luminance contrast locally (Knierim and van Essen, 1992). This undirected inhibition of divisive inhibition type (see Chapter 2, Equation 2.5) is distributed according to a Gaussian profile with a half-width of 4 neurons distance, reaching as far as 6 neurons. Divisive inhibition leads to local normalisation.

Hansen and Neumann (2004) discuss shunting inhibition as neu-

ral correlate of divisive inhibition. Though there has been some critique (Holt and Koch, 1997) that shunting transmitted by $GABA_A$ and $GABA_B$ has subtractive effects on the firing rate rather than divisive, Hansen and Neumann (2004) point out evidence for shunting nonetheless being a candidate for explaining divisive inhibition: Mitchell and Silver (2003) and Prescott and Koninck (2003) showed that for large synaptic input with high variance and dendritic saturation, shunting can have divisive effects. There are several mechanisms explaining shunting on a cellular level. One type of shunting is suggested to be transmitted by $GABA_B$ (Molyneaux and Hasselmo, 2002), which is relatively slow (Molyneaux and Hasselmo (2002): ca.100-200ms). We chose our divisive inhibition decay time constant to be 100ms. Due to the long decay, divisive inhibition will mainly take effect during the tonic response. For the network effects of our divisive inhibition it is not necessary to use slow inhibition, though.

Both types of surround inhibition, parallel subtractive inhibition and radial divisive inhibition, will take little effect during the transient and more effect during the tonic response. This is mainly due to inhibition taking effect via an inhibitory interneuron. By the time this is activated (threshold) and an excitatory neuron receives feedback from it, the excitatory neuron's transient answer is finished.

Lateral Modulation

Neurons with collinearly and curvilinearly arranged cRFs facilitate each other (Figure 3.3.A/C). BO neurons (Area-1b) only link to BO neurons with the same BO preference. The coupling strength has a Gaussian profile (Figure 3.3.E). This lateral connectivity profile is a possible network-level implementation of the Gestalt law of continuity (Figure 1.2.A) and is supported by physiological findings (e.g., Ts'o et al., 1986). The linking decay time constant is 50ms, according to fast NMDA channel time constants found in experiments (for details see Chapter 2.3.3).

Parallel Orientation Inhibition

An effect further supporting the Gestalt property of continuity is the inhibition of neurons with iso-orientation tuning with cRFs in parallel (*parallel-cRF inhibition*) (Figure 3.3.B). In Area-1a the range of inhibition is r=1, in Area-1b it is r=3. The longer range of the latter was chosen to counterbalance the BO feedback: Since feedback is divergent, not only neurons encoding a stimulus object's contour but also neurons in their surround receive feedback. Thus, also neurons not encoding the object would show a higher firing rate if they did not receive *parallel cRF* inhibition. Since inhibition from neurons encoding the object's contour is strongest, neurons encoding the surround are the losers in a soft *winner-take-all* (WTA) competition.

The two types of surround inhibition, parallel subtractive (*parallel-cRF*) inhibition and radial divisive inhibition, complement

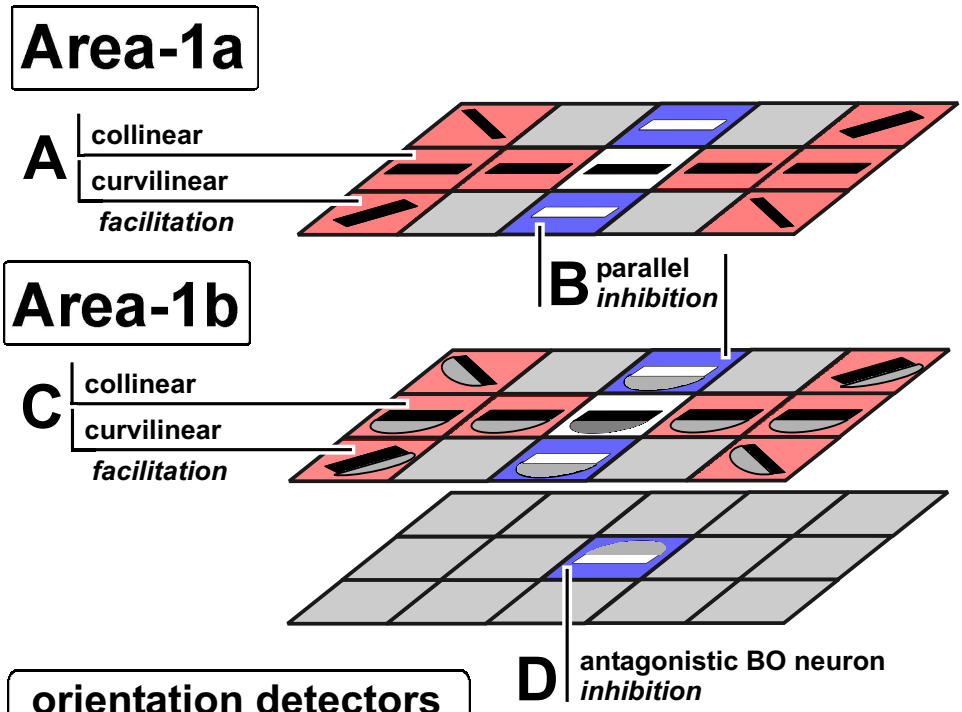
Area-1a
A
collinear
curvilinear
facilitation
B
parallel
inhibition
Area-1b
C
collinear
curvilinear
facilitation
D
antagonistic BO neuron
inhibition

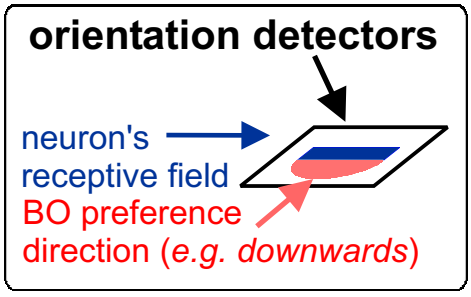
orientation detectors
neuron's
receptive field
BO preference
direction (e.g. downwards)

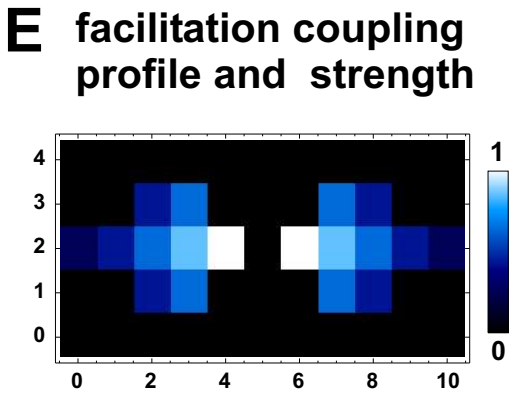
E
facilitation coupling
profile and strength
4
3
2
1
0
0
2
4
6
8
10
1
0

each other. Divisive inhibition inhibits the surround in general (independent of orientation), whereas parallel inhibition inhibits a subset of neurons in a soft *winner-take-all* (WTA) (Itti et al., 2000) manner, thus increasing the contrast of contours. The network would also work with only one of these mechanisms, but not as well.

Therefore, all lateral connections in Area-1 either strengthen the contrast of continuous contours (*figure*) or inhibit the surround (*ground*). These mechanisms support local figure-ground segregation.

3.4 Area 2: Curvature Detectors

Area-2 neurons are activated by curved contours (*curvatures*). Each of four layers of curvature detectors encodes curvatures of a different orientation (Figure 3.1: Area-2). CRF properties of neurons in Area-2 result from converging connections from Area-1a neurons, each of

Figure 3.3 *(facing page)*: Lateral connectivity in Area-1a and Area-1b for an example neuron. A-D: For an exemplary neuron for each of the two areas its lateral connections are shown schematically. The exemplary neurons are marked with white background. All neurons are symbolised by a rectangle with a bar indicating their preferred orientation inside. Further, for Area-1b the direction of BO preference is indicated by a semicircle. Neurons with red background are facilitated by linking, neurons with blue background are inhibited. **A/C:** Neurons with linearly and curvilinearly arranged cRFs facilitate each other, thus the encoding of contours is supported. In Area-1b (**C**) only neurons with the same or similar BO preference are linked. **E:** The lateral coupling profile with coupling strengths is plotted for a neuron with horizontal orientation preference located at position x=5 (horizontal) and y=2 (vertical). The coupling strength is weighted with a Gaussian. The linear coupling reaches to up to a distance of 5 neurons. The curvilinear coupling facilitates two neurons in each quadrant. **B:** Neurons with the same orientation tuning whose cRF is parallel adjacent to the source neuron are inhibited. This inhibition reaches to each side with a distance of 1 (Area-1a) resp. 3 (Area-1b). **D:** The neurons with identical cRF properties but differing in BO preference (i.e. the BO neuron's antagonist) is also inhibited. **Not shown:** Lateral divisive inhibition.

which encode a segment of a curve.

In Area-2, for each of 4 curvatures, there is a layer of 7x7 excitatory/inhibitory neuron pairs.

Area-2 neurons are curvature detectors with complex cell properties: Area-2 neurons respond (1) specifically to curvatures and (2) to a range of curvatures within their cRF.

Figure 3.4 illustrates the convergence from Area-1a to Area-2 for example curvature detectors. Area-1a neurons of three different orientation selectivities converge on each Area-2 neuron. In order for an Area-2 neuron to be selective to a particular range of curvatures from a confined region, several mechanisms are used:

MAX-Operation

Several neurons of *each* Area-1a neuron orientation preference converge on one Area-2 neuron. In order to avoid that Area-1a neurons only of the same orientation preference suffice to bring an Area-2 neuron above threshold, we implemented a MAX-operation (Riesenhuber and Poggio, 1999). This is done by computing the highest firing rate of each group of neurons with the same orientation preference converging on the same Area-2 neuron. For the example shown in Figure 3.4 this means that the maximum firing rate of all neurons marked yellow is computed and the same for the neurons highlighted blue and red. After the MAX-operation the convergence of the different orientations is computed with an AND-gate.

AND-Gate

The activation converging on one Area-2 neuron from *different orientation selective* Area-1b neurons is multiplied (AND-operation). Input from all three Area-1 orientation detector types converging on an Area-2 neuron is a necessary condition for it to fire. If there is only input from one or two orientation types, on the other hand, the Area-2 neuron is not activated. In order to bring an Area-2 neuron above threshold, activity significantly above spontaneous activity from all converging orientations is necessary.

This mechanism allows the detection of curvatures of a wide range of luminances: A high contrast line stimulus will activate neurons of one orientation preference to a very high firing rate but will not trigger any other types of orientation detectors. Thus, the product of orientation detectors converging in Area-2 via an AND-gate will be very low or nil. In contrast, a low contrast curve-stimulus will activate three types of orientation detectors converging on the same Area-2 neuron. Though all Area-1a neurons will only be active with a low firing rate due to the low contrast of the stimulus, the product of their firing rates will be big enough to activate the appropriate Area-2 curvature detector.

Saturation Function in Area-2 Neurons

Due to the multiplication in the AND-operation, the range of resulting values is increased compared to the usual adding of pre-

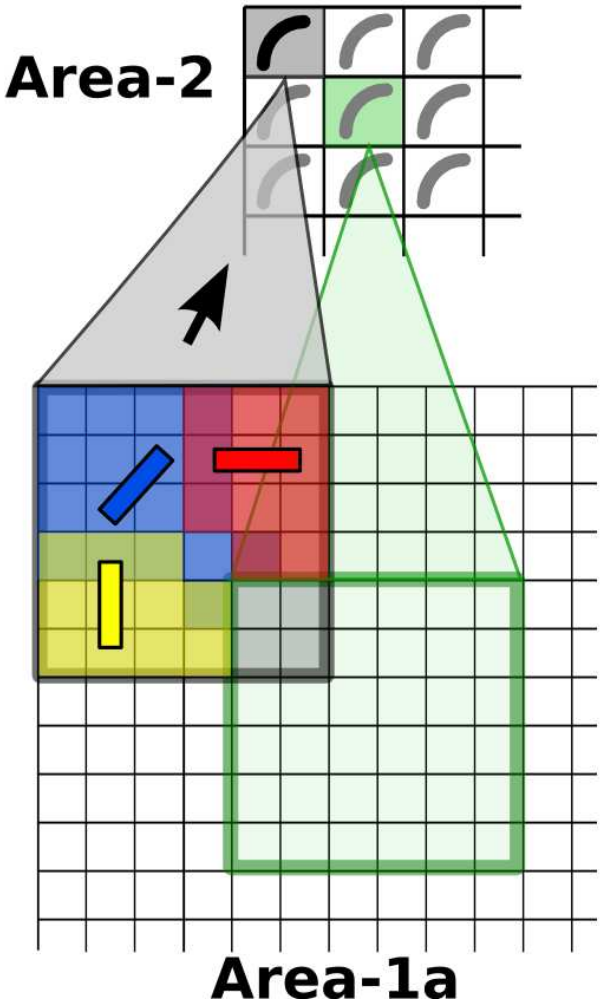

Figure 3.4: Area-2 Curvature Detectors. Exemplary, the convergence of Area-1a orientation selective neurons to Area-2 curvature detector neurons is shown. The lower part of the figure shows a clipping of Area-1a, each grid squared symbolising a neuron. The *yellow, blue* and *red* bars indicate the orientation selectivity of the neurons shaded in those resp. colours. These neurons converge on the same Area-2 neuron (highlighted *grey*). There is an overlap of the receptive fields of curvature detectors, as shown by the example of the cRF and neuron highlighted in *green*, but the overlap is not functional. One stimulus curvature can only elicit activity in one curvature detector.

synaptic activity in a postsynaptic neuron. In order to transform the product of the AND-operation in a reasonable firing rate of curvature neurons, we implemented Area-2 neurons with a saturation function (see Equation 2.7; in the rest of the network we used a transfer function which is linear above threshold). Thus, a certain input is necessary to bring an Area-2 neuron above threshold. When input strength has reached saturation, increase of input firing rate will not increase the output firing rate of the neuron.

As an alternative to introducing a saturation function, the root (here: $\sqrt[3]{}$) of the result of the AND-product could have been used. That approach did not work as well since the setting of the Area-2 neurons threshold became more difficult, making the mechanism less robust.

Neural Correlates of AND-Gate

Physiologically, an AND-gate can be motivated by non-linear dendritic interactions (Koch et al., 1983). For example, different area V1 neurons project to the same V3 neuron. Each V1 neuron (e.g. encoding a different orientation preference each) elicits a postsynaptic potential on the V3 neuron's dendritic tree via a synapse. Thus, a V1 neuron of one orientation preference can trigger only a certain maximal depolarisation in the postsynaptic V3 neuron. Only if several V1 neurons (encoding different orientations) provide input, the combined depolarisation will trigger an action potential. AND-gates are also used by Grossberg (1994) for his model bipolar-cells, which will only be active when receiving input at both sides.

Complex Cell Properties

Area-2 neurons are activated by a (limited) range of curvature radii, thus showing complex cell properties. From Figure 3.4 it can be inferred which types of curves and right angles elicit Area-2 activity. In the Area-1a region, where the top left (second quadrant) curvature detector receives its input from, a stimulus curve has to activate at least one of each type of orientation detector in order to bring the appropriate Area-2 neuron above threshold.

As indicated by the green rectangle in Figure 3.4, the cRFs of curvature detectors overlap. The convergence onto Area-2 and overlap in Area-1a were designed so that a stimulus curve will elicit the same Area-2 activity (of different neurons) independent of their position in the visual field.

Lateral Connections

There are three types of lateral connections in Area-2: (1) Curvature detectors, which correspond in their bending sense, facilitate each other. (2) Curvature detectors, which complement each other to a curvature change (*S-curve*), inhibit each other. (3) Curvature detectors of the same type subtractively inhibit each other locally with Gaussian distribution of coupling strength.

3.5 Area-3: Convex Object Detection

Area-3 neurons are activated by convex contours. The cRF properties of neurons in Area-3 result from the following feed-forward convergence from Area-2: Curvature detectors of orientations and spatial relations, appropriate to encode a convex contour converge on the same Area-3 neuron. In our model, it is not necessary that the cRFs of these curvature detectors are adjacent. The object's contour can be interrupted (occlusions, gaps) and the object will still be detected. Even if only three curvature detectors are activated by the corners of a rectangle (e.g. due to one of the corners being occluded), activation is still elicited in Area-3 by the remaining three detectors, but at a lower firing rate. If only two curvature detectors are activated, it is still possible that Area-3 activity is elicited, yet at an even lower firing rate.

Area-3 consist of one layer of 21x21 excitatory/inhibitory neuron pairs.

Area-3 Encodes Probability of Presence of an Object

The activation strength of a neuron in Area-3 is interpreted as the probability of the presence of an object in the stimulus at the location coded by this neuron. Thus, a preference is encoded for contour detectors complementing each other to what would be perceived as a closed contour (according to Gestalt law of closed contour, Figure 1.2B). This property is supported by psychophysical experiments (Elder and Zucker, 1993, 1994; Kovács and Julesz, 1993). Through the convergence of curvature neurons with different spatial relations to different Area-3 neurons, information about size and position of an object in visual space is preserved and encoded in Area-3 (Figure 3.5.A).

Due to the low pass characteristic of the orientation filter and due to the increase of cRF size with each layer in the forward path, stimulus shifts by less than 6 pixels will activate the same Area-3 neuron.

Lateral Connections in Area-3

In Area-3 neighbourhood property is defined by lateral connections. Neurons encoding objects that share parts of their contour inhibit each other. There are two classes of inhibitory connections: Inhibition between neurons encoding objects (1) extending to the same side from the shared contour and (2) extending to opposing sides.

Ghost Inhibition

When a stimulus object is presented, not only the Area-3 neuron encoding the object best is driven, but also neurons encoding similar (in size and position) objects receive input by curvature detectors. The objects encoded by the Area-3 neurons being co-activated, we call *ghost objects*, since they are not actually contained in the stimulus but neurons encoding them are nonetheless active. Since the co-activation of neurons encoding ghost objects is unwanted, we intro-

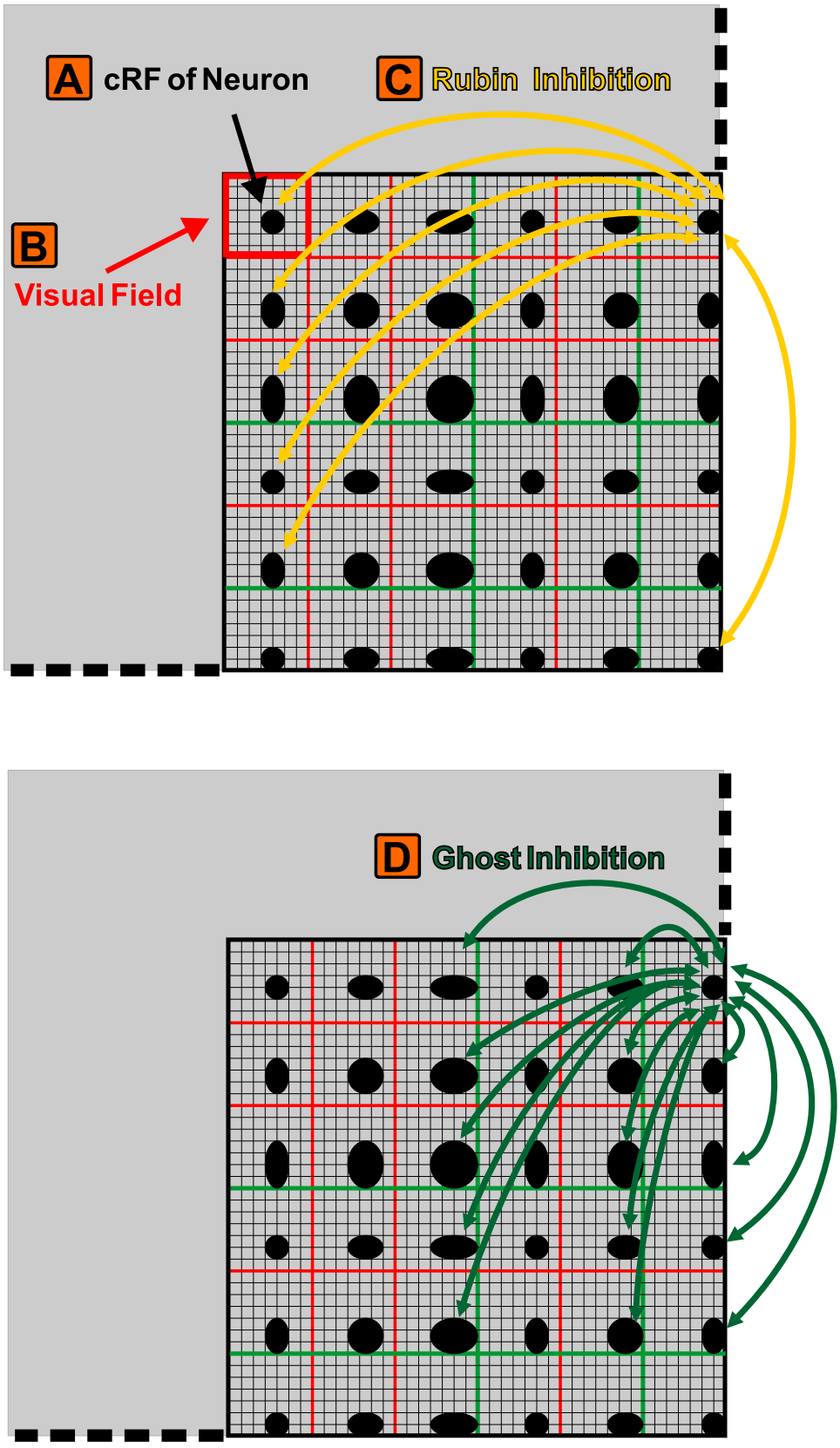
A cRF of Neuron
C Rubin Inhibition
B
Visual Field
D Ghost Inhibition

duced lateral subtractive inhibition, which we named *ghost inhibition*. This form of inhibition is implemented between all Area-3 neurons encoding neurons sharing parts of their contour.

Figure 3.5 shows neurons from Area-3, each neuron is indicated by a visual field (Figure 3.5.B) with the cRF specific to the neuron (Figure 3.5.A).

Let us go back to the initial example: When a stimulus object is presented to the network, a high response firing rate is elicited in the most fitting Area-3 neuron. Co-activated neurons show a lower initial firing rate. Due to ghost inhibition the correct (regarding the stimulus) Area-3 neuron exerts high inhibition on the co-activated neurons due to its high firing rate. Thus, the firing rate of the co-activated neurons is nearly completely inhibited. A significant activation of the *ghost* Area-3 neurons would lower the network's performance, since these neurons would project BO feedback back to neurons not encoding the stimulus object.

In Figure 3.5.D all neurons[II] inhibited by the neuron in the top right of the grid and vice versa inhibiting this neuron are pointed out by an arrow.

Rubin Inhibition

The second type of lateral subtractive inhibition in Area-3 is the inhibition occurring between all neurons that encode objects that share parts of their contour but extend to opposing directions. One example case of such a scenario is Rubin's vase (Rubin, 1921), where two objects (vase and face) are contained in a stimulus which share a part of their contour. Hence, we named this type of inhibition *Rubin inhibition*. Such two objects can be encoded in Area-3 at the same time. This will result in feedback from these Area-3 neurons encod-

[II] i.e., all neurons shown in this excerpt of the entire layer

Figure 3.5 *(facing page)*: Area-3 Topology. Area-3 neurons encode object position and size. A sample of 6x6 neurons from Area-3 (lower right corner) with each neuron's respective cRF is displayed. **Upper graph:** Rubin inhibition for the neuron in the top right corner of the grid. **Lower graph:** Ghost inhibition for the neuron in the top right corner of the grid. **A:** The cRF location in the visual field of the neuron represented here. **B:** The visual field of the neuron represented. **C:** Arrows indicate all neurons that inhibit and are inhibited by the neuron in the top right corner of the grid with *Rubin inhibition*. **D:** All neurons that inhibit and are inhibited by the top right neuron with *ghost inhibition*.

ing the objects to antagonistic BO neurons encoding the shared contour. If one of the two Area-3 neurons encoding the Rubin-type objects is activated with a much higher firing rate, then due to the soft *Rubin* inhibition, the more activated neuron will prevail.

Figure 3.5.C indicates all neurons in the sample inhibiting and vice versa inhibited by the neuron in the top right of the grid by Rubin inhibition. With all but the lowest neuron in the first column the top right neuron shares parts of its left contour.

3.6 Feedback

Feedback from Area-3 facilitates the activity of those Area-1b neurons that encode the contour of the object detected in Area-3 via a linking synapse (Section 2.3.3). Area-3 neurons encode the position and size of an object. The spike density (i.e. firing rate) of an Area-3 neuron encodes the probability of presence of an object in a stimulus at one location. Furthermore, the side of the contour to which the object extends, can be inferred from the object's position and size encoded in Area-3. This information is also encoded into the feedback by selectively facilitating the appropriate Area-1b neurons.

In Area-1b there are two neurons which encode the same part of an object's contour, only differing in the feedback they receive. Feedback from the neuron that encodes the probability of an object's presence is only sent to one of them. Thereby, the neuron receiving feedback is given *border-ownership* property. It has a preferred direction for an object's surface to extend to from the contour it encodes.

The antagonist is facilitated with feedback from Area-3 neurons activated by stimulus objects, of which the surface extends to the opposite direction.

Antagonistic pairs of such BO-neurons mutually inhibit each other subtractively (Figure 3.3D).

Due to the increase of cRF size from the lower to the higher areas, an Area-3 neuron can be activated by a certain range of object sizes and positions. Thus, feedback is projected not only onto neurons encoding one specific contour but to neurons encoding a range of contours. This divergence does not pose a problem, since local inhibition in Area-1b suppresses activity of neurons inappropriately receiving feedback.

Chapter 4

Results of the Main Border-Ownership Model

Outline

We describe the behaviour of the network responding to the presentation of a range of stimuli in order to demonstrate object presence detection (in Area-3) and the effect of BO-feedback (in Area-1b). Further, the object detection performance of the model in scenes with noisy input is analysed.

4.1 Overview Over Stimuli

The network was presented with the stimuli used by Zhou et al. (2000) and others. With these stimuli we demonstrate the network response regarding the following variations of stimulus objects:

- size
- form
- position (translation)
- number of objects
- correlation of objects
- completeness

Further, we investigate how the model handles noisy stimuli. For that purpose we overlayed a stimulus containing an object with noise.

4.2 Response of the Network Areas to an Example Stimulus

We give an overview over the network's behaviour by describing its response to an example stimulus. A rectangle stimulus (Figure 4.1.A) is presented for 100ms with stimulus onset at t=100ms. The stimulus onset delay was chosen in order to allow the system to relaxate into a steady state after it is switched on. There is immediate input to the network, since background brightness of 25% of the object's brightness is added to the stimulus (after convolution with the orientation filter) throughout the entire simulation.

Area-1a

Area-1a neurons exhibit cRF properties corresponding to orientation-selective simple cells (Hubel and Wiesel, 1962) (Figure 4.1.B, filters: Figure 3.2). There are four layers, each encoding a different orientation preference ($0°, 45°, 90°$ and $135°$). Their average response to the example stimulus (Figure 4.1.A) is displayed in Figure 4.1.C. Each square pixel in the 30x30 grid represents a neuron. Each neuron's average rate is colour-coded. The average activity was computed for the time during stimulus presentation (100-200ms) and normalised to the maximum activity of the four layers (maximum=1). The development of firing rate over time is plotted for several example neurons encoding the object's contour (indicated by arrows) in Figure 4.1.D. All these neurons show a high transient and a lower sustained tonic response.

In the layers encoding horizontal and vertical orientation (Figure 4.1.C.a/c) the effect of lateral divisive inhibition can be seen. The activity of neurons in the vicinity of the neurons encoding contours is completely inhibited during stimulus presentation.

Area-2

Excitatory feed-forward projections from Area-1a to Area-2 (for details see Section 3.4) activate curvature detector neurons matching the stimulus. In Figure 4.2.A the average activity evoked by the example stimulus (Figure 4.2.B) for each of the four curvature layers is depicted. The average was computed for the time of stimulus presentation and normalised to the maximum over all four layers. The cRF property of each layer is indicated in the top left corner in Figure 4.2.A. Every corner of the stimulus object activates a different type of curvature detector. Further, since the four corners of the rectangle are at different positions, each corner activates a curvature detector with a different cRF. In Figure 4.2.C the firing rate of all Area-2 neurons significantly activated are plotted. Due to the saturation transfer function of the Area-2 neurons, the optimally activated neurons all reach saturation and thus exhibit very similar dynamics. Hence the

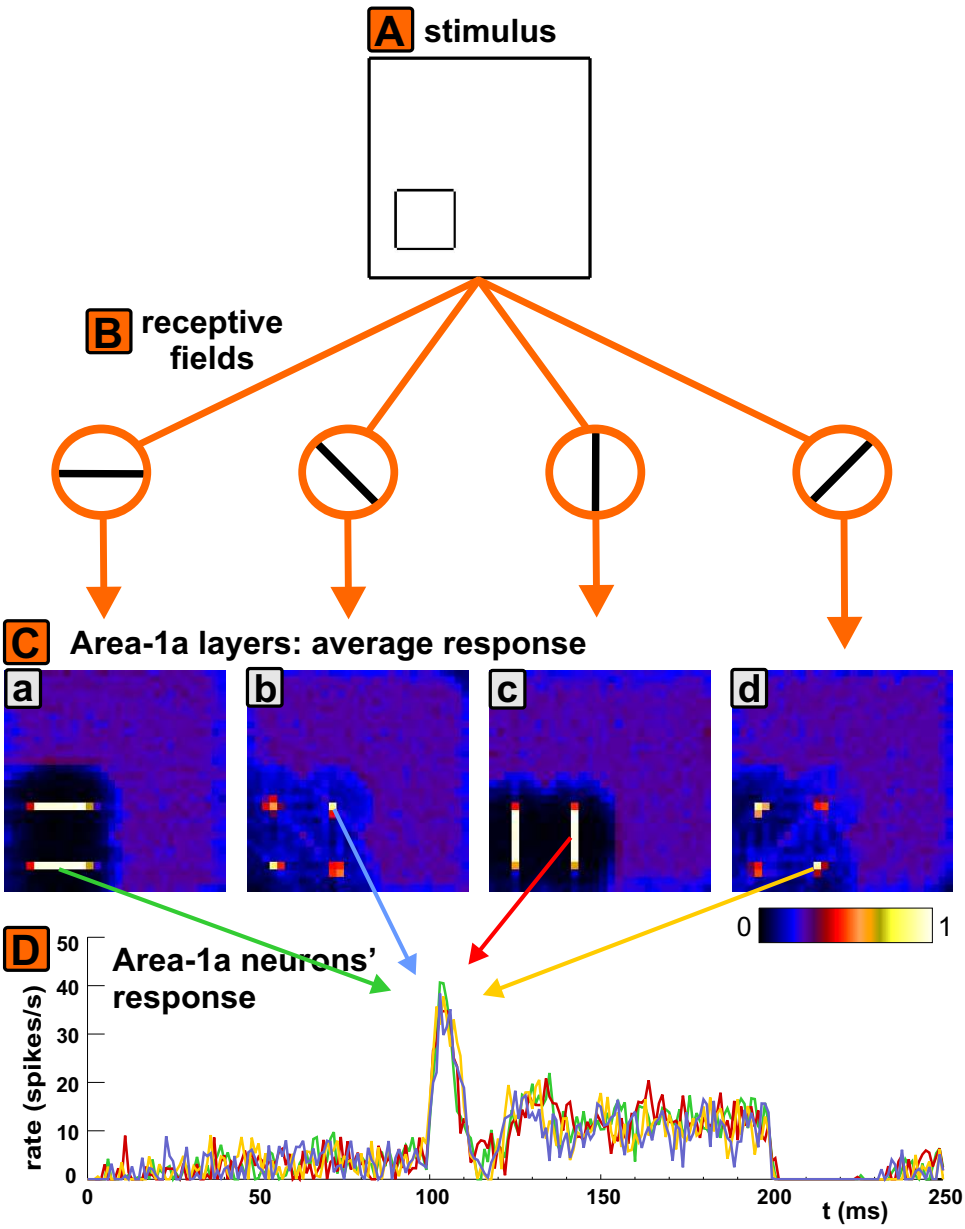

Figure 4.1: Area-1 activity elicited by example stimulus. The stimulus (**A**) is convoluted with orientation detectors (**B**) giving each neuron in Area-1a (**C**) different classical receptive field (cRF) properties. In **C** the neurons' average rate during stimulus presentation is displayed. In **D** the development of firing rate over time for some exemplary neurons (indicated by arrows) is plotted.

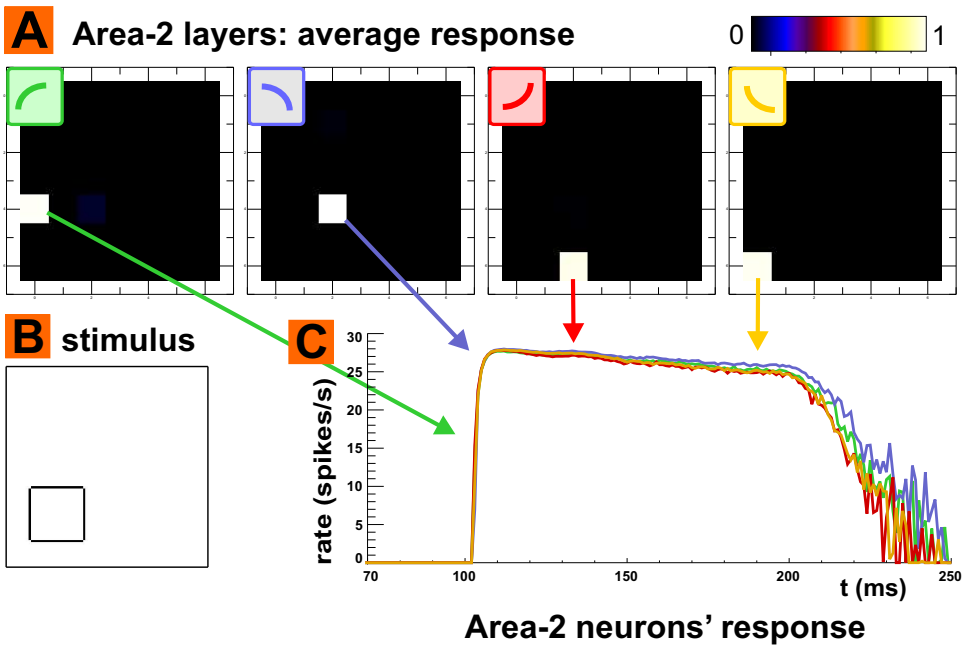

Figure 4.2: Curvature detection: Area-2 activity elicited by example stimulus. Average activity during stimulus presentation (100-200ms) evoked in the four curvature detector layers (**A**) by a rectangle stimulus (**B**). **C:** The firing rate of all significantly active neurons. For assignment of neuron activities to location in layers arrows and activity graphs are colour coded.

computed average in Figure 4.2.A is nearly the same for all neurons significantly activated.

Area-3

As described in Section 3.5 curvature detectors converge via excitatory feed-forward connections to Area-3 neurons. With Area-3 neurons having a very high threshold, accumulated input from several curvature neurons is necessary to drive a neuron. In Figure 4.3.B the average activity of the excitatory layer of Area-3 neurons is shown. The sample stimulus (Figure 4.3.A) brings only one Area-3 neuron above threshold. Its rate is plotted in Figure 4.3.C. Due to the high tonic activity in Area-2 and the value of Area-3 neuron time constants and inhibition strength, Area-3 shows a high sustained activity for the time of stimulus presentation.

Area-1b

Area-1b differs from Area-1a in that it receives the identical input *delayed* and that there are two detector layers for each orientation. In these layers identical neurons inhibit each other (Figure 3.3.D). An-

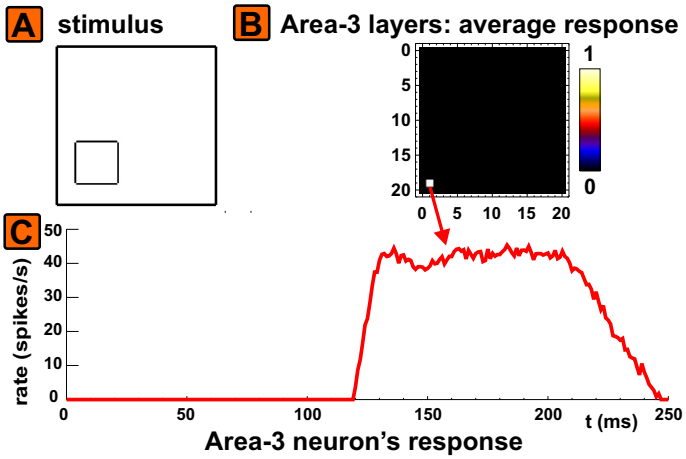

Figure 4.3: Area-3 activity elicited by example stimulus. **A:** This rectangle stimulus was presented to the network. **B:** One neuron in Area-3 is driven by the stimulus. **C:** The firing rate of the only active Area-3 neuron plotted over time.

other difference is that Area-1b additionally receives feedback from Area-3. The effect of feedback can be seen in Figure 4.4 for the example rectangle stimulus. In Figure 4.4.B the average rate for all BO-layers from response onset to end of stimulation (125-200ms) is shown. The icons in the top left corner of each graph indicate the orientation and BO preference (the black bar shows orientation preference, the grey semi-circle preferred BO direction relative to the bar). In Figure 4.4.B antagonistic layers are arranged in columns. The rate is normalised to the maximum activity in each pair of antagonistic layers[I]. In the third column, e.g., the upper layer has a BO preference to the right, whereas the lower layer has a BO preference to the left. Since these neurons encode parts of the right vertical contour of the stimulus object, the neuron with the BO preference leftwards receives BO-feedback input, thus has a higher rate and inhibits the other antagonistic neuron. The effect of inhibition can be seen in Figure 4.4.A. In Figure 4.4.A the rates of two neurons with identical cRFs, one with BO preference rightwards (blue), the other with BO preference leftwards (red) is plotted. For comparison of rates of neurons of the same BO preference encoding opposing contours of a stimulus object, in Figure 4.4.C the rate of two exemplary neurons is plotted. Due to BO-feedback the rates of neurons start to differ already during the transient answer of the response. The rate of the neuron encoding

[I]This is done since the maximum rate in layers encoding orientation preference $45°$ and $135°$ is higher than in the other layers. This is due to divisive inhibition having less effect if one neuron is more active than its entire surround.

the left vertical contour (green) is low due to inhibition from its antagonist in the layer encoding the opposite BO-direction.

After now having demonstrated the response of all areas of the network to the example stimulus, we will direct our attention to the key features of the network. For that purpose we made simulations with stimuli that make these features most explicit.

4.3 Stimuli Eliciting Opposite BO Preference in One Neuron

Figure 4.5 shows the activity of one model BO neuron (Area-1b) to two different object stimuli. One stimulus extends leftwards from the neuron's cRF (Figure 4.5A), the other one rightwards from the cRF (Figure 4.5B). The neuron shows a BO preference to the left (Figure 4.5D), i.e., it responds stronger to objects extending leftwards from its contour.

4.4 Stimuli of Varying Position, Size and Form

Variation of Position and Size

Area-3 neurons encode position and size (see Chapter 3.5). In Figure 4.6 we demonstrate that the same rectangle at a different position in visual space (see Figure 4.6.A.a/b) activates a different Area-3 neuron (Figure 4.6.B.a/b). Also, stimulus objects of different size (Figure 4.6.A.a/c) activate different Area-3 neurons (Figure 4.6.B.a/c). The response onset and magnitude of firing rate in Area-3 to an appropriate stimulus is however independent of position and size (Figure 4.6.C).

Variation of Form

Detection of object presence is widely invariant of stimulus object form. A rectangle and a C-shaped form of the same size (Figure 4.7.A.a/b) are detected by the same Area-3 neuron (Figure 4.7.B.a/b) whereas a smaller rectangle stimulus (Figure 4.7.A.c) sharing three of its edges with the other two objects, activates a different Area-3 neuron (Figure 4.7.B.c). As in the previous example of varying position and size, the response onset and magnitude of Area-3 activity is very similar for all three stimuli (Figure 4.7.C).

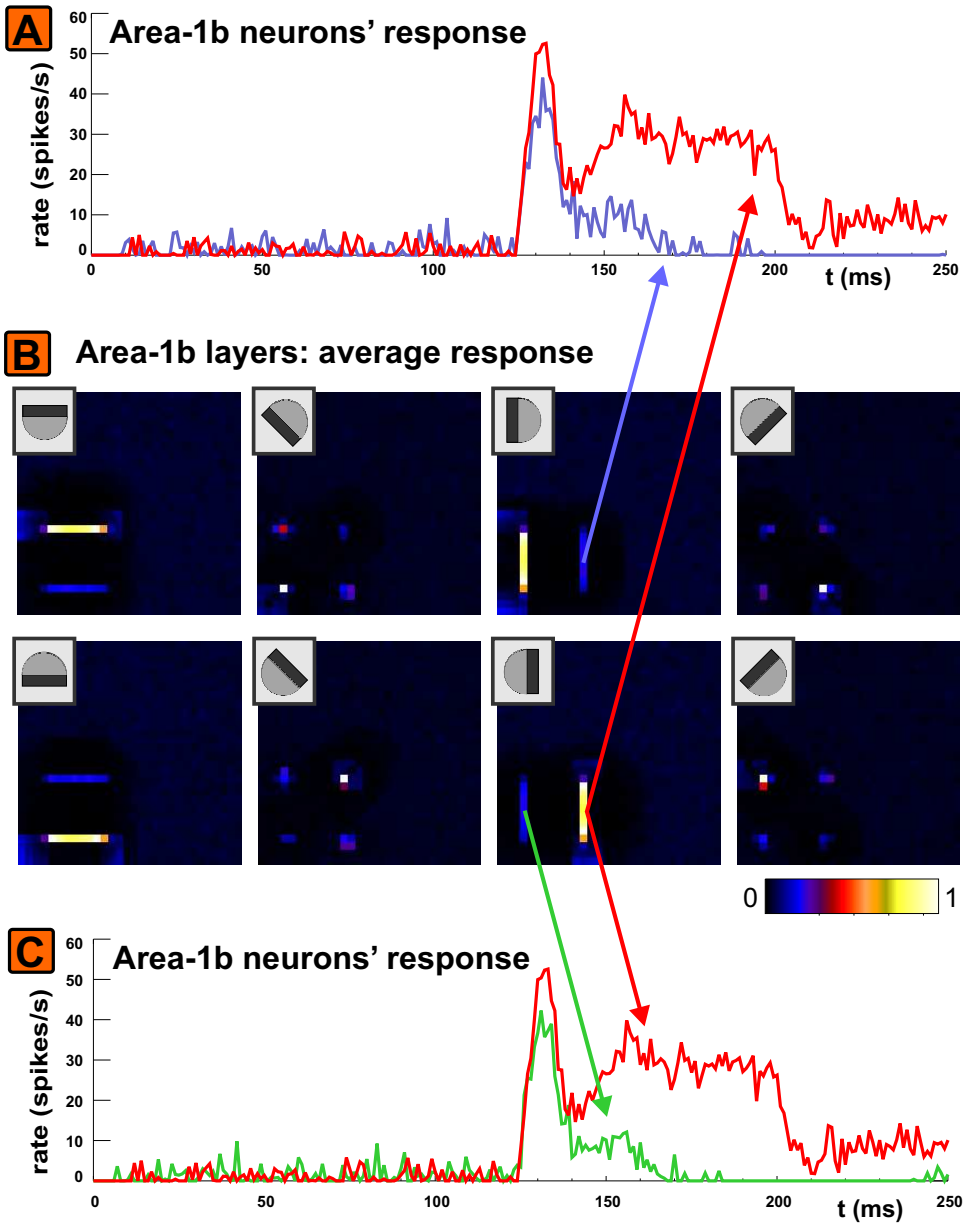

Figure 4.4: Area-1b: BO-layers response to an example stimulus. B: Average activity of BO-layers during stimulus presentation. Layers encoding antagonistic BO properties are arranged in columns. The activity is normalised for each column of layers. **A:** Response of two antagonistic BO neurons with identical cRF encoding parts of the contour of the stimulus object. **C:** Response of two neurons with identical BO property encoding opposite contours of the stimulus object.

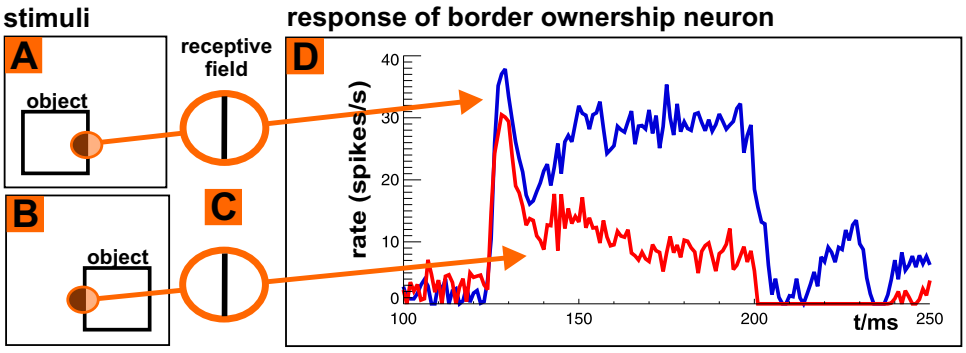

Figure 4.5: Border-ownership neuron activity. A,B: Two simulations are done with different stimuli. **C:** The stimuli are identical within the receptive field of the neuron plotted. **D:** The response of an Area-1b border-ownership neuron to each of the two stimuli. The neuron shows a higher response for objects extending leftwards from the contour it encodes. The simulations reproduce the experimental data (Figure 1.1).

4.5 Feedback Effect Quantification

Figure 4.8 shows results of simulations with and without feedback. With identical stimuli (Figure 4.8.A) for the same neuron (Figure 4.8.B) the difference in activity (Figure 4.8.C) is due to the feedback.

With the *normalised accumulated feedback effect* E_{fb} we quantify the difference in activity between simulations with and without feedback to Area-1b:

$$E_{fb}(t) = \frac{\int_{\tau_1}^{\tau_1+t} A_f(\tau) - A_n(\tau) d\tau}{t \int_{\tau_1}^{\tau_1+t} A_n(\tau) d\tau} \tag{4.1}$$

with time of response onset τ_1, window of integration $\Delta\tau = t$, activity with feedback A_f and without feedback A_n. The effect is normalised to the activity without feedback.

The feedback effect $E_{fb}(t)$ is plotted in 4.8.D. Figures 4.8.E/F show the average activation of a layer of BO neurons with a preferred contour orientation of $90°$ and BO preference to the left.

4.6 Multiple-Object Stimulus

Our network is capable of detecting the presence of several objects at the same time. In case of ambiguities, such as when two objects

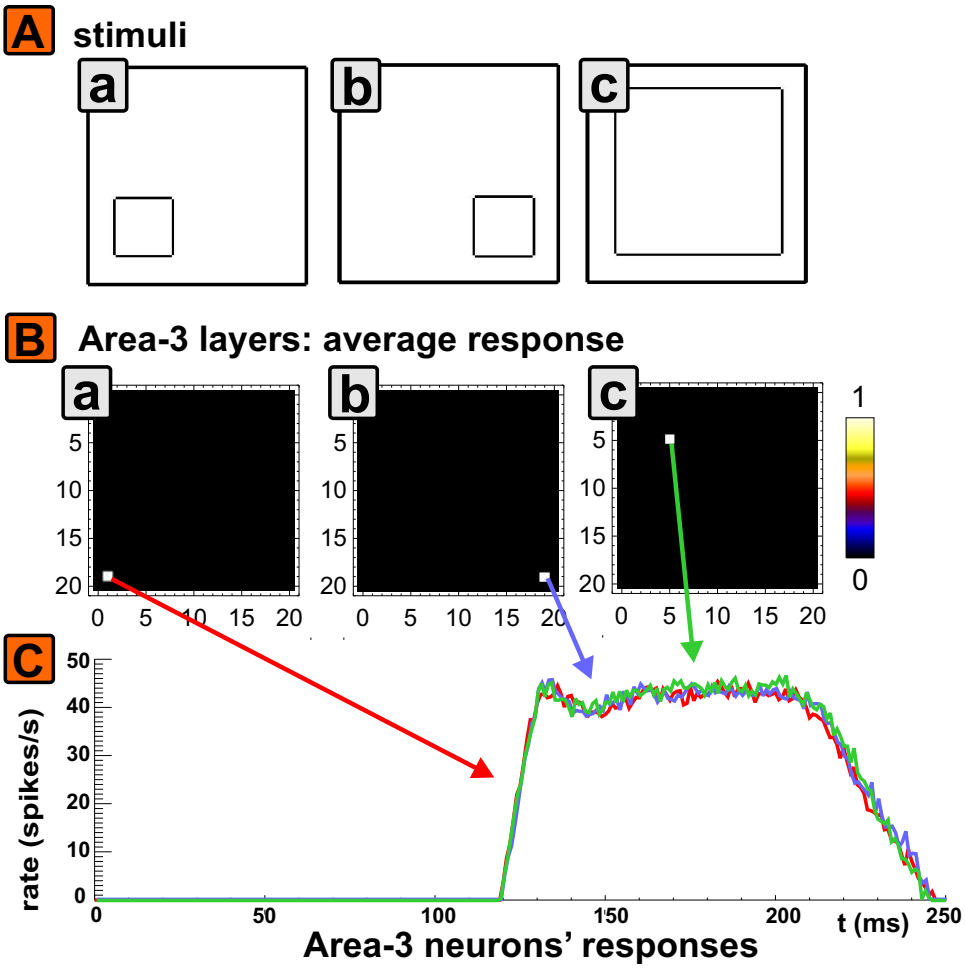

Figure 4.6: Variation of position and size. For different stimulus object location and size (**A**) different Area-3 neurons are activated (**B**). **C:** Area-3 neuron response onset and magnitude to an appropriate stimulus are independent of location and size.

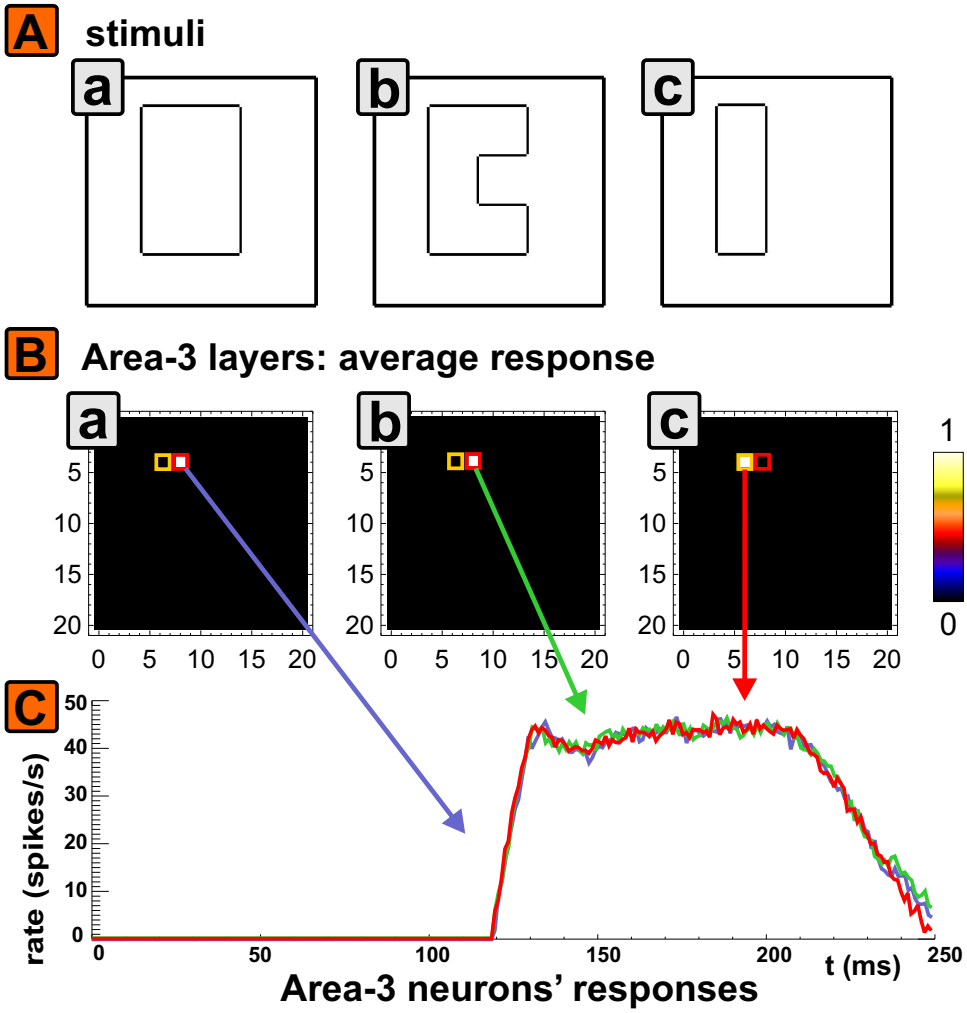

Figure 4.7: Stimuli of different form. A: Stimuli of different form but same size (a and b) and different size (c). **B:** Area-3 activity evoked by the three respective stimuli normalised to the maximum activity of all three simulations. **C:** Rate of active Area-3 neurons for each of the three stimuli.

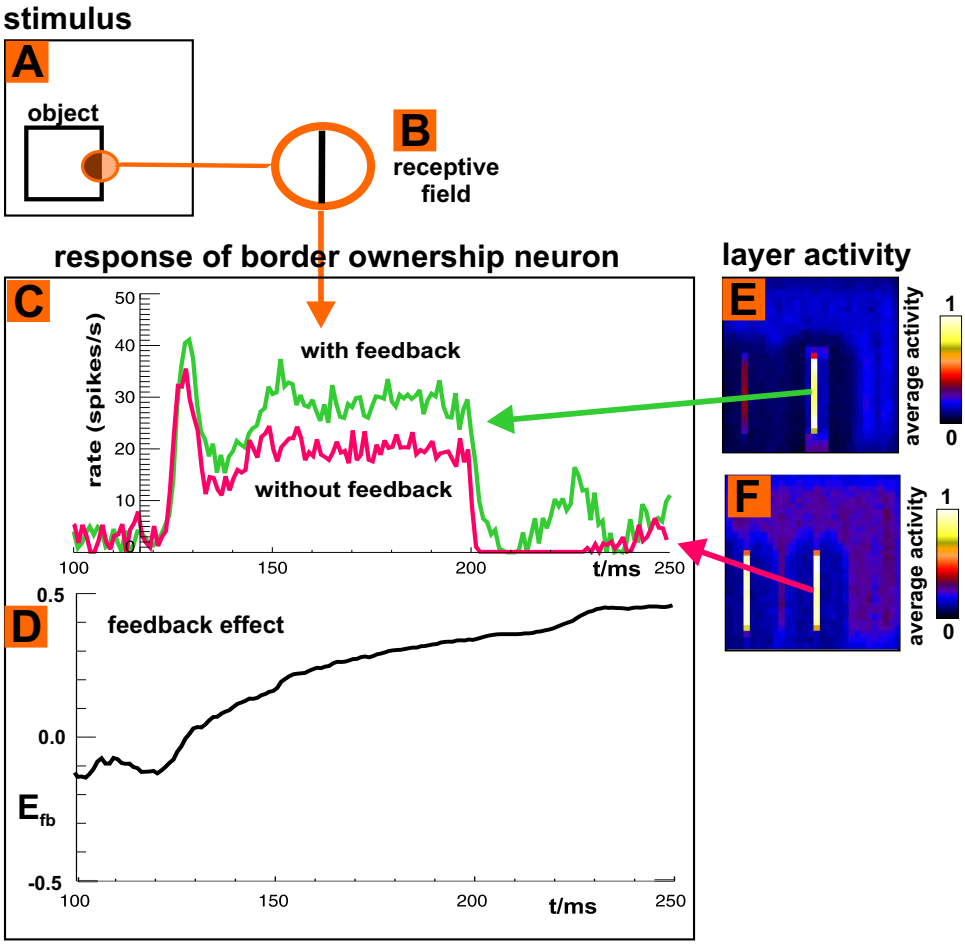

Figure 4.8: Effect of feedback. For the stimulus in **A** the activity of a BO neuron (Area-1b) with a preferred contour orientation of $90°$ (**B**) and a BO preference to the left is plotted. The activation is shown with (green) and without (red) feedback (**C**). The *normalised accumulated feedback effect* indicating difference between active and inactive feedback is plotted over time (**D**). **E,F** show the average activity during stimulus presentation (0-100ms) of the BO-layer in Area-1b. All neurons in that layer have an orientation preference of $90°$. Neurons in **E** have a BO preference to the left.

have a contour in common, neurons in Area-3 encoding these objects inhibit each other. Here we present the network's response to several stimuli with different constellations of multiple objects.

4.6.1 Separate Stimulus Objects

We demonstrate the network's ability to detect several objects at a time with a stimulus containing two rectangles (Figure 4.9.A). The stimulus drives two Area-3 neurons, each encoding size and position of one of the stimulus objects (Figure 4.9.D). Feedback from these neurons activates neurons in the appropriate BO layers. Figure 4.9.B/C/E/F show the average activity (110-220ms) of four BO layers. The neurons encoding any stimulus object's contour having a BO preference towards the inside of the object show a far greater rate than the neurons with the same cRFs encoding the opposite BO preference. Therefore, BO feedback can also introduce correct BO properties in Area-1b for stimuli containing more than one object.

4.6.2 Stimulus Objects Sharing an Edge

We investigated stimulus scenarios where two stimulus objects share an edge. This class of stimuli is interesting, since unlike with separate objects it is not trivial which BO property will be assigned to the shared edge. We presented three different stimuli of this class to the network:

- two objects sharing an entire edge (not shifted), extending to opposing sides
- two objects sharing parts of an edge (shifted), extending to opposing sides
- two objects sharing parts of an edge, extending to the same side, one object located within the other

Stimulus Objects Sharing an Edge Without Shift

We presented the network with two rectangular stimulus objects sharing an entire edge (Figure 4.10.A). In Area-3 initially three neurons are activated by the stimulus (Figure 4.10.D). The neurons that are only briefly active are marked with circles in Figure 4.10.D, since their average activity is far lower than the one of the prevailing neuron and thus can be hardly made out in the graph. The firing rate of all neurons active in Area-3 is plotted in Figure 4.10.H. Area-3 detects initially three objects: each rectangle by itself and the rectangles combined. The neuron encoding the latter prevails against the other

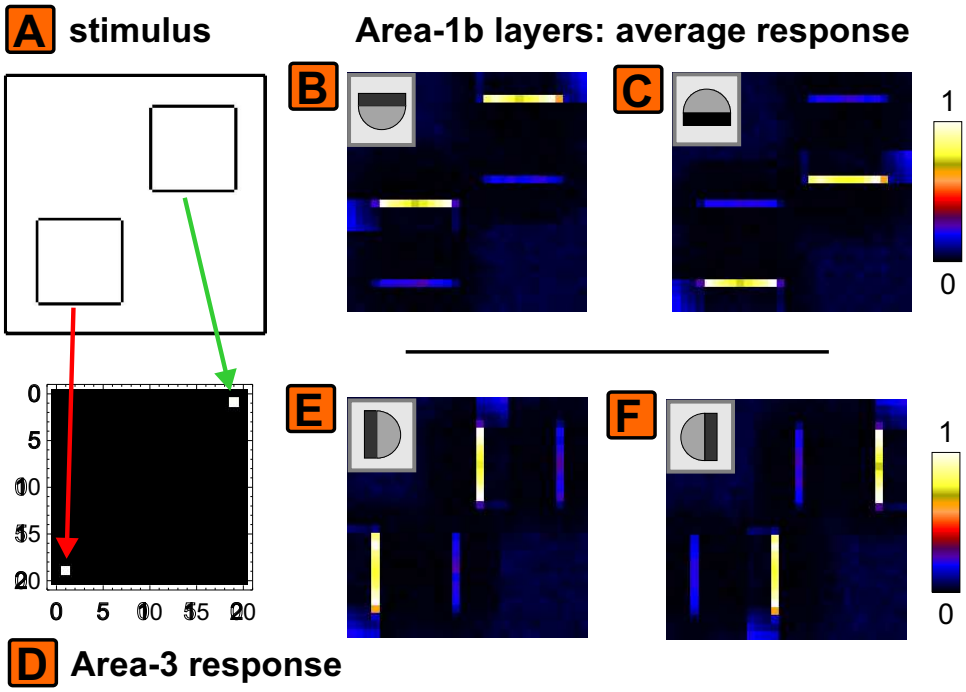

Figure 4.9: Network response to stimulus containing two objects. A: Stimulus containing two rectangles presented for 100ms starting at t=100ms. **D:** Average Area-3 activity evoked by the stimulus. **B,C,E,F:** Average response of selected BO layers (110-220ms). BO preference is indicated in the top left corner. In antagonistic layers **B** and **C** resp. **D** and **E** feedback activates opposing edges. Activity is normalised to their maximum for both antagonistic layer pairs.

two. Hence, BO feedback is mainly provided to the contour of the combined object, i.e. the shared contour does not receive any feedback but in the first 25ms of response onset. Since the feedback from the neurons encoding the two single objects projects to antagonistic neurons encoding the shared edge, the edge is not attributed to one or the other object during that time. As can be seen from the irregular activation of the shared edge (Figure 4.10.E/F), in some cases a BO neuron with the preference rightwards is slightly more active than its antagonist neuron or vice versa. Once, the Area-3 neurons encoding the single stimulus objects are completely inhibited ($t > 135ms$), there is no BO feedback at all to the shared edge. Figure 4.10.G shows the activity of sample neurons of the same BO property [II] encoding three different edges. The response is very similar to the response of a neuron encoding a contour receiving no feedback (see Figure 4.8.C).

The mechanism that leads to a winner-take-all of the Area-3 object detector neuron encoding the combined object is the following: There is inhibition between Area-3 neurons encoding shared contours: Inhibition between neurons encoding objects extending to opposite sides is less ($.002$, *Rubin inhibition*) than inhibition between neurons encoding objects extending to the same side ($.005$, *ghost inhibition*) for reasons given in Chapter 3.5. Thus, the neurons encoding the single objects inhibit each other reciprocally with weak inhibition, whereas the neuron encoding the combined object and the other two neurons inhibit each other reciprocally stronger. This would imply, that the neuron encoding the combined object is inhibited most and thus the

[II] vertical orientation preference, BO preference rightwards

Figure 4.10 *(facing page)*: Two objects sharing an entire edge. A: Stimulus with two objects sharing an entire edge. **D:** Area-3 average activity during the simulation (0-250ms). Sparsely active neurons are indicated by circles. **H:** Single unit activity of all active Area-3 neurons. Same color code as arrows in D. Neurons encoding single objects are only briefly active, whereas the neuron encoding the combined object shows high sustained activity. **B/C/E/F:** Average activity of selected BO layers between response onset and end of stimulation (110-220ms). The outer contours show BO properties, whereas the shared contour (**E/F**) shows no significant BO preference. **G:** Exemplary single cell activity of neurons encoding different edges. Which neurons' activations are plotted is indicated by the arrows.

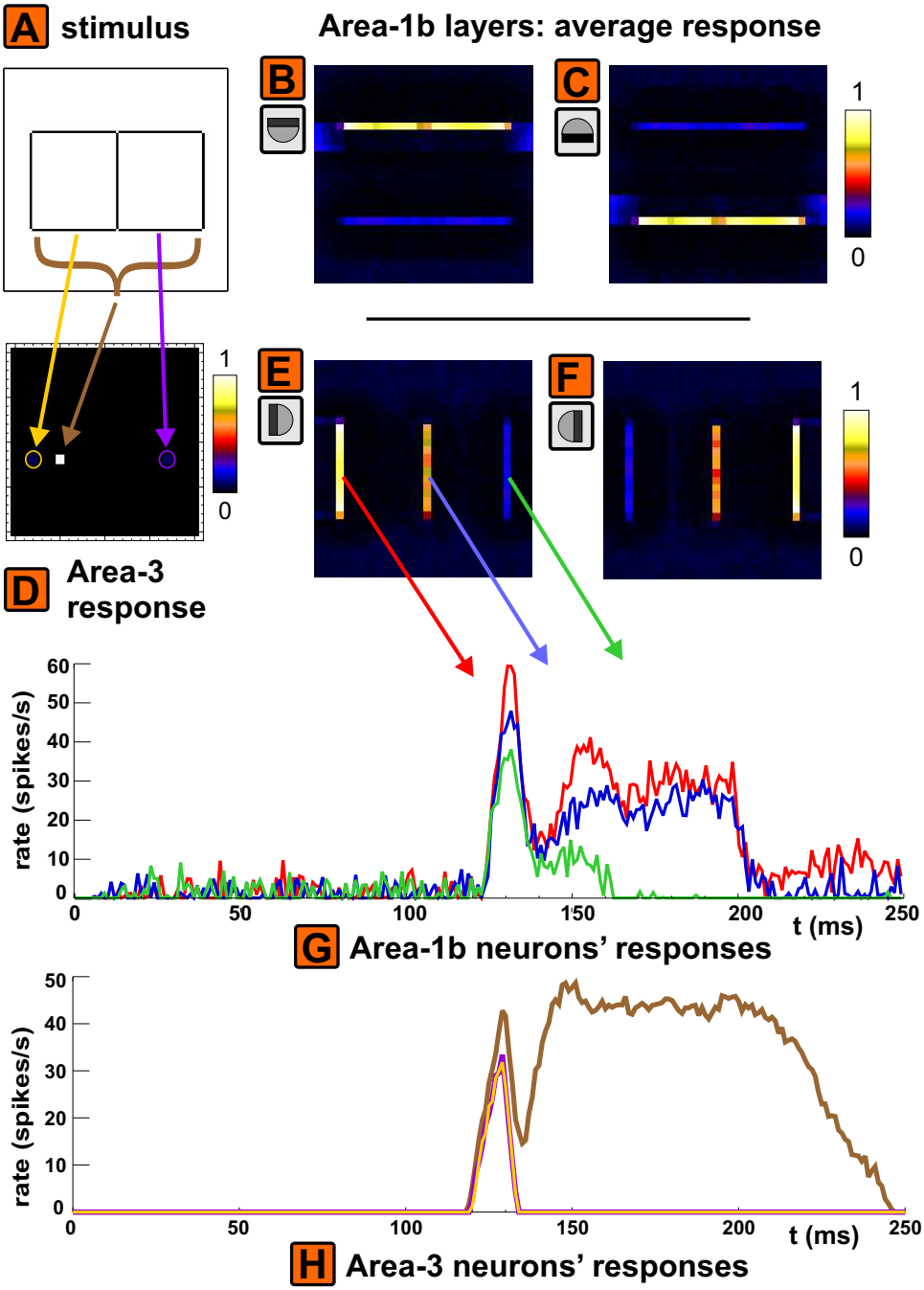
A stimulus
Area-1b layers: average response
B
C
1
0
E
F
1
0
1
0
D Area-3 response
rate (spikes/s)
60
50
40
30
20
10
0
0
50
100
150
200
250
t (ms)
G Area-1b neurons' responses
rate (spikes/s)
50
40
30
20
10
0
0
50
100
150
200
250
t (ms)
H Area-3 neurons' responses

other two will prevail. Yet, another aspect has to be taken into account for the explanation. Due to the shared contour, the curvature detectors driven by the corners verging on the shared contour are not activated as much, since the T-junction does not drive the curvature detectors as well as a single edge. Thus, the neurons encoding the single objects are not activated as much as the neuron encoding the combined object. For that reason, the combined object prevails.

Stimuli Objects Sharing an Edge With Shift

When a stimulus with two objects that share an edge but are shifted against each other (Figure 4.11.A) is presented, the presence of two objects is detected in Area-3 (Figure 4.11.D). BO feedback to Area-1b modulates the correct BO neurons encoding the outer edges of each of the two objects (see e.g. Figure 4.11.B/C). The shared edge shows, as in the previous example, no significant BO property (Figure 4.11.E/F). This is due to antagonistic BO neurons encoding the shared contour both receive feedback of the same magnitude. Thus, no BO neuron exhibits such a high rate that it could inhibit its antagonist drastically.

Stimuli Objects Sharing a Contour Extending to the Same Side

A stimulus with two objects extending to the same side from a shared edge (Figure 4.12.A) evokes activity in two Area-3 neurons (Figure 4.12.D). To be precise, the stimulus contains small gaps in the shared edge where the smaller object branches off of the shared contour. Thus, the upper and lower right corners of the smaller rectangle activate curvature detectors. As described above (Figure 4.10), T-junctions activate curvature detectors far less. The real world stimulus equivalent to our stimulus would be that the smaller rectangle overlaps the bigger one on the shared edge and that the rectangles are e.g. of different luminance. Then, the upper and lower right corners of the smaller rectangle are visible as curvatures.

Figure 4.12.H shows the activity of the two active Area-3 neurons over time. The smaller rectangle elicits a slightly lower response in Area-3, especially in the late tonic response. These two neurons provide feedback to Area-1b (Figure 4.12.B/C/E/F). As can be seen, the rate of the contour detecting neurons encoding the “correct” (regarding the stimulus) BO direction is greater for the bigger object (compare blue to red neuron rate in Figure 4.12.G). The activity on one edge varies considerably (compare orange and blue in Figure 4.12.G). The rate of some neurons encoding the “wrong” BO direction is in some cases very similar to the rate of a neuron encoding the “correct” BO direction (compare red and yellow in Figure 4.12.G). Nonetheless, the ratio between antagonistic BO neurons is still correct (compare red and yellow in Figure 4.12.F and their antagonists in Figure 4.12.E.) Thus, not absolute rate, but relative rate compared to the antagonistic BO neuron encodes BO property. This allows the

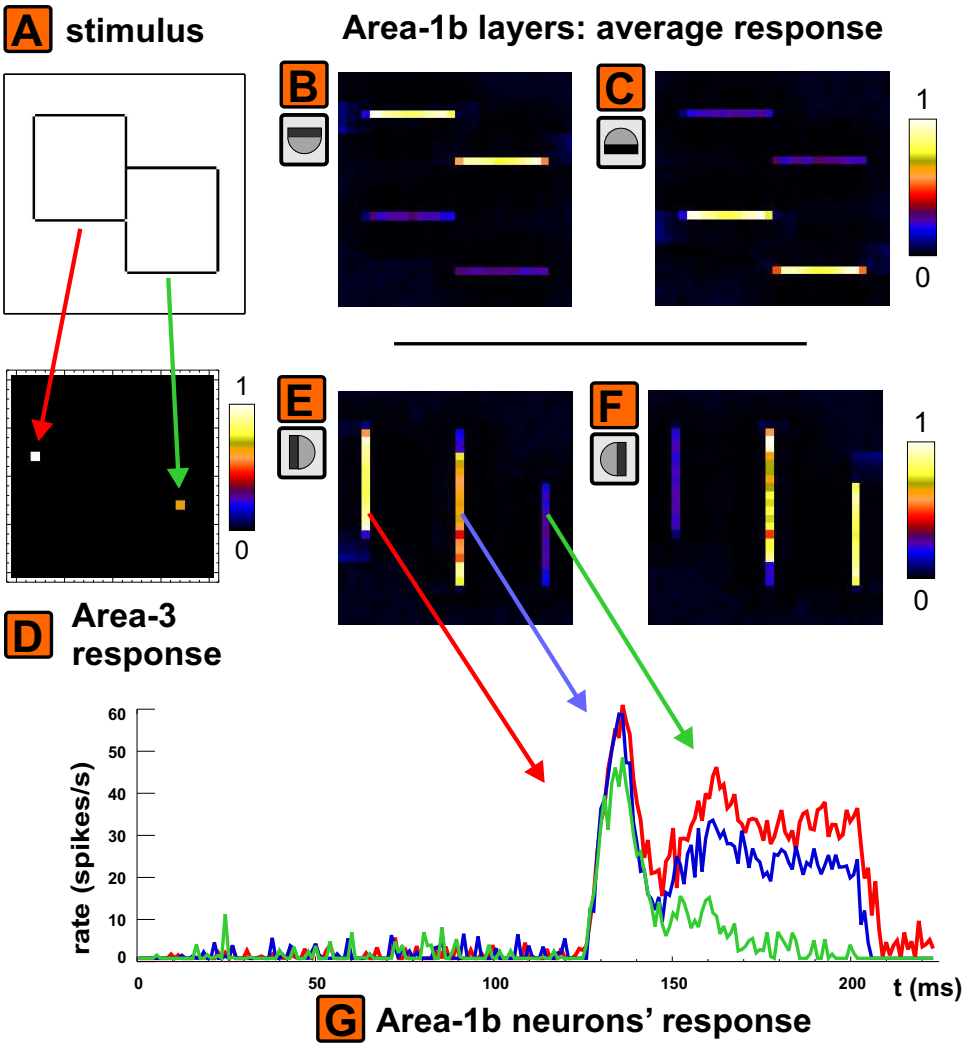

Figure 4.11: Two objects shifted against each other sharing parts of an edge. A: The stimulus. **D:** Area-3 activity evoked by stimulus. Average activity during stimulus presentation normalised to 1. **B/C/E/F:** Area-1b layers being modulated by BO feedback. The average activity is plotted, normalised to the maximum of **B** and **C** resp. the maximum of **E** and **F**. **G:** Sample single unit activity of neurons of the same BO property with cRFs at different edges of stimulus objects.

differences in unambiguity of object detection to be encoded.

4.6.3 Overlapping Stimulus Objects

We presented a stimulus of two overlapping rectangles to the network (Figure 4.13.A). With the stimulus we incidently demonstrate that the curvature detectors respond also to rounded corners. The stimulus evokes activity in four Area-3 neurons (average activity for all layer neurons: Figure 4.13.D; rate over time of active neurons: Figure 4.13.I). Two neurons are only briefly active (*red, green*), hence their average activity is very low (they are marked by circles in Figure 4.13.D). Figure 4.13.G shows where the Area-3 neurons project to in Area-1b. Thus, the Area-3 neuron marked *green* was activated by two corners (the lower left and right corners of the overlapped rectangle) and a T-junction (the lower left intersection of the rectangles). Since the T-junction activates the appropriate curvature detector less than a corner, the *green* neuron exhibits a lower rate than the Area-3 neuron encoding the overlapped object. Because these two neurons encode objects sharing parts of their contour, the neurons inhibit each other. The neuron encoding the overlapped object prevails since its rate is higher (Figure 4.13.I). The same as for the *green* neuron holds true for the neuron circled *red* in Figure 4.13.D. Figure 4.13.H shows the firing rate for a few example neurons (indicated by arrows originating at Figure 4.13.E/F). The BO neuron encoding the bottom right corner of the overlapped object receives for some time feedback from three Area-3 neurons, whereas the bottom left corner of the overlapped object receives slightly less feedback. This manifests in the slightly lower BO neuron rate in the latter region (see Figure 4.13.H blue vs. red firing rate graphs.)

Figure 4.12 *(facing page)*: Network response to two objects sharing an edge, extending to the same side. A: Stimulus containing two objects. **D:** Evoked Area-3 average activity (100-200ms). **H:** Activity of all (2) active Area-3 neurons. **B/C/E/F:** Area-1b average activity (110-220ms). Neurons encoding contours show BO preferences. **G:** Activity trace of Area-1b sample neurons, showing activity on edges encoding the BO preference suiting the stimulus object (*orange, blue, red*) or encoding the opposite BO reference (*green, yellow*). Neurons encoding the smaller object receive less feedback and show a lower rate. But the difference of activity between antagonistic BO neurons is still unambiguous.

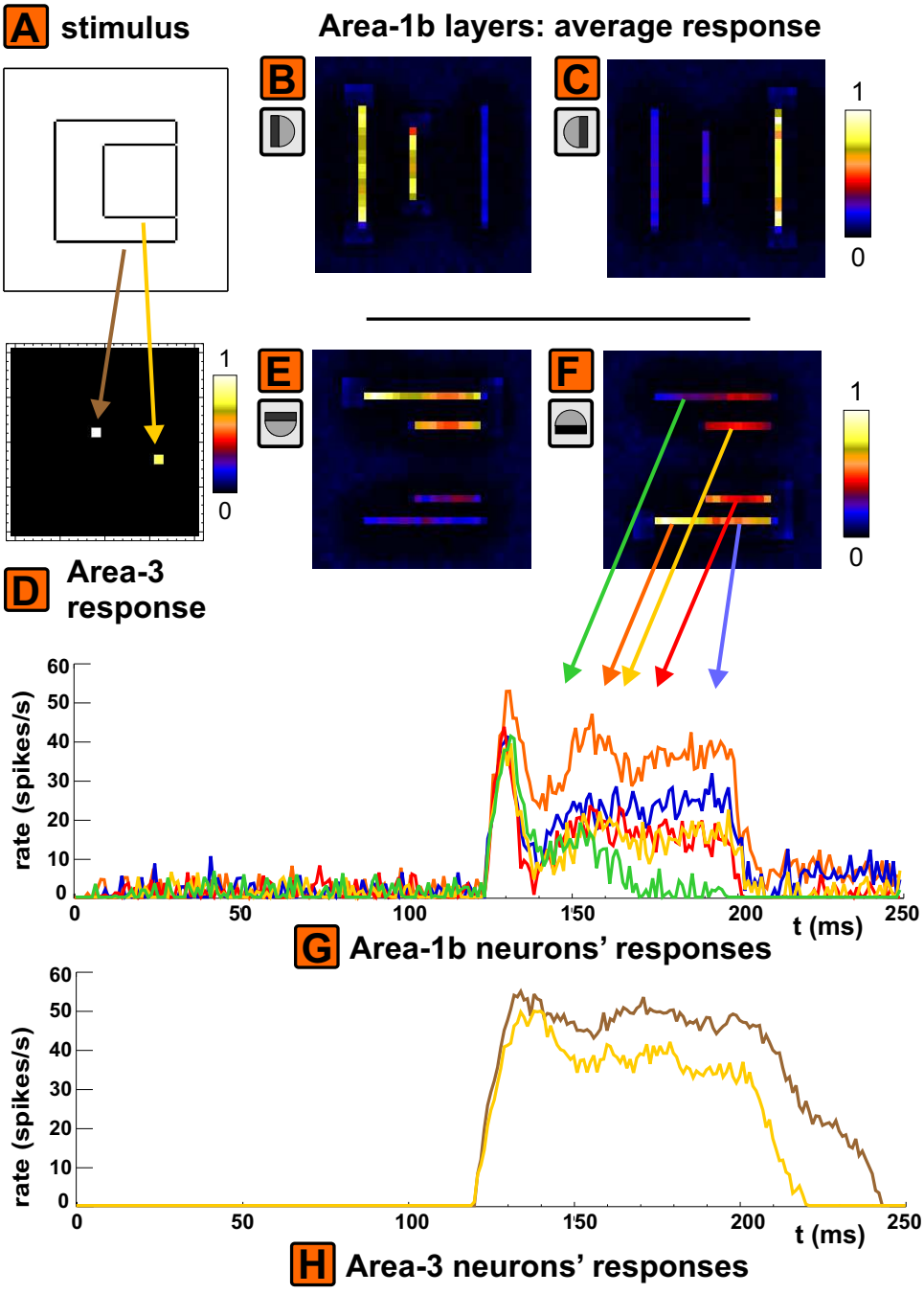
A stimulus
Area-1b layers: average response
B
C
1
0
1
0
E
F
1
0
D Area-3 response
rate (spikes/s)
60
50
40
30
20
10
0
0
50
100
150
200
250
t (ms)
G Area-1b neurons' responses
rate (spikes/s)
60
50
40
30
20
10
0
0
50
100
150
200
250
t (ms)
H Area-3 neurons' responses

Altogether, all contours are assigned with the "correct" BO preference regarding the stimulus objects. Further, the neurons encoding the contour of the overlapping object and the "correct" BO preference show a uniformly high rate. Neurons encoding the contour of the overlapped object and the "correct" BO preference show a slightly more irregular and partially lower firing rate.

4.7 Incomplete Objects and Non-Objects

Area-3 detects complete as well as incomplete objects, as we have shown in the previous example (Figure 4.13), where an incomplete overlapped rectangle elicits a response in Area-3. We investigate the response stimulus objects of varying completeness elicit in Area-3. Further, we document how that effects the emergence of BO properties in Area-1b.

Figure 4.14.B shows that Stimuli *a, b* and *c* (Figure 4.14.A) elicit Area-3 responses which increase with the degree of stimulus object completeness. Stimuli *d* and *e* do not cause any activity in Area-3.

In Figure 4.14.C the average activity (110-220ms) of the layer with

Figure 4.13 *(facing page)*: Overlapping stimulus objects. **A:** Stimulus with rounded corners. **D:** Average Area-3 object detector neuron activity. Two neurons with very low average rate are marked by circles. **G:** Regions in Area-1b where active Area-3 neurons project feedback to (color coding as in D). **I:** Activity of all active Area-3 neurons over time (color coding as in D and G). **B/C/E/F:** Average Area-1b activity for example BO layers. Edges encoded by neurons having the "correct" BO property show far greater average activation than their antagonistic neurons encoding the opposite BO property. Some BO neurons encoding the edges of the overlapped object show lower activity than the neurons encoding the contour of the overlapping object. **H:** Sample single Area-1b neuronal activity for neurons encoding an edge of the overlapping object with the right BO property (*green*), encoding an edge with right BO property of the overlapped object (*orange* and *violet*) and encoding an edge of the overlapped object with the "wrong" BO property (*red* and *blue*). This shows that BO encoding works well in most parts, but that for some parts of the overlapped object the difference between "correct" and "wrong" BO neuron regarding the stimulus is very low (*violet* and *blue*).

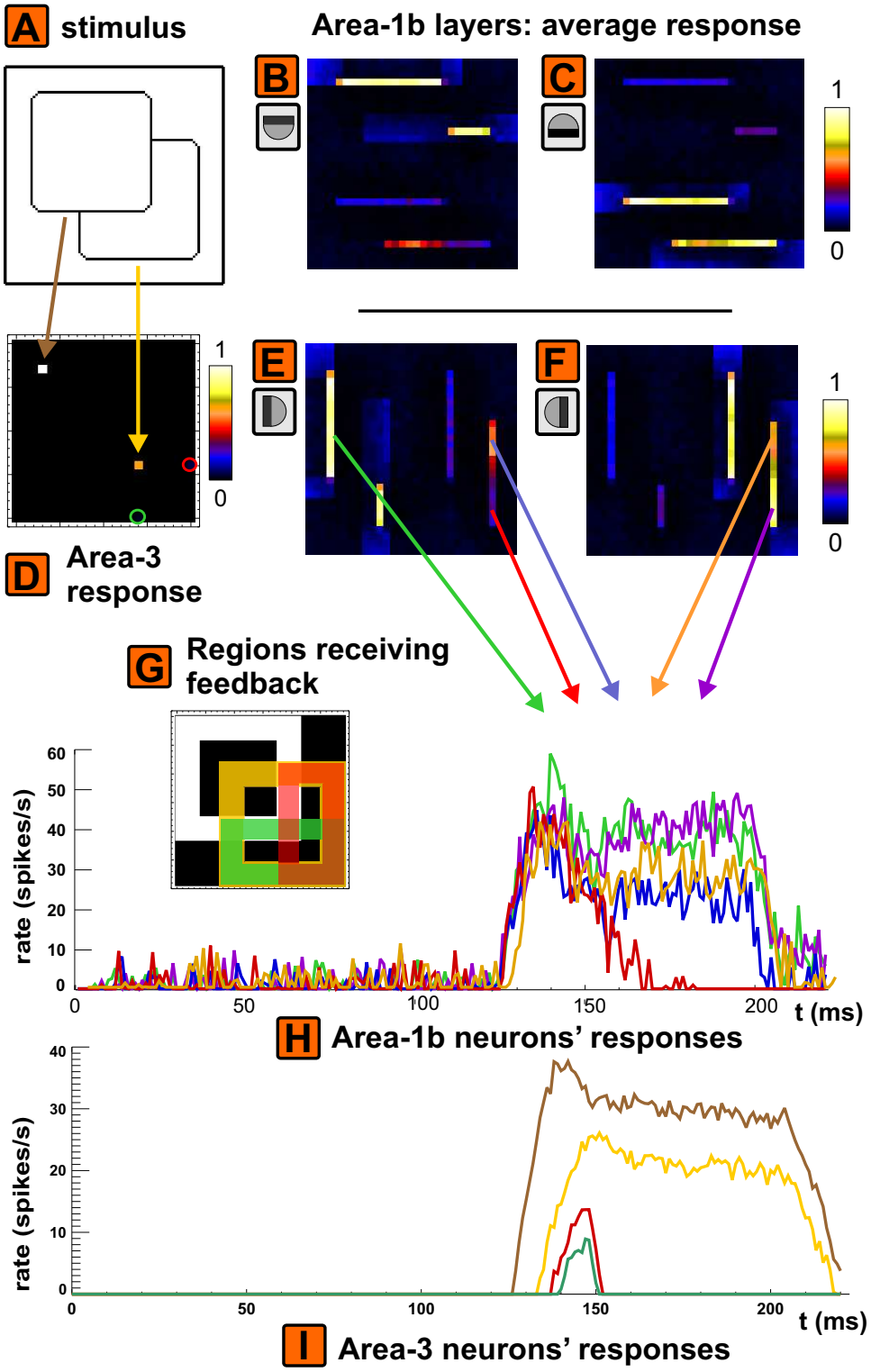
A stimulus
Area-1b layers: average response
B
C
1
0
E
F
1
0
1
0
D Area-3 response
G Regions receiving feedback
rate (spikes/s)
60
50
40
30
20
10
0
0
50
100
150
200
t (ms)
H Area-1b neurons' responses
rate (spikes/s)
40
30
20
10
0
0
50
100
150
200
t (ms)
I Area-3 neurons' responses

horizontal orientation and upward BO preference in Area-1b is plotted for all five stimuli. Figure 4.14.F shows the activity in layers of the opposite BO preference. In Figures 4.14.D/E for every stimulus the activities of two antagonistic BO neurons encoding parts of the stimulus object's contour are plotted. Figure 4.14.D shows the activity of neurons encoding the "correct" BO property regarding the stimulus (except the neurons encoding Stimuli *d* and *e*, since there is no correct/incorrect BO direction, since the stimuli do not contain an object). The non-object stimulus *e* shows the steepest transient response. The neuron encoding the complete stimulus object (Stimulus *a*), shows the highest tonic answer, though the tonic responses only differ slightly. In contrast, the responses of the neurons encoding the "wrong" BO property regarding the stimulus objects (Figure 4.14.E) show very different rates. The neurons encoding the non-objects (Stimulus *d* and *e*) and the most incomplete object (Stiumulus *c*) show a response rate similar to their antagonists', whereas the tonic response of the other neurons decrease with increase of completeness of the stimulus object.

4.8 BO in Neurons Not Receiving Direct Feedback

The presentation of a C-shaped stimulus (Figure 4.15.A) demonstrates a further important property of our model: BO coding in concavities of stimuli.

As can be seen in Figure 4.15.B-E the BO neurons encoding the outer convex part of the C-shape show strong BO preference (e.g. the top edge of the C-shape has a high BO preference downward, see

Figure 4.14 *(facing page)*: Complete and incomplete stimulus objects. A: Stimulus objects of varying completeness and non-objects. **B**: Stimuli A.a/b/c each elicit an Area-3 response plotted here. **C/F:** Average Area-1b activity (110-220ms) for horizontal orientation preference and BO preference upward (**C**) resp. downward (**F**) for all stimuli (*a*-*e*). **D:** Firing rate of sample neurons encoding "correct" (insofar there is an object detected in Area-3) BO property regarding the stimulus object. **E:** Firing rate of sample neurons encoding the "wrong" (if an object is detected in the stimulus) BO property regarding the stimulus object.

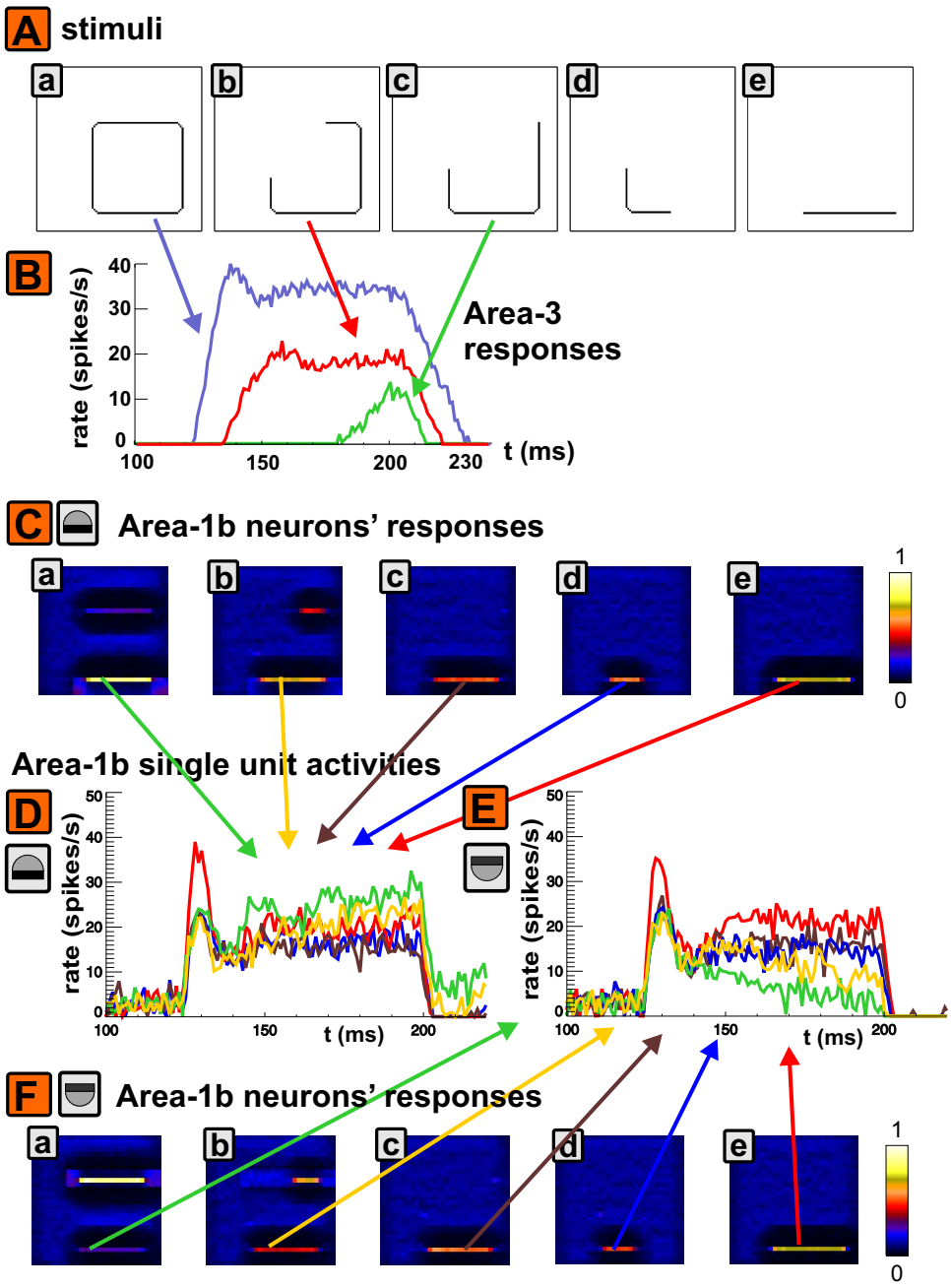
A stimuli
a
b
c
d
e
B
rate (spikes/s)
40
30
20
10
0
100
150
200
230
t (ms)
Area-3
responses
C
Area-1b neurons' responses
a
b
c
d
e
1
0
Area-1b single unit activities
D
E
rate (spikes/s)
50
40
30
20
10
0
100
150
200
t (ms)
F
Area-1b neurons' responses
a
b
c
d
e
1
0

Figure 4.15.B). But also the concave inner part of the C-shape exhibits correct BO properties, i.e. the salient BO preference is directed inside of the C-shaped object. In Figure 4.15.B (BO preference downward) e.g. the neurons encoding the lower edge of the concave part of the C-shape show a higher average response than their antagonists (Figure 4.15.C). Therefore these neurons encode that the object extends downward from this edge. All edges encoding the inner part of the C-shape show the "correct" BO property regarding the stimulus.

BO Coding Without Direct Feedback

The correct BO coding of the entire contour of the C-shape does not trivially follow from the network's architecture. This is, because the inner part of the C-shape does not receive direct BO feedback — unlike the outer convex contour.

Area-3 only detects the presence, position and rough size of a stimulus object, but does not encode information about the specific form of the object. The BO feedback from an Area-3 neuron is constrained to a limited region in which the contour of a blob shaped object is inferred to lie in order to activate this particular Area-3 neuron. Hence, only the outer convex contours of the C-shape receive BO-feedback.

Role of Lateral Linking

The BO preference of neurons encoding the inner concave part emerges due to lateral linking from BO-neurons encoding the outer contour.

An essential element of lateral linking in Area-1b is that linking is restricted to BO neurons with the same or similar BO preferences. Lateral linking is transmitted between neurons whose cRFs are linearly and curvi-linearly arranged (see Figure 3.3). Thus, the "correct" BO property encoded strongly on the outer (convex) contour of the C-shape, propagates along the contour into the concave part.

Ratio Between Feedback and Lateral Linking Strength

A key factor of filling-in along contours into concavities is the ratio of feedback strength to strength of lateral coupling. Our simulations showed that a ratio of about $10 : 1$ of feedback to lateral coupling[III] worked best for lateral transmission of induced feedback. With less feedback lateral coupling dominates along contours receiving feedback over feedback, i.e. the effect of lateral linking is so strong, that feedback does not make a significant difference. In the

[III]The feedback strength was $w_{feedback} = 3 \cdot 10^{-4}$, the strength of lateral linking was $w_l = 10^{-5}$, weighted with a Gaussian profile. If several neurons are active with the same rate encoding a linear stimulus, then lateral linking sums to $w_{l,sum} = 3.18 \cdot 10^{-5}$. If we now assume equal rates in Area-3 and Area-1a, then the ratio is $w_{feedback}/w_{l,sum} \approx 9.43$. If we assume a rate of the magnitude measured in our simulations (50 spikes/s in Area-3 and 40 spikes/s in Area-1b) we get a slightly different ratio of $(w_{feedback}O_{Area-3})/(w_{l,sum}O_{Area-1b} \approx 11.79$. Since both approaches are plausible we just give a rough approximation of the ratio 10:1.

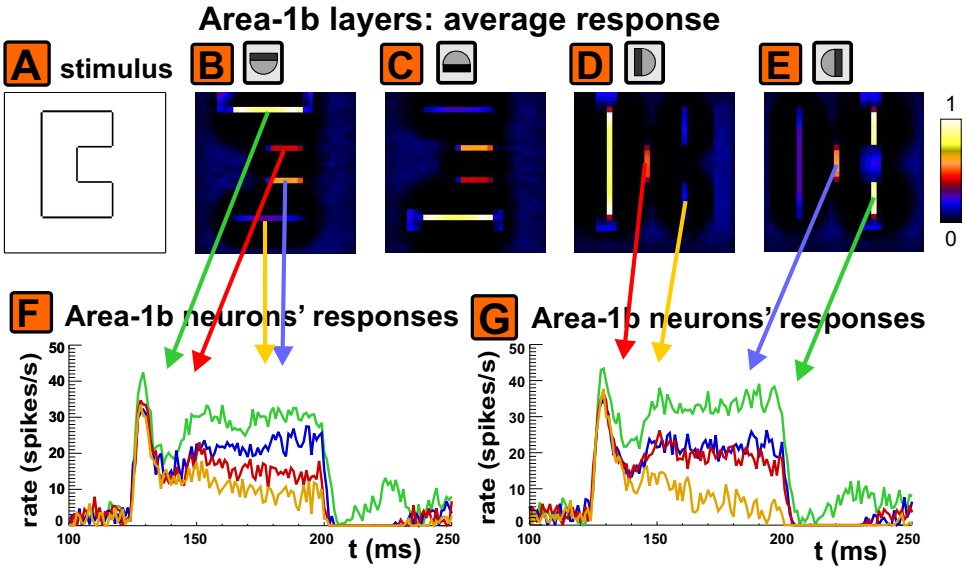

Figure 4.15: BO at concave contours of stimulus objects. **A:** A C-shaped stimulus was presented to the network (100-200ms). The inner part of the C-shape is concave. **B-E:** Averaged response of Area-1b layers encoding different BO properties. The inner part of the C-shape shows BO preferences directed inside the C-shape, i.e. "correct" BO coding with respect to the stimulus object. **F/G:** Firing rate of sample neurons.

other extreme, if feedback dominates over linking, BO coding along contours receiving feedback works fine, but BO properties laterally transmitted along contours e.g. into concavities does not work.

Objects and Ghost Objects (Not) Detected

When the C-shaped stimulus was presented to the network, only one Area-3 neuron became active. The inner part of the C-shape describes two aligned corners of an incomplete rectangle missing one edge. This *ghost* object was not detected in Area-3 for the following reason:

1. The Area-2 neurons encoding the two inner corners of the C-shape modulate each other laterally. But at the same time each of these neurons is also inhibited laterally by the Area-2 neurons encoding the curvatures where the concavity starts on the C-shape contour. The second derivatives of these curvatures have the opposite sign of the inside curvatures, thus the Area-2 neurons encoding these curvatures inhibit each other.

2. Since the *ghost* object and the object detected from the C-shape stimulus share parts of an edge, the Area-3 neurons encoding them inhibit each other. Since the neuron encoding the C-shape is quickly active, it inhibits the other neuron, also keeping it from exceeding the threshold.

Simulations with Lateral Delay Render More Realistic Dynamics

The above simulations were all done without lateral delay. Since the lateral spreading of BO activity does not occur instantly in visual cortex and since the dynamics of the neurons' responses will be significantly different when lateral delay is considered, we included lateral delays in our model. The results of those simulations for a C-shaped stimulus are presented and discussed in Chapter 5.

4.9 Figure-Ground Segregation

Facilitation of the activity of neurons encoding object presence by feedback can strongly support *figure-ground-segregation*. The following results show that with feedback, *figure* and *ground* can be much better distinguished than without. We quantified the consequences of feedback for figure-ground-segregation by analysing the discriminability of neurons coding figure and ground *with* and *without* feedback. As stimulus we used the same rectangle as shown in Figure 4.8. Figure 4.16 shows that feedback makes figure-ground-segregation more robust against noise. The standard deviation σ of the noise

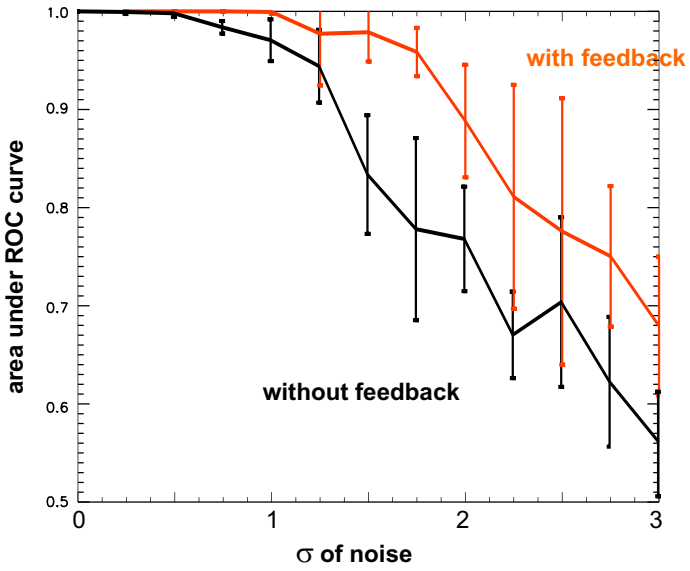

Figure 4.16: Separability of figure and ground. The standard deviation σ of broadband Gaussian amplitude noise added to the membrane potential of the neurons was varied. Discrimination between figure and ground was analysed by applying detection theory (**receiver-operator characteristic, ROC**). Separability of figure vs. background from the activity just before the end of stimulus presentation for 3ms was analysed. The separability works significantly better for areas receiving feedback for lower and medium noise levels. σ was normalised to the average membrane potential around a neuronal maximum of neurons encoding background. The vertical bars indicate the standard deviation of the ROC values.

added to the neurons' membrane potential (see Equation 2.5 in Section 2.2) was systematically varied. Figure 4.16 shows the separability, measured as area under a ROC curve (Green and Swets, 1988), between all neurons encoding the object and the same number of randomly picked background neurons. For every neuron the average activity around its maximum (+/-1ms) is used, since (1) information density is highest in the peak and (2) in rapid processing consecutive layers integrate only over a limited time-window. We normalised σ to the average membrane potential of background neurons during the time-window of integration. The ROC values are averages over about 20 runs for every σ value.

Chapter 5

Model with Delays

Outline

Lateral conduction delays are added to the previous border-ownership model. This allows better comparison with other models. The model with delays predicts later BO property differentiation in concave than in convex parts of a stimulus object's contour.

5.1 Lateral Conduction Delays

Types of Indirect Delay

So far conduction delays between neurons connected to each other were only implicit in our model. There are several sources for indirect delays:

- discrete time steps due to our numeric approach (1 time step = 1 ms), thus at least 1ms delay
- delays due to neuron properties (e.g. membrane time constants, firing threshold)
- delays due to indirect activation via interneurons

Delays for Comparison

Since in other BO models (see Chapters 1.1.2 and 8.3) lateral conduction delays play a crucial role we added delays to our simulation framework for comparison. Since the conduction of activity along inter-areal connections is very rapid (Girard et al., 2001) we introduced delays for lateral intra-areal connections only.

Neurologic Determination of Lateral Delay

We assume that our visual input space covered a visual angle of $20°$. Hence 90 pixels of the stimulus, i.e. a distance of 30 Area-1 neurons, correspond to $20°$ visual angle. The visual field used by Zhou

et al. (2000) was of the same size. For simplicity, we assume a uniform lateralaxonal conduction velocity independent of eccentricity. Further, we use the cortical magnification factor at 3° eccentricity[I] of $2.3mm/^\circ$ (Virsu and Hari, 1996; Adams and Horton, 2003, the latter in monkey). Lateral velocity in cortex is known to be in the range of $.1 - .2m/s$ which is equal to $.1 - .2mm/ms$ (Slovin et al. (2002) in monkey; see Nowak and Bullier (1997) for review). For the following computations we used the medium of this range of $v = .15\ m/s$:

$$v = .15\frac{mm}{ms}\left(2.3\frac{mm}{^\circ}\right)^{-1} \approx .0652\frac{^\circ}{ms} \mathrel{\widehat{=}} .098\frac{neurons}{ms} \quad (5.1)$$

$$\Rightarrow \quad v^{-1} = \sim 10\frac{ms}{neuron} \quad (5.2)$$

Thus, the time for one AP to propagate from one neuron to an adjacent neuron takes approximately 10 ms from one neuron to the next.

5.2 Delays in the Model

In our model feed-forward activation reached Area-3 about 20ms after stimulus onset (see Figure 4.3). These delays are due to the neuron and network properties.

Lateral Inhibition without Delay

Lateral divisive inhibition (Gaussian weighted, HWFM 4 neurons far, reaching a maximum of 6 neurons far) was implemented without conduction delay. Due to the Gaussian-weighted coupling strength a slight delay comes about indirectly, since weak inhibition has to be integrated longer to take the same effect.

Lateral Linking with Delay

The lateral conduction velocities were implemented as computed in the previous section. As in our previous simulations linking had spatially a Gaussian profile. Neighboring neurons received the linking input with a delay of 10ms, neurons in a distance of 2 neurons range with 20ms and so forth. For implementational reasons (handling of queues) lateral linking reached only up to 3 neurons far. In order to keep the total lateral linking strength at the same value as in the simulations without delays with lateral linking reaching a maximum of 5 neurons far, we normalized the total synaptic weight of the modulatory linking kernel to the same value as in Chapter 4.

[I] i.e. 3° visual angle away from the fovea

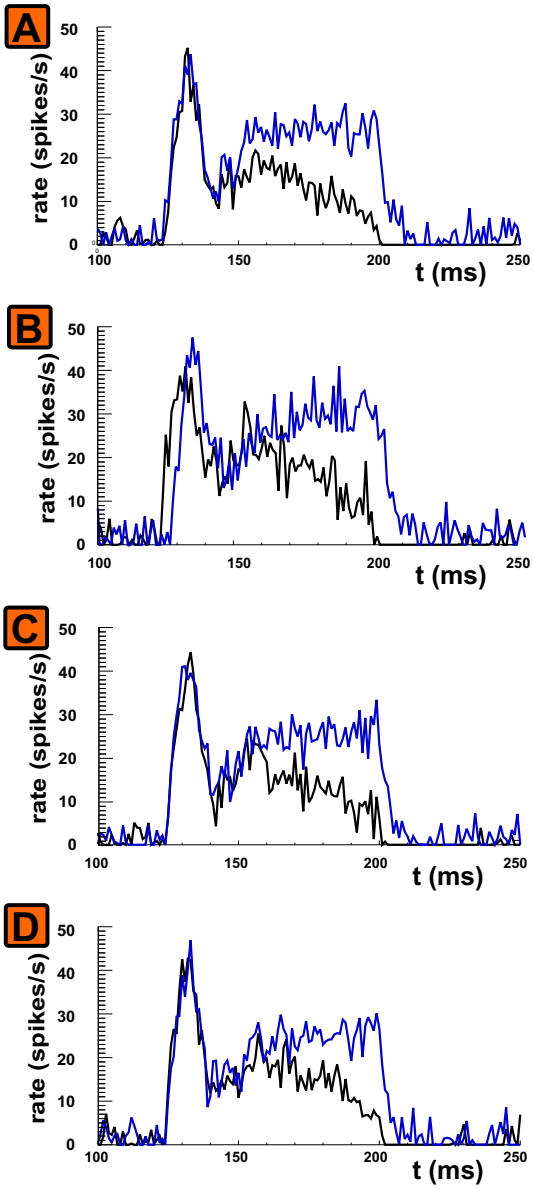

Figure 5.1: Firing rate of antagonistic BO neuron pairs encoding the concave contour of C-shape. For 4 positions of the horizontal part of the concave contour of a C-shape the activity of antagonistic BO pairs is plotted. The position where the firing rate start to significantly diverge is approximately the point in time when the laterally transmitted BO preference information reaches these neurons. The neurons in **A** are positioned closest to the convex contour, **D** is next to the inner corner, **B** and **C** are located A and D.

5.3 Results

As stimulus we used the same C-shape as in the simulations without delays (Figure 4.15).

In Figure 5.1 the spreading of BO activity into the concavity of the C-shape is plotted. We plotted the rate over time for antagonistic BO neurons encoding the concave contour. As can be seen, for neurons located closer to the convex part of the C-shape the rate of the antagonistic BO neurons begins to differ earlier than for neurons encoding the more inner parts of the concavity.

Prediction of Model with Delays

Thus, we predict, that in recordings of neurons encoding the contour of an object, the BO effect can be discerned earlier in neurons concoding convex parts of the contour than in neurons encoding concave parts.

Chapter 6

Closed Feedback Loop

Outline

We investigate the effect of adding feedback connections from Area-3 to Area-1a on the model's performance. We show that with this closed loop, fi gure-ground segregation in Area-1a is improved.

6.1 Feedback to Area-1a

So far we have shown how feedback from higher Area-3 of our model can induce border-ownership properties in lower Area-1b and how feedback at the same time improves the signal-to-noise ratio.

Closed Loop

Here we investigate feedback from Area-3 to Area-1a. Through projecting back to Area-1a a loop is closed, i.e. feedback modulates an area from which itself receives input. This is an interesting property, since during the presentation of a stimulus object detection can be continuously refined in all areas of the loop. Closed loops are used in a number of models (e.g. Grossberg, 1994; Neumann and Sepp, 1999; Siegel et al., 2000; Corchs and Deco, 2002).

Modulation of Tonic Response Only

Unlike the feedback to Area-1b, the onset of the feedback modulation is too late to have an effect on the transient answer. But closed loop feedback can positively modulate the tonic activity of a lower area neuron. Through lateral inhibition, in turn, local contrast is improved.

6.2 Modifications to the Model

Feedback Architecture

The feedback connections to Area-1a were constructed nearly iden-

Neuron	excitatory	inhibitory
transfer function slope m	2	2
threshold $\theta/\frac{spikes}{s}$	6 (A1) 2 (A2) 10 (A3)	30 (A1) 0 (A2,A3)
τ_e/ms (excitatory)	5 (A1) 30 (A2,A3)	23 (A1) 7 (A2,A3)
τ_l/ms (linking/facilitatory)	150 (A1) 50 (A2,A3)	10 (A1) 50 (A2,A3)
τ_1/ms (subtractive inhibitory short)	5	-
τ_2/ms (subtractive inhibitory long)	17	-
τ_3/ms (divisive inhibition)	100	-
σ	2.0 (A1) .5 (A2,A3)	.5

Table 6.1: Closed loop model parameters. The slopes, thresholds and time constants of neurons in all areas (A1, A2, A3) are listed. A dash indicates that the neuron does not receive any activation through that synapse type.

tical to the feedback connections to Area-1b. The only difference was that feedback was not BO preference direction specific. I.e. feedback from an Area-3 neuron to the Area-1a layer with neurons encoding vertical orientation preference is projected to the neurons (potentially) encoding the upper *and* the lower contour.

New Parameters Allow Continuous States

We adjusted the network parameters so that Area-1a and Area-2 neurons showed two basic modes of activation beyond the transient response: (1) high and (2) low tonic response. The parameters are detailed in Table 6.1. Unlike in the previous model we used a linear threshold function in Area-2 instead of a saturation function. When the saturation function is used Area-2 neurons are basically in one of two states. Either they are hardly active at all or their rate is close to saturation. This performance is not appropriate for the closed feedback loop, since once one of the two states is adapted, a change of state is very unlikely. In a closed loop, on the other hand, change of states should be possible after the transient response.

Figure 6.1 *(facing page)*: Closed loop feedback with example stimulus. A: The stimulus contained an object and a non-object. **E/F:** Average response of Area-1a layers (100-200ms). **B:** Firing rate over time of two neurons, one encoding a part of the contour of the stimulus object, the other encoding the contour of the non-object. **G/C:** Two Area-2 neurons are activated by the curvature indicated at the top of **G** – one far more than the other, though the patterns they are activated by are very similar. **H/D:** In Area-3 only on neuron fires with a rate significantly above 0 spikes/s.

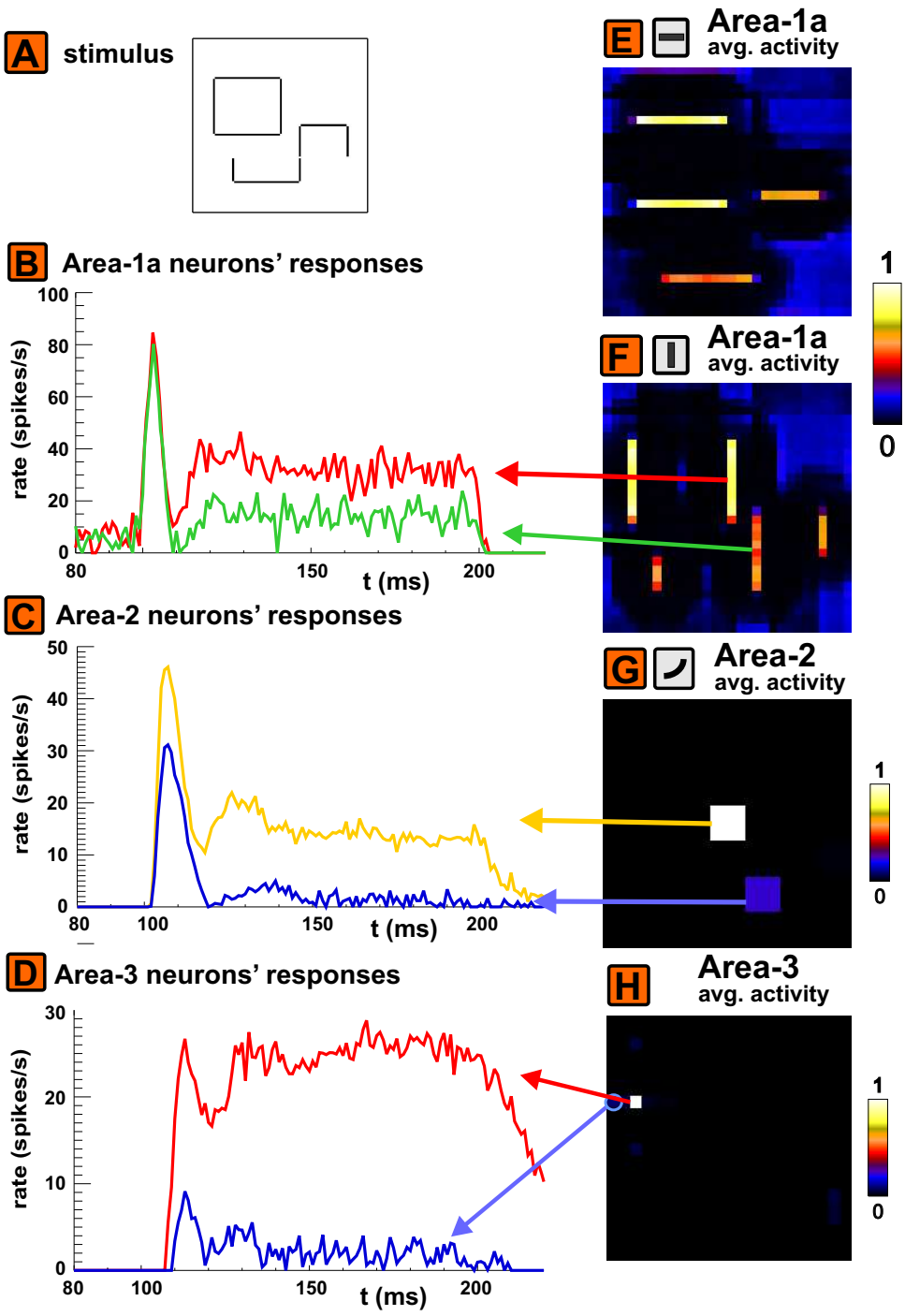
A stimulus
B Area-1a neurons' responses
rate (spikes/s)
t (ms)
C Area-2 neurons' responses
rate (spikes/s)
t (ms)
D Area-3 neurons' responses
rate (spikes/s)
t (ms)
E Area-1a avg. activity
F Area-1a avg. activity
G Area-2 avg. activity
H Area-3 avg. activity
1
0

6.3 Results

Area-1

The network's response to an exemplary stimulus is shown in Figure 6.1. We included a rectangle as stimulus object and a curvy contour as non-object into the stimulus (Figure 6.1.A). Figure 6.1.B shows the development of firing rate over time for an Area-1a neuron encoding parts of the contour of the rectangle and the firing rate of a neuron encoding parts of the non-object. Figure 6.1.E/F show the average rate (100-200ms) of the Area-1a layer with orientation preference horizontal (E) resp. vertical (F). The activity over time of the neurons marked in Figure 6.1.F is plotted in Figure 6.1B. The Area-1a neuron encoding the object shows a significantly higher tonic response than the neuron encoding a part of the non-object.

Area-2

The two neurons active in Area-2 encode simliar curvatures (Figure 6.1.G). One neuron shows a far greater tonic activity (Figure 6.1.C) because it encodes a part of an object's contour.

Area-3

In Area-3 (average rate see Figure 6.1.H) one neuron shows a high firing rate (Figure 6.1.D), whereas a few other neurons detecting ghost objects (Chapter 3.5) of the stimulus object and non-object show a very low firing rate (Figure 6.1.D).

Contours of Objects Show High Rate in Area-1a

As a result Area-1a neurons encoding the contour of the stimulus object show a continuously higher firing rate during the tonic response than neurons encoding contours not being part of objects (Figure 6.1.B).

6.4 Discussion of Closed Feedback Loop

Activity in All Layers Affected by Object Detection

The exemplary simulation shows that feedback perpetuates high tonic Area-1a activity. As a result not only do neurons coding objects show a higher rate in the lowest area of the network, but also in intermediate (Area-2) and highest (Area-3) areas neurons encoding features of the stimulus object or the entire stimulus object show higher rates compared to neurons not encoding the stimulus object. This difference is greater than in the simulations with the network that had no closed feedback loop (e.g., see Chapter 4.2).

Closed Loop Improves Segregation

To conclude, a closed feedback loop is a good mechanism to further improve segregation between neurons encoding stimulus objects and neurons encoding the rest. In our model the closed loop can support BO coding, since object coding in Area-3 is improved.

Chapter 7

Learning Feedback

Outline

Support for the connection architecture of our model is provided by showing that feedback connections can be learned with a biologically plausible learning rule. We used a Hebbian learning rule. We show the main principles necessary for learning feedback modulation in a simple network. Finally, we demonstrate, that our network model learns connections which are similar to the hand wired connections which we used in previous chapters.

7.1 Why Learn What?

Aim: Support for the Model Through Learning

So far, the architecture of our model was based on knowledge of anatomy, physiology and inferences from Gestalt laws and psychophysics. This engineering-type approach is an accepted and often used method in computational neuroscience (e.g. Grossberg et al., 1995; Riesenhuber and Poggio, 1999; Neumann and Sepp, 1999). The aim of this section is to show that core aspects of our model (Figure 3.1) are confirmed by learning.

Epistemology

Developing neural network models of parts of the cortex is part of an iterative process of experimenting, modelling, making predictions, experimenting and refining the models. Through this process our understanding of the brain advances.

The central epistemological question in computational neuroscience is how to ensure that a model captures essential elements of a cortical process (Amit, 1989). Core strategies commonly used are:

- Basic building blocks are used, in our case the model neurons and their types of interactions (Chapter 2). These building

blocks are chosen to show emergent behaviour on the network level that is qualitatively similar to cortical activity on the network level.

- Models designed from the building blocks try to reproduce known experimental data (Chapter 4) and make predictions for future experiments (Chapter 8).

- Unsupervised, biologically motivated learning of a model's connectivity is aimed to reproduce essential connection features of a preliminary designed ("hand wired") model (this chapter).

In learning the strength of synapses is de- or increased according to pre- and postsynaptic activation. Hebbian learning (Hebb, 1949) is the most basic and common learning rule. There are many variations to this rule, e.g. trace learning (Földiak, 1991) used for learning invariances. For reasons detailed below we use classical Hebbian learning.

Limits to Learning

Learning in a biologically plausible neural network should be subject to neurologic constraints. As it is implausible to assume that the visual system is fully developed at birth, it is neither reasonable to propose that everything has to (and can) be learned from scratch. The visual cortex is pre-structured genetically to a significant degree, so that certain specifications of the network to be learned can be assumed. Further, learning connections to and in higher cortical areas before lower areas develop their specificities, cannot render any meaningful results.

Focus on Feedback

For that reason and due to computational constraints we had to focus learning on a part of the model. We focused on the model's modulatory feedback connections, for several reasons:

- Feed-forward paths similar to ours have been learned by others (e.g. Deco and Rolls, 2004; Kayser et al., 2001; Rolls and Milward, 2000)

- Lateral connections have been learned before (e.g. Prodöhl et al., 2003; Mel and Fiser, 2000; Spratling, 1999)

- In contrast, there is no model explaining border-ownership by feedback, let alone a model where this has been learned.

- In general, there are only few models explaining how feedback connections can be learned.

Goal

We show that through Hebbian learning information about the probability of object presence, its position and size can be learned to positively modulate those neurons that encode the detected object in lower visual areas.

We first introduce the learning rule used by us, then demonstrate the mechanisms involved in learning feedback connections in a simple model and finally integrate learning in our comprehensive model.

7.2 Learning Rule

Hebbian Learning

For learning modulatory feedback we used the most common learning principle, Hebbian learning (Hebb, 1949). Hebb's learning rule states that the connection strength between neuron A and neuron B is to be increased, if neuron A fires an action potential within a certain small time window before neuron B fires. The reasoning behind it is, that if the described scenario occurs above chance level, the information encoded by the two neurons is correlated. Hence, neuron A, firing earlier, can support neuron B in eliciting an action potential. The influence of neuron A on neuron B can be increased for this purpose by increasing the synaptic strength of the connection from neuron A to neuron B. The plasticity of weights thus depends on the current rate of presynaptic (O_i) and postsynaptic (O_j) neuron and on the current weight w_{ij} (Gerstner and Kistler, 2002):

$$\frac{d}{dt}w_{ij} = F(O_i,O_j,w_{ij}) \tag{7.1}$$

There is physiological evidence for Hebbian learning, e.g. Bi and Poo (1998). We used the following implementation of the Hebbian learning rule. Every time step weights are changed according to:

$$\frac{d}{dt}w_{ij} = \alpha(w_{max} - w_{ij})O_iO_j \tag{7.2}$$

with learning rate α, maximum weight w_{max} (upper bound), activity of presynaptic neuron O_j, activity of postsynaptic neuron O_i, and current weight w_{ij} (Gerstner and Kistler, 2002). Since the weights are confined by w_{max} and normalisation (see next paragraph) avoids all weight eventually reaching w_{max}, the decay factor γ continiously decreasing the weights contained in the original formula by Gerstner and Kistler (2002) was not needed and thus removed[I].

[I] corresponds to setting it to 0, since γw_{ij} was a summand

Normalisation

The sum of all connections converging on the same neuron are normalised. Thus, the total synaptic weight of every target neuron is kept constant. This can be physiologically motivated by a limited capacity of the dendritic tree of the postsynaptic neuron. Royer and Pare (2003) found conservation of total synaptic strength by synaptic depression compensating potentiation. Normalisation is computed by:

$$w_i = w_{max} \frac{w_i}{\sum_j w_{ij}} \tag{7.3}$$

Through the upper bound w_{max} (in equation 7.2) for learning, weights are avoided to increase indefinitely. Further, weights are avoided to eventually all reach w_{max} by normalisation. Through normalisation synaptic competition is introduced leading to selectivity of neurons. By lateral inhibition in the network neurons are decorrelated. Thus, neurons become selective for different stimuli.

7.3 Learning Feedback: Simple Model

We discuss the prerequisites for and mechanisms involved in learning modulatory feedback connections on the basis of a simplified model. The feedback connections provide lower layers with border-ownership information. The central question is: How do neurons, although they receive identical input, develop opposing BO preferences?

Prerequisites

For orientation contrast selective neurons to develop BO preference, there have to be at least two neurons with identical cRFs, in order to learn opposite BO preferences. The neurons of every antagonistic pair have to mutually inhibit each other. Further, to potentially learn any feedback connection, all object detector neurons (source neurons) are connected to all BO neurons (target neurons).

Architecture of a Simplified Model and its Stimuli

In the simplified model we reduced the object detection area (Area-3) to two neurons, each representing another object detected. The BO encoding area (Area 1b) was also reduced to two neurons mutually inhibiting each other (Figure 7.1). Alternating, two stimuli were presented for t=100ms with a pause in between of t=100ms[II]. Each stimulus activated a different neuron in the object detection layer, whereas both BO layer neurons were activated by both stimuli (see Figure 7.1). The BO neurons can be thought to encode a contour,

[II] A random presentation of stimuli would have rendered the same results. It would have possibly taken longer, though.

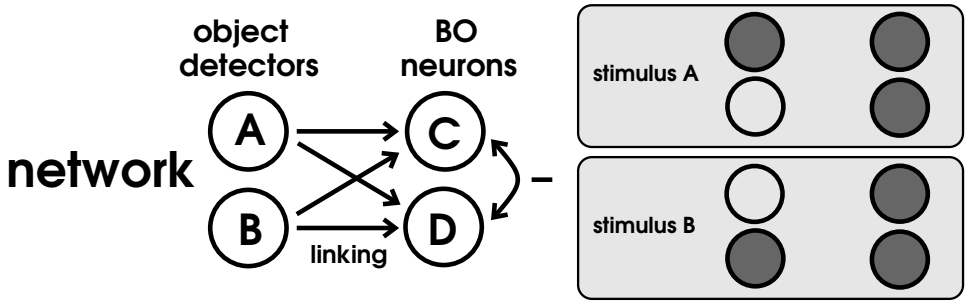

Figure 7.1: Simple model demonstrating aspects of learning feedback. A,B: Source neurons, analogue to Area-3 object detector neurons. **C,D:** Neurons analogous to two Area-1b BO neurons with identical cRFs. The neurons mutually inhibit each other. **Stimulus A/B:** Two stimuli are presented to the network. Both stimuli activate neurons C and D (both BO neurons), whereas each stimulus activates another object detector neuron, either A or B.

which is equally activated by two different stimuli, each stretching to a different side from the contour.

Initialisation and Delays

All weights were initialised with the same value ($w_{i,j}$=.009). The learning rate was set to $\alpha = 10^{-6}$. The offset of the input between the layers was 8ms with the object detector layer stimulated first.

Leaning was done with high BO inhibition (w_{ij}=.3) letting the two neurons behave in a winner-take-all (WTA) manner. Thus, in the beginning (Figure 7.3.A/B) it is chance which neuron wins.

Target Neurons Specialise on One Stimulus Each

After 50s (50,000 network iterations) the network reached a stable state. Each BO neuron learned to respond preferably to a different stimulus. In Figure 7.2 the change of weights over time during learning is shown. The connection from the object detector neuron encoding one stimulus to the BO neuron it learns to prefer increases during learning. Due to normalisation the connection from the other object detector neuron to this BO neuron is decreased by the same amount as the weight from the first neuron is increased. In Figure 7.3 the responses of BO neurons before and after learning are shown. Before learning it is random which target neuron wins (Figure 7.3.A/B). Though always one neuron prevails, occasionally the loosing neuron shows a slight tonic activation. After learning target neurons respond to the preferred stimulus with a higher maximum transient firing rate than before learning (Figure 7.3.C/D). Also, there is only a slight transient response and no tonic response at all by the target neuron when the non-preferred stimulus is presented.

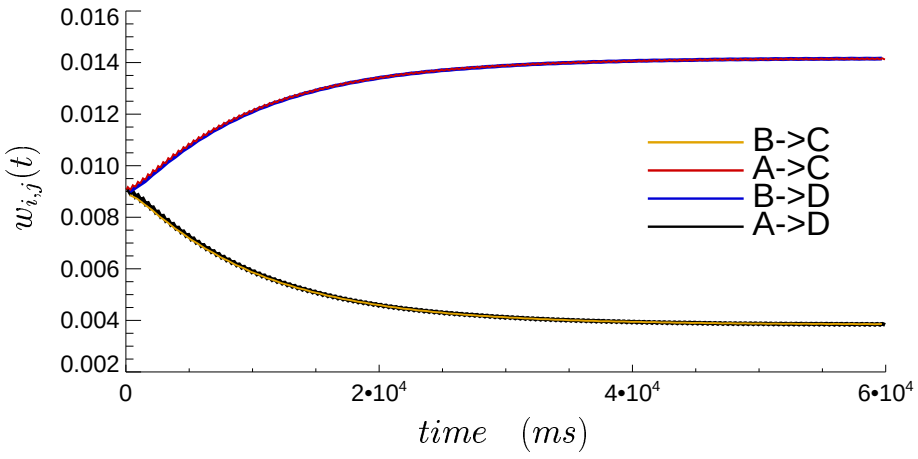

Figure 7.2: Dynamics of learning BO properties in a simplified model. The changes of all four weights during learning is plotted. The dynamics were averaged over 30 simulations. The network converges to the steady state after about 50s (50,000 simulation time steps). Object detector neuron A (see Figure 7.1) provides mainly BO neuron C with "feedback" and neuron B does so to neuron D.

Therefore, our extremely simplified model shows how neurons receiving identical input develop opposing BO preferences. In the following section we show how feedback connections are learned in the big network.

7.4 Learning Feedback: Complex Model

With the simple model we showed how antagonistic neurons can be learned. Here, we present the results from our simulations in the big network. The simple model showed how antagonistic BO neurons specialise on different stimuli. An important question to investigate in the big model is how different Area-3 neurons encoding objects that share a contour learn to project to the same BO neuron encoding the contour and not on antagonistic BO neurons encoding opposing BO preferences. We designed our stimuli according to this question.

Stimuli

We presented 4 stimuli, each with a different rectangle, all sharing one edge. Two of them extended to one side from the shared edge, the other two stimuli to the other side (Figure 7.4.A).

Learning Parameters

The stimuli were presented alternately for 100 ms with a pause

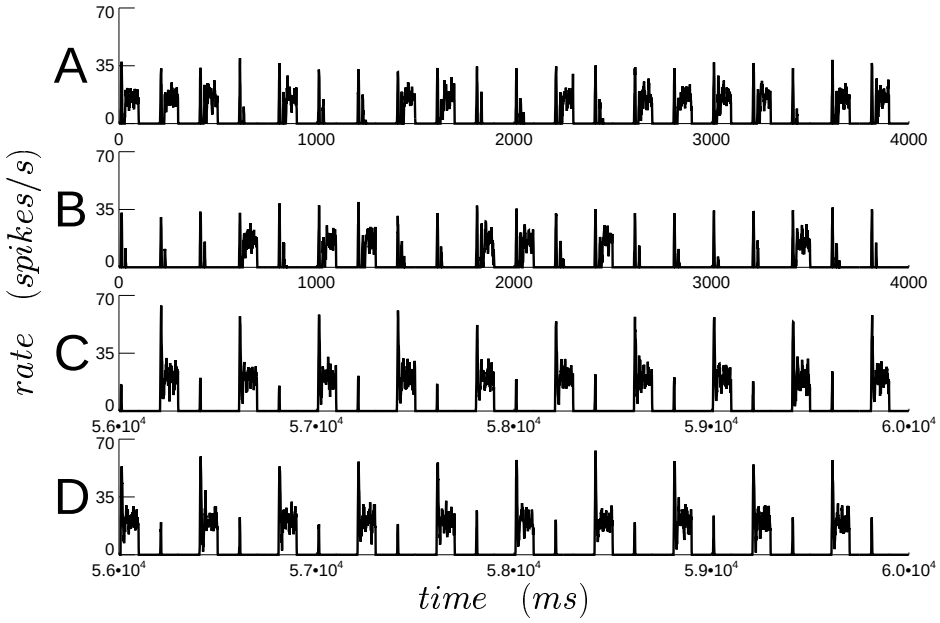

Figure 7.3: Neurons response before and after learning. The presentation of the two stimuli alternated. **A:** The response of target neuron C (see Figure 7.1) before learning plotted for 20 stimulus presentations. **B:** The response of target neuron D before learning. **C:** The response of target neuron C after learning in the converged network. The neuron responds pronounced to every other stimulus. The neuron shows only a brief low transient response to the non-preferred stimulus. **D:** The response of target neuron D after learning. It has learned to respond to the other stimulus.

between stimulus presentations of 200 ms. Between presentations of different stimuli a pause is necessary because the negative membrane potential has to relaxate to assure equal opportunity for learning. The learning was $\alpha = .5 \cdot 10^{-6}$ and the upper bound of summed weight converging on a BO neuron was $w_{max} = .001$. The weights were initialised to 0.

Results

In Figure 7.4 the development of weights during learning for some exemplary connections and the final learned weight matrices is shown.

The network was stimulated repeatedly with the 4 stimuli shown in Figure 7.4.A. Figure 7.4.B shows that weights of connections from two Area-3 neurons encoding objects extending to the same side from the shared contour to the same Area-1b neuron either increase conjointly (*red* and *orange*) or decrease conjointly (*light green* and *dark green*). Thus the weights from different Area-3 neurons to the same Area-1b neuron are either all high or all low when the Area-1b neuron encodes a part of a contour shared by the objects encoded by the two Area-3 neurons *and* if these objects extend to the same side.

Figure 7.4.C.a shows the weights at the end of the simulation of 100,000 time steps (100s). At that time not all weights have reached a stable state. These are the weights between the Area-3 neurons activated by Stimulus **a** (Figure 7.4.A.a) and one Area-1b layer. Figure 7.4.C.b/c/d show the same for the other 3 stimuli and the same Area-1b layer. In Figure 7.4.C.a/b the connections to the same neurons encoding the shared contour show similar weights, either high

Figure 7.4 *(facing page)*: Learning of feedback connections in big network. A: We presented repeatedly these 4 stimuli to the network. All 4 stimuli share one edge. Two extend from this shared edge leftwards, two rightwards. **B:** The development of weights over time for 4 weights converging on the same Area-1b neuron from the 4 Area-3 neurons which each encode one of the stimuli objects. **C:** Four weight matrices, one from each Area-3 neuron encoding one of the stimuli to an entire Area-1b layer with preference for vertical oriented stimuli. **D:** Four weights matrices connecting from the same 4 Area-3 neurons to the Area-1b layer holding the potentially antagonisitc neurons of the layer shown in **C**. Weights between Area-3 and Area-1b neurons encoding the same stimulus object are learned. If the weight from one Area-3 neuron to one Area-1b neuron is high then the weight from the same Area-3 neuron to the Area-1b neuron's antagonist is low (C/D).

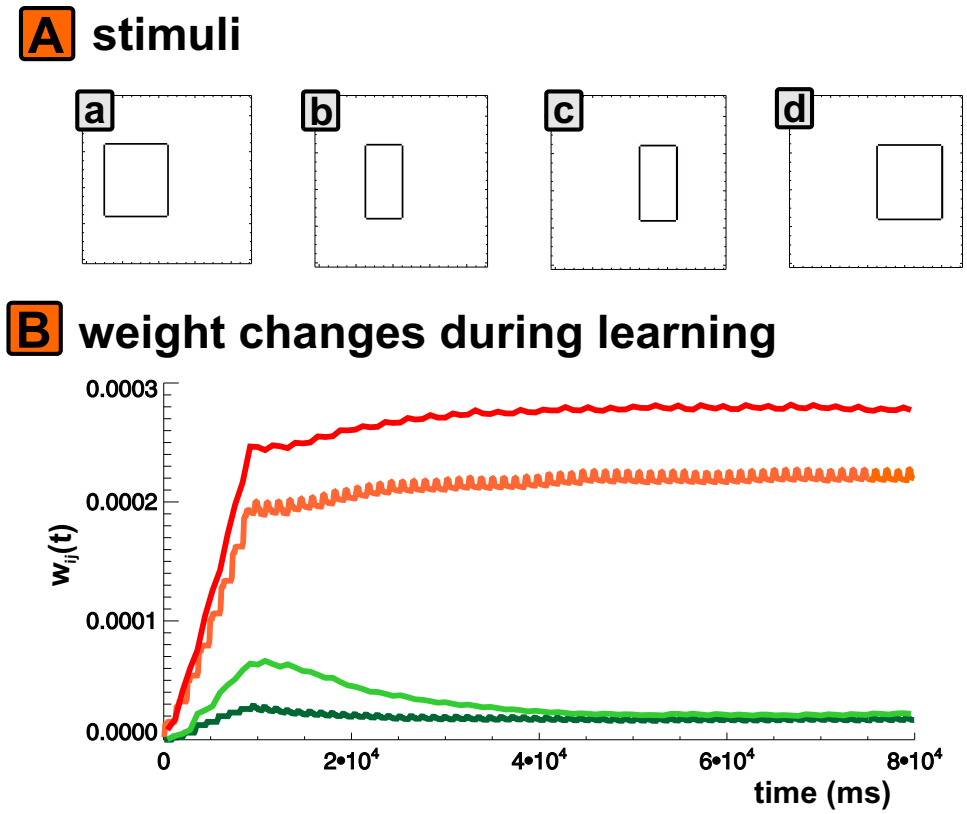
A stimuli
a
b
c
d
B weight changes during learning
0.0003
0.0002
0.0001
0.0000
$w_{ij}(t)$
0
$2 \cdot 10^4$
$4 \cdot 10^4$
$6 \cdot 10^4$
$8 \cdot 10^4$
time (ms)
weight matrices:
C
a
b
c
d
D
a
b
c
d

or low (red circles). Figure 7.4.D.a/b weights induce the opposite BO preference (yellow circles). The same holds true for Figure 7.4.C.c/d (green circles). This shows that not only the exemplary connections (Figure 7.4.B) developed a coherent BO preference but that this is the case for most connections.

Learning did not result in all neurons of one layer to encode the same BO preference. For BO properties to develop we initialised two layers of identical neurons inhibiting each other. Unlike in our hand-wired model, the two preferences are not assigned to the layers. From this we conclude that the lateral modulation in these layers was not strong enough to force neighbouring neurons to encode the same BO preference. That would have rendered patches of neurons in each layer encoding the same BO preference. Since our model is very abstract, we cannot derive from this that first BO feedback and then lateral connections are learned during the development of the brain.

Explanation for Learning Results

These results bring up an interesting question: Why did different Area-3 neurons learn to connect correctly to the same Area-1b neuron?

It turns out that one important property of Area-3 is that when a stimulus is presented not only the Area-3 neuron best encoding the stimulus is activated, but there are co-activation of Area-3 neurons encoding similar objects (*ghost* activation). This plays an important role in learning, since the ghost objects extend to the same side from a contour shared with the stimulus object. Thus when feedback is learned from the "correct" Area-3 neuron to an Area-1b neuron that prevailed in the competition against its antagonist, then also connections from Area-3 neurons encoding the ghost objects to this Area-1b neuron are learned a little bit. If later a stimulus object is presented that activates one of the ghost neurons, then already having slightly learned the connections to the Area-1b neuron mentioned above, this Area-1b neuron receiving slightly more feedback than its antagonist is likely to prevail against its antagonist. As a result the connection between this Area-1b neuron and the Area-3 neuron is learned again.

Due to this mechanism every Area-3 neuron activated and its ghost neurons will learn feedback to the same Area-1b neurons. Thus, these Area-1b neurons will encode the same BO preference for all stimuli presented. This mechanism has to be confirmed by more intense simulations with sets of more than 4 stimuli.

In our simulation we used a relatively high learning rate. Thus, there are high fluctuations in the weights with every stimulus presentation. Since it is not plausible that one stimulus presentation causes such a great difference in connection strength, future simulations should be performed with lower learning rate. The results of

our simulations are nonetheless valid, since the fluctuations do not keep the weights we plotted (Figure 7.4.B) from reaching a stable state.

Summary

We have shown that our hand-made feedback connections can be confirmed by learning these connections with a biologically plausible learning rule.

Chapter 8

Discussion

Outline

Our model reproduces basic properties of object-presence coding in the dorsal visual pathway. We demonstrate how feedback from a higher level visual area can specifically facilitate the activity of neurons at lower stages of the processing hierarchy. This modulation can indicate border-ownership and improve figure-ground segregation.

We compare the properties of our model with electrophysiological results of Zhou et al. (2000). We show how our results relate to other physiological and psychophysical findings and discuss what our model predicts and which cortical areas could correspond to the modules of our model. Further, we compare our model with other models on BO and discuss implications of BO coding to figure-ground segregation.

8.1 Comparison of Our Model to Properties of BO Neurons

8.1.1 Reproducing Effects Measured in BO Experiments

Our model qualitatively reproduces the experimental data measured by Zhou et al. (2000). As in the experiments, our network codes BO independent of stimulus object size and position (Chapter 4.4). In our model a BO neuron responds with a high firing rate when encoding a contour owned by an object extending to one side from the contour. The same neuron responds with a low firing rate when the stimulus object owning the contour extends to the other side (Figure 4.5).

Our model shows BO properties for different stimulus object forms, among others the rectangular and C-shapes used by Zhou et al. (2000) (see Figure 4.7). The model is able to reproduce the early differentiation between "correct" and "wrong" BO responses with respect to the stimulus object (Figure 4.4). Also quantitatively our model reproduces the temporal dynamics and firing rates measured by Zhou et al. (2000).

Incomplete and Non-Objects

When Zhou et al. (2000) presented rectangular objects extending beyond the boundary of their screen, thus appearing only incomplete, these objects elicited nonetheless "correct" BO response, only with lower intensity. When a rectangle extending nearly over the entire half of the stimulus screen was shown, the BO neurons showed no BO preference, i.e. a neuron that previously showed BO properties fired with the same rate independent to which side the object extended. The latter stimulus was likely to be perceived just as a contrast polarity edge.

We were able to reproduce these results by presenting incomplete objects and non-objects to our network (see Chapter 4.7). Incomplete objects such as a rectangle missing one or two corners, elicit a BO response, just not as pronounced as a complete rectangle. A curve by itself, however, does not elicit any BO activity. Also, other non-objects, such as a line, showed no BO preference.

Overlapping Stimuli

When presenting two overlapping rectangles (Figure 4.13), our network reproduced the results found by Zhou et al. (2000). All neurons encoding the border shared by the two stimulus objects showed a BO preference in the direction of the object on top.

Stimuli Sharing a Contour

In their experiments Zhou et al. (2000) also varied the size of shift between two overlapping stimulus objects. They recorded neurons encoding the edge shared by the two objects. When the shift between the objects was clearly visible and thus also the visual identification of the overlapping object, the shared edge encoded the correct BO property with BO preference directed to the overlapping object. When a stimulus with two unshifted objects sharing an edge was presented (ambiguous situation), the neurons encoding the shared contour did not show any BO preference. Our network reproduces this behaviour (Figures 4.10 and 4.13).

We further tested our model with stimuli which were not used by Zhou et al. (2000): Objects sharing parts of their contour (Figures 4.11 and 4.12). Our model predicts that for these stimuli neurons encoding the shared part of the contour do not show any significant BO property wen the objects extend to opposing sides from the shared contour (Figure 4.11). Thus, these neurons respond as in the previous example with the unshifted stimulus objects. On the other hand,

neurons encoding the outer parts of the partially shared edge that only belongs to one stimulus show BO preference. This response behaviour is a direct result of the network architecture: Two objects are detected in Area-3. Antagonistic neurons encoding the shared edge both receive feedback neither prevails, thus no BO preference develops. The neurons encoding the outer side belonging only to one of the two stimulus objects only receive feedback from one Area-3 neuron and thus show an unequivocal BO response.

8.1.2 Coding BO by Feedback

Our model suggests fast feed-forward object detection and feedback to a lower level area with finer resolution to explain the BO effect. In Chapter 1.1.1 we suggest that there is feedback from high area neurons encoding an object's presence and location to neurons in lower primary visual cortex area (V1) encoding the object's contour and surface. There we show that fast feed-forward and feedback connections would allow feedback to coincide with the longer-latency input from the retina to area V1 of the parvocellular pathway.

BO in the Ventral Pathway

We suggest that V1 neurons, receiving parvocellular input and encoding BO properties, project to visual areas V2 and V4 of the ventral pathway. As a result, BO information is available to neurons of those extrastriate ventral areas. Zhou et al. (2000) showed that most neurons in areas V2 and V4 exhibit BO properties.

Thus, BO could play an important role in solving the initially posed problem of segregating an object from its ground. Once this is achieved through feedback in lower areas, further processing including object recognition can take place.

8.1.3 Coding BO by Feedback Only

In our model the only source for BO encoding is the feedback from Area-3. The lateral facilitatory coupling profile in Area-1b is unspecific regarding BO coding (Figure 3.3). Lateral connections encoding Gestalt properties (Figure 1.2) in our model thus only transmit BO information (see Figure 3.3), but do not extract it.

Support for BO via Feedback

There is experimental support for feedback as a mechanism of BO. Zhou et al. (2000) recorded from the same V2 cells for simple rectangular stimuli and more complex C-shaped or overlapping stimuli, i.e., including contradictory BO cues. Over 50% of the cells showed BO properties for simple but not for complex stimuli. In some cases, neurons were selective to contrast polarity as long as

they did not show BO properties. Zhou et al. (2000) concluded that there are a variety of figure-ground separating mechanisms, each using a different strategy.

Further Properties of BO Neurons in Experiment

The neurons recorded by Zhou et al. (2000) were not only selective to orientation and showed border-ownership but some showed further preferences, such as for contrast polarity. A number of neurons did only show a preference to contrast polarity when the contour they encoded was not part of an object. When the neuron encoded an object contour, it only showed BO preference, but no significant polarity preference anymore.

BO Property Only "Overwrites" Other Properties When Object Is Detected

In our model BO properties are absent from the network as long as no object is detected. This allows other preferences to be encoded, which are not "overwritten" as long as there is no BO feedback. Our model only codes preference for oriented lines, thus further preferences would need to be added to demonstrate this property in our network. In other models (Kikuchi and Akashi, 2001; Li, 2005, discussed later in detail) BO coding is always present.

Our model fails to encode "correct" BO when too much noise or clutter is contained in the stimulus.

8.1.4 BO Coding in Concave Objects

Inner Side of C-Shape

Our model reproduces the effects measured by Zhou et al. (2000) for a C-shape stimulus. They found neurons encoding parts of the vertical inner (concave) part of a C-shape to encode the "correct" BO preference (directed to the inside of the object). This is noteworthy since local curvature Gestalt cues suggest that the contour belongs to an object extending to the side opposite of the C-shape.

Delay

Our simulations with a C-shaped stimulus show "correct" BO encoding for the entire concave contour of the C-shape (Figure 4.15). When introducing lateral delays in Area-1b, the latency of the BO response[I] increases compared to the simulations without delay, but only by a few milliseconds (Figure 5.1).

BO Less Pronounced at Concave Than Convex Contour

The difference in firing rate of antagonistic neurons is significantly lower for neurons encoding the inner contour (concave) of the C-shape than for the neurons encoding the outer contour - especially during the transient answer. This reproduces the result of Zhou et al. (2000).

Nonetheless, our results show that BO feedback and its lateral spreading may be fast enough to propagate BO preference informa-

[I]The BO response is defined to take effect when the activity of a pair of antagonistic neurons starts to differ.

tion along an object's contour. The BO activation in the model reaches the BO neuron encoding the center of the concavity fast enough for the experimental results of Zhou et al. (2000) to be reproduced.

For the C-shaped stimulus Zhou et al. (2000) only measured the BO property of the neuron encoding the central part of the concavity. Our model predicts that not only neurons encoding this edge but also all neurons encoding the horizontal edges of the concavity encode BO. This could be tested in future experiments.

8.1.5 Limitations of the Model

Form Detection Limitation

Our network uses fairly simple object detection mechanisms. Due to the lack of appropriate connections from Area-2 to Area-3 horizontally and vertically elongated objects, but not diagonally elongated ones can be detected. Since Zhou et al. (2000) presented many of their stimulus objects tilted, strictly speaking, our network would not have detected them. This is not a principle limitation, though. Our framework could be extended to also detect otherwise elongated forms.

Limited Radius

Further, due to the restricted radius of curves, Area-2 curvature detectors cannot detect stimulus objects with curvatures greater than radius r = 6 neurons distance[II].

Limited Spatial Frequencies

In order to enable our network to deal with a wider range of stimuli (greater range of curvatures, different spatial frequencies) one can do the following: (1) The Gabor input filters could be set to a low spatial frequency. Thus, the spectrum of spatial frequencies resulting from filtering would be in a range of lower frequencies. The task of object presence detection according to Gestalt properties would not be obstructed. (2) Alternatively, our architecture could be replicated at different spatial frequencies. Supporting and competing mechanisms would need to be introduced between the different frequencies.

Object Size Limitation

The network is limited to detecting objects in the range of 15x15 to 90x90 pixels, the latter being the size of the entire input stimulus.

[II] I.e. in Area-1 neurons describing a curvature with a radius of 6 neurons distance are activated by the stimulus. In our 90x90 stimulus this translates to a radius of r = 18 pixels.

8.2 Comparison Between Model and Physiology

In Chapter 2 and 3 we argued that our network is a biologically plausible model of parts of the visual cortex. In the following section we discuss several aspects of our model with regard to physiology:

- processing of input
- cortical areas corresponding to our model areas
- plausibility of our feedback connections
- possible extensions of the model

8.2.1 Input - Filtering - Processing

Static Contour Detectors

Our model is limited to detecting only contour stimuli. Zhou et al. (2000) recorded BO properties for stimuli with objects encoded by contrast polarities as well as by lines. Besides these features, there are many more cues defining an object, e.g. surface, texture or depth cues (disparity) (Grossberg, 1994).

Alternative Detectors

By changing the spatial and temporal properties of the input filters of our network it could also process various other types of stimuli. Instead of linear contours also luminance or disparity could be detected. With temporal filters motion could be encoded. This would be interesting, since the dorsal pathway is known to detect motion signals better than static images (e.g. Goodale and Milner, 1992; Ungerleider and Haxby, 1994). Though the dorsal pathway also responds to static images with a transient response (Thorpe et al., 1996), it would be more plausible if our model received moving input and was able to respond to it. To implement this, the network's architecture could be maintained, only the network input would need to be filtered differently, e.g. by Reichardt type detectors (Hassenstein and Reichardt, 1956). The detectors could be implemented as proposed by Bayerl (2006) with integration over temporal consecutive images to compute motion vectors.

Since our aim was to demonstrate basic mechanisms we abstained from implementing motion detection. For further development of the model motion detectors would be one of the first features to add.

8.2.2 Gestalt Rules and Intra- and Inter-Areal Connectivity

The performance of the network arises from the interplay of lateral and inter-areal connections. Facilitatory and inhibitory local connections according to the Gestalt law of good continuation and proximity (Figure 1.1) aid object feature extraction. Neuronal activity that cannot be attributed to object features is suppressed. The remaining activation encodes object features, which are bound together step by step by inter-areal feed-forward connections.

8.2.3 Correspondence of Network Areas and Visual System Areas

Here we discuss what cortical areas could correspond to the areas of our model.

Dorsal Pathway

We argued that the feed-forward path of our network models the dorsal pathway of visual cortex (see Chapter 1.1.1). The dorsal pathway leads from Area V1 via V2 and V3 to MT (medial temporal cortex; also referred to as V5) and further to the parietal cortex with MST (medial superior temporal), AIP (anterior intraparietal), LIP (lateral intraparietal) among others (Wallis and Bülthoff, 2003). There are also direct connections from V1 to MT and V2 to MT.

Model Area-1

Our model Area-1 neurons show receptive field properties found in area V1 in primate (Hubel and Wiesel, 1968) and cat (Hubel and Wiesel, 1962) visual cortex.

Model Area-2

The Area-2 neurons of our model respond to a range of curvatures of a specific orientation within their cRF. Cells with similar cRFs have been found in area V2 of visual cortex. Hegdé and van Essen (2000) recorded V2 cells in macaque monkey that explicitly responded to complex shapes, among others, curvatures. The stimulus most effectively eliciting activity in a neuron caused the neuron to show a significantly larger responce than elicited by the most effective bar or sinusoid. About one-third of the neurons recorded showed significant differential responsiveness to various complex shapes. Many neurons selectively responded to a particular orientation, size and/or spatial frequency of the preferred shape. Ito and Komatsu (2004) recorded from V2 cells that were selective to angles. The responses were highly selective to a particular angle in approximately one-fourth of the neurons.

Model Area-3

Area-3 of our model shares many properties with area MT in primates. The cRFs of Neurons recorded in Area MT are selective to reti-

nal position, direction of motion, speed of motion, binocular disparity, and stimulus size (Born and Bradley, 2005). Their cRFs are much larger (about ten times in linear dimensions) than in V1 (Born and Bradley, 2005). Nontheless, the range of lateral interaction in MT is not greater than the one in V1. The range is not greater than fractions of a degree of visual angle, with the MT cRF being many degrees wide (Churchland et al., 2005).

Many MT cells show center-surround properties, with stimuli extending into the surround region eliciting a much lower response than stimuli only covering the center part of the cRF (Born and Bradley, 2005). Due to this cRF property the extent of the cRF of these neurons is well defined.

The cRFs of our Area-3 also cover up to the entire stimulus field. Further, both MT and model Area-3 are selective to retinal position and stimulus size. We did not implement motion detection. Thus, area MT and model Area-3 are different in that concern, which is not a principal limitation, as discussed in Section 8.2.1 .

Motion Detection and Feedback

If motion detection is implemented, the feedback projections need to be adapted. Feedback has to projet into the lowest area not to where the object was detected but where it is expected to be once the feedback reaches the lowest area.

8.2.4 Alternative Localisation of Feed-Forward Path of Model in Ventral Pathway

We argued that the dorsal pathway could correspond to the feed-forward path of our network (Chapter 1.1.1) because response onset to a stimulus is so much earlier in higher dorsal areas than in lower areas of the ventral pathway, that feedback from the dorsal path can reach lower ventral areas when afferent input reaches that area.

Feedback Within Ventral Path

Alternatively, the feed-forward path could correpond to the ventral pathway. Due to the variation observed in response onset of ventral areas (Schmolesky et al., 1998) it is possible that feedback from a higher area elicited by a first activation wave could coincide with response onset of lower area neurons receiving late afferent input.

Areas of Ventral Path

The ventral pathway extends from V1 via V2 and parts of V3 to V4 and further to IT (inferior temporal cortex) and other areas in the temporal lobe. There are also direct connections from V2 to V4.

Properties of V4

We already described in the previous section the properties of V1 and V2. Area V4 neurons respond preferrably to objects that are more complex than the ones V2 prefers. In experiments Pasupathy and Connor (2002) and Kobatake and Tanaka (1994) found that V4

neurons respond to specific complete shapes made up of linear, convex and concave boundary fragments. At the same time, the spatial invariance of neurons compared to V2 and especially V1 increased. With encoding these properties, area V4 could correspond to our model's Area-3. The only property required in our model architecture that is not matched well by V4 is the spatial selective coding of objects. Our model requires rather specific spatial coding of object position in order to allow relative precise feedback to the neurons encoding the object's contour in lower areas.

Latency in Ventral Pathway

Measurements of the delays in the visual system (Bullier, 2001; Schmolesky et al., 1998) show, that the range of response onset to a stimulus varies greatly within the areas:

- **V1:** 26-122ms (Bullier, 2001), 34-98ms (Schmolesky et al., 1998)
- **V2:** 56-118ms (Schmolesky et al., 1998) 56-120ms (Bullier, 2001)
- **V4:** 72-159ms (Schmolesky et al., 1998)

Since in comparison inter-areal delays are very short (Fellemann and Van Essen, 1991) it is feasable that V1 and V2 neurons with late response onset receive feedback from higher ventral areas that were activated on the first activation wave.

This is an interesting alternative, since feedback from higher areas in the ventral pathway would show different properties than feedback from the dorsal pathway. Object detection would not occur independent of form. Hence, feedback could be given much more precisely onto object contour.

8.2.5 BO Feedback: Selective to Orientation

When a stimulus object is detected in Area-3 of our model, feedback is projected to all those Area-1b neurons which can potentially encode a convex stimulus object that could elicit activation in this Area-3 neuron. This feedback is selectively projected back to neurons of specific orientations and BO preferences.

Selective or Non-Selective Feedback in the Brain?

There are no experimental results about the orientation selectivity of feedback projections from area MT or other higher areas of the dorsal pathway. For feedback from V2 to V1 there exists contradicting evidence. Selective feedback is supported by measurements of Angelucci et al. (2002) (in macaque). Stettler et al. (2002) on the other hand found experimental evidence that V2-V1 feedback is not selective to orientation (also in macaque). What would be the effect to our network if feedback was not selective?. If feedback is projected to all

orientations in a limited region equally, then, obviously, the activity of all neurons receiving feedback increases compared to the background activity. If within the region receiving feedback there are neurons encoding the contour of the stimulus object, these neurons exhibit locally the highest rate. Thus, these neurons will also exhibit the highest rate when additionally receiving feedback. Since our feedback acts multiplicative the firing rate of neurons with a high rate increases absolutely more than the rate of neurons with a low firing rate. Thus, also after unselective feedback our model neurons encoding the stimulus object contour will prevail against their surround. From this we conclude that orientationally unselective feedback can also provide lower layer neurons with BO properties. Nonetheless, unselective feedback would not render as good BO coding in Area-1b as the selective feedback we use in our model.

8.2.6 Predictions for Future Experiments

Latencies

the analogue of our model's Area-1 (e.g. V1) to receive direct BO feedback from the object detection area (Area-3 in our model). If this was the case, then the latency of BO-specific activity should be shorter in V1 than in other, higher areas of the ventral stream. If this was not the case, then this suggests that V1 receives BO feedback only indirectly, e.g. via area V2 or V3. This could be investigated in future experiments.

Further, the latency of BO coding in the areas of the ventral pathway, such as V4, would give a hint whether they receive direct BO feedback or, as we propose with our model, indirectly via V1 or V2.

8.2.7 Extension of Architecture: Indirect BO Feedback via Area-2

In our model feedback is projected back only from the highest area (Area-3) to Area-1. This architecture could be extended by feedback from Area-3 to Area-2 and from Area-2 to Area-1 and an adequate bi-layer extension of Area-2.

Feedback From and Via Area-2

Area-2 neurons activated by a simulus would modulate Area-1 activity by feedback. Area-2 neurons additionally receiving feedback from Area-3 would fire with a higher rate and would modulate Area-1 even more. Feedback from lower areas could be projected more precisely to the contour of a stimulus object than feedback from higher areas, because the spatial specificity is usually higher in lower areas of the dorsal pathway. Consequently, concavities that receive BO ac-

tivation only indirectly via lateral connections in the current model would receive direct BO feedback in the extended architecture.

Divergence of Feedback

Curvature invariance is modelled in our network in the connections from Area-1 to Area-2. From Area-2 to Area-3 no further spatial invariance is added. Therefore, feedback from our model's Area-2 to Area-1 would not be more precise than feedback from Area-3. Thus, the above mentioned advantage of feedback from multiple areas does not work for our concrete implementation.

Change in Response Dynamics

Probably new dynamic properties would be the result. Area-2 would provide Area-1 with BO feedback gathered from its vicinity due to lateral activation in Area-2 until Area-2, in turn, receives BO feedback from Area-3. Thus, new dynamics could probably be observed on the concave inner contour of a C-shape. First, feedback would arrive in Area-1 with BO encoded only by Area-2, providing Area-1 with the "wrong" BO property due to the inner contours of the C-shape hinting at an object to extend to the other direction from the contour than the C-shape. Once Area-2 receives BO feedback from Area-3, Area-2 would begin to encode the "correct" BO preference, the opposite from what it encoded previously. As a result Area-1b neurons encoding the concave part of the contour would first receive feedback with the "wrong" BO preference.

8.3 Comparison with Other Border-Ownership Models

As described in the introduction there are several models trying to explain BO. They utilise one or more of the following mechanisms:

- feed-forward connections to V1 and lateral connections in V1, where:
  - activation spreads along the contour of the object (Li, 2005; Kikuchi and Akashi, 2001)
  - long-range connections between neurons encode opposing contours of the object (Nishimura and Sakai, 2004)
- feedback modulation of BO properties to explain Rubin's vase and other attentional effects (Li, 2005)

8.3.1 Review of Other BO Models

Recently, several mechanisms explaining the BO effect were suggested (Kikuchi and Akashi, 2001; Nishimura and Sakai, 2004; Li,

2005). Since BO neurons were mostly found in V2 and V4 (>50%) (Zhou et al., 2000) and only few in V1 (18%), modelling focussed on V2. BO properties in V1 are often explained by fast feedback connections from V2 (Girard et al., 2001). Previous models argued for BO properties to arise by feed-forward connections to and lateral connections in V2 (Li, 2005; Kikuchi and Akashi, 2001; Nishimura and Sakai, 2004). Feedback from higher areas is attributed only a modulatory effect to BO perception (Li, 2005) to explain attentional effects leading to switches in perception as in the famous example of Rubin's vase (Rubin, 1921).

BO Explained by Intra-Areal Connections

There have been two approaches explaining BO by intra-areal connectivity: (1) chains of activation running along the object's contour (Kikuchi and Akashi, 2001; Li, 2005) and (2) long-range connections between neurons encoding opposite contours of the object (Nishimura and Sakai, 2004).

8.3.2 Border-Ownership and Delays

Lateral Delay Determined by Physiological Constraints

Li (2005) argues that lateral connections in V2 allow fast BO coding. She argues that the correlate of her BO area is area V2 of visual cortex. She assumes 8-10 ms activation latency of monosynaptic connections independent of the distance between neurons. Further, she assumes 3° visual angle as greatest distance of lateral connections. However, lateral latencies in V2 are too long to explain the effects measured by Zhou et al. (2000), who found the latency of the BO effect to be largely independent of object size. Physiological data about V2 (Roe and Ts'o, 1995, in macaque monkey) indicate a cortical magnification factor of 4 mm per degree *across* orientation-, colour-, and disparity-stripes together (~ 1.3 mm per degree each) and ~ 0.7 mm per degree *along* each stripe. Assuming the lowest cortical magnification factor (along stripes) of 0.7 mm per degree, this results in an axonal velocity of 0.26 mm/ms. This is in the range of spike velocities measured in horizontal connections (Slovin et al. (2002): 0.1–0.2 m/s in monkey; see Nowak and Bullier (1997) for review). If BO information would propagate along the object's contour representation, as in the models by Li (2005) and Kikuchi and Akashi (2001), the direct distance from the outer corner of the C-shape from where the "correct" BO information is transmitted to the neurons recorded at the inner side of the C-shape would exceed 10 degrees of visual angle[III].

[III] In Zhou et al. (2000) the C-shaped stimulus covered 10° (horizontal) x 20° (vertical). That makes $\sim 15^\circ$ distance going along the contour from the outside edge to the cRF location of the neuron recorded and more than 10° distance assuming the

Thus, even with the shortest distance and the shortest delay, it would take longer than 25 ms for the signal to arrive at the neuron with cRF at the inner side of the C-shape. For the neuron to start showing the "correct" BO property it would take even longer, since the neuron encodes the "wrong" BO property at arrival of the "correct" signal due to misleading local cues having arrived earlier. Thus, inversion of the BO neuron's activation would still be necessary. Therefore, the mechanism suggested by Li (2005) and Kikuchi and Akashi (2001) cannot explain the BO properties measured by Zhou et al. (2000) by lateral connections in V2 for larger stimulus representations.

Lateral Coupling Perpendicular to Contour

Nishimura and Sakai (2004) developed a BO model suggesting long-range lateral connections with their main axis perpendicular to the contour encoded. In their model, BO properties arise from connections between linking neurons encoding opposite sides of an object. This model can explain BO properties arguably for mid-sized objects due to employing direct lateral connections. But Li (2005) noted that it cannot explain some of the observations by Zhou et al. (2000).

Intra-areal connections, as suggested by Li (2005), Kikuchi and Akashi (2001), and Nishimura and Sakai (2004), may support BO encoding.

Feedback Support

Kikuchi and Akashi (2001), Nishimura and Sakai (2004) and Li (2005) explain BO mechanisms by integration of local cues. Thus, BO selective activity should be present for C-shaped or overlapping objects, since local cues are available. The models by Li (2005) and Kikuchi and Akashi (2001) predict initially "wrong" BO classification, induced by misleading local cues, and later in the response encoding of "correct" BO property. Their models and the model by Nishimura and Sakai (2004) cannot explain neurons *only* significantly encoding contrast polarity when BO is *not* encoded.

Fast Laterally Induced BO Effect in Our Model

In our model the "wrong" BO property is not initially encoded in concavities (e.g. in the C-shape) until the "correct" BO property is laterally relayed. Further, all neurons encoding the convex parts of the object contour receive direct BO feedback. Thus, "correct" lateral BO activation into a concavity is significantly faster in our model than in the model by Li (2005), since (1) BO coding does not have to be reversed and (2) the distance along the contour to the nearest neuron encoding the "correct" BO property is at least as short, usually shorter.

most direct connection.

8.4 Feedback and Figure-Ground-Segregation

8.4.1 Closed Loop

When feedback is projected from Area-3 to Area-1a in our model (see Chapter 6) neurons encoding the contour of an object detected are modulated by linking. Thus, Area-1a neurons receiving linking input exhibit a higher firing-rate. Due to the properties of the feed-forward path, only Area-1a neurons receiving feedback show tonic firing-rates significantly greater than 0.

In the closed loop, in contrast to Area-1b feedback does not reach Area-1a neurons during their transient response.

8.4.2 Feedback Improves Figure-Ground-Segregation

Our model demonstrates that figure-ground segregation can be significantly improved by feedback encoding object presence.

Segregation by Feedback

In our model, fast feedback connections from Area-3 to Area-1 play an important role in improving figure-ground segregation by facilitation of BO neurons, i.e., in the low level area where neurons represent visual objects at high spatial resolution. Thus, segregation of object and background representations in early visual areas is improved. Feedback may enhance the activity of BO neurons encoding the contour of an object. These neurons, in turn, may suppress non-object activity in their surround by lateral inhibition. (See also Gewaltig et al., 2003, for a related idea.).

Besides many feed-forward models mainly dealing with object recognition in the visual system (e.g. Riesenhuber and Poggio, 1999), there are a number of other models, suggesting recurrent networks for improving figure-ground segregation.

Inhibitory Feedback

Locally limited feedback via inhibitory interneurons to improve contrast locally, as in Area-1 and Area-2 of our model, has been used in our group for some time. Eckhorn et al. (1992) demonstrate a two layer network, in which inhibitory connections from higher to lower layer serve as control loops. Feedback is diverted to the association field of a local neuron assembly. This feedback reduces mainly uncorrelated noise, since neurons encoding an object facilitate each other by lateral connections. This mechanism locally improves separation of figure and background.

Feedback Using Bigger cRFs in Higher Areas

An often implemented feedback mechanism in models of the visual system is to use integration over greater distances due to greater cRFs. Lateral connections in higher areas and feedback can then aid figure-ground segregation in lower areas.

Gove et al. (1995) use bipolar cells in V2 with two collinear receptive fields for long range grouping. They encode surface brightness by modelling filling-in in V4. This so-called *boundary contour system* gives feedback to lower areas, encoding form and surface (*feature contour system*). This, in turn, projects to higher areas encoding object identity (*object recognition system*).

Similarly, Weitzel et al. (1997) developed a multi-layer network of spiking neurons encoding vertex presence in its highest layer. Through a synchronisation layer and feedback, *linking waves* propagate along detected edges and vertices in lower layers. Further, representations of contours belonging to different objects are temporally separated.

Also Neumann et al. use integration over greater distances in higher areas to provide V1 neurons with information from outside their cRFs (feedback from V2 (Neumann and Sepp, 1999); motion detection in MT and feedback (Bayerl and Neumann, 2004)). Their models areas only differ in spatial scale of integration. Higher areas have greater fields of integration, lower areas allow more detailed representation due to smaller cRFs. Neumann and coworkers modelled feedback modulation as we did (Equation 2.5). They also compute lateral inhibition by divisive inhibition in order to enhance local feature contrast. This can be subsequently used to improve figure ground segregation, as done by us.

8.4.3 Model of Dorsal and Ventral Pathway

Deco and Rolls (2004) developed a model linking dorsal and ventral pathways.

They use a mechanism very similar to the one used by us: Feedback from a higher area modulates the activity of neurons encoding a stimulus object in a low area of the visual system, which in turn is used for further feed-forward processing. In their model attention from higher areas can trigger one of two modes: (1) visual spatial search and (2) visual object identification. In the latter case a bias is given to a neuron in an area modelling posterior parietal cortex (PP), where a spatial map of an object's location is encoded. Feedback from PP to V1 modulates neurons encoding the detected object. In their model V1 functions as an *active blackboard* (Bullier, 2001) mediating

between higher visual areas. Unlike us, Deco and Rolls (2004) modelled the ventral pathway, whereas their dorsal path is reduced to one layer. In our model feedback takes effect with far shorter delays with respect to response onset in the lowest layer than in the model by Deco and Rolls (2004), where attention effects reach V1 neurons as late as 120–200 ms after response onset.

8.4.4 Our Model and Bistable Stimuli

Bistable Stimuli

There are stimuli, where an observer experiences fluctuations in perception despite unchanging visual stimulation.

The best known example is Rubin's vase (Rubin, 1921), where either two faces or a vase are seen. Another example is the necker cube (Necker, 1832), a cube wth transparent sides which is perceived to either extend towards the front from a focussed corner or to the back (multistable depth reversal). For review of further bistable patterns see Leopold and Logothetis (1999).

For some bistable stimuli such as Rubin's vase the shared contour of the two objects plays an important role for which object of a bistable stimulus is seen. Modulations of BOLD signals from V1 correlate with rivalry states when the rival targets are more complex (Lee and Blake, 2002).

Area-3 Inhibition

In Area-3 of our model there are two types of (divisive) inhibition:

- *Ghost inhibition* between objects sharing parts of their contour extending to the same side
- *Rubin inhibition* between objects sharing parts of their contour extending to opposite sides from there

The Rubin inhibition is implemented as a weak subtractive inhibition. As a result BO feedback from an Area-3 neuron activated more than its Rubin counterpart will be stronger and thus the contour is assigned to that object. If Area-3 neurons show about the same firing rate, then they inhibit each other equally, resulting in a slightly reduced rate for both. Feedback will be of about equal strength and thus BO activation will be ambiguous (Figure 4.10).

Adding Bistability to Model

In order to reproduce activity likely to trigger bistable perception, we would need an attentional mechanism modulating either one or the other Area-3 neuron. Then one Area-3 neuron would show a higher firing rate, inhibit the other significantly, BO neurons of one direction preference would prevail and in consecutive areas

the shared contour would be assigned to the stimulus object that received attention.

Alternatively, the Rubin effect could be explained by introducing harder competition either in Area-3 or Area-1b of our model. Thus, one of the possible two interpretations would be forced to win. This is not a plausible mechanism, since the other experimental results could not be reproduced by the model.

8 Discussion

Chapter 9

Conclusions

Our model of the dorsal pathway proposes a realistic mechanism for fast detection of object presence. We encode Gestalt properties in the network to support extraction of object boundary features. Our results demonstrate that, with feedback, figure-ground segregation is possible under higher noise levels. Furthermore, our model produces BO properties by feedback in lower area neurons as found by Zhou et al. (2000). Unlike BO models using intra-areal connections, our model can explain BO selectivity of the response transient and independence of object size. Finally, our model explains that BO information is present in the ventral pathway, since ventral areas receive input from BO neurons in lower areas. Feedback not only provides neurons with BO properties but contributes to object recognition in the ventral stream by improving figure-ground segregation.

For future research, we suggest – besides what was already suggested in the discussion – cooling experiments as done by Hupe et al. (2001) on area MT combined with electrophysiological recordings in V1, V2 and/or V4. If as a result BO properties would seize to occur in thse areas, this would be an evidence for BO properties being induced by feedback from the dorsal pathway. Further, our alternate proposal of BO feedback coming from higher areas of the dorsal pathway, could be examined by cooling ventral areas such as V4.

9 Conclusions

Bibliography

Adams, D., Horton, J., 2003. A precise retinotopic map of primate striate cortex generated from the representation of angioscotomas. The Journal of Neuroscience 23 (9), 3771–89.

Amit, D., 1989. Modeling brain function - the world of attractor neural networks. Cambridge University Press.

Angelucci, A., Levitt, J., Walton, E., Hupé, J., Bullier, J., Lund, J., 2002. Circuits for local and global signal integration in primary visual cortex. The Journal of Neuroscience 22 (19), 8633–46.

Bayerl, P., 2006. A model of visual motion perception. Ph.D. thesis, University of Ulm, Germany.

Bayerl, P., Neumann, H., 2004. Disambiguating visual motion through contextual feedback modulation. Neural Computation 16, 2041–66.

Bi, G., Poo, M., 1998. Synaptic modifications in cultured hippocampal neurons: dependence on spike timing, synaptic strength, and postsynaptic cell type. The Journal of Neuroscience 18 (24), 10464–72.

Born, R., Bradley, D., 2005. Structure and function of visual area MT. Annual Review of Neuroscience 28, 157–89.

Braitenberg, V., Schüz, A., 1991. Anatomy of the cortex statistics and geometry. Springer-Verlag.

Bullier, J., 2001. Integrated model of visual processing. Brain Research Reviews 36 (2-3), 96–107.

Chance, F., Nelson, S., Abbott, L., 1998. Synaptic depression and the temporal response characteristics of V1 cells. The Journal of Neuroscience 18 (12), 4785–99.

Churchland, M., Priebe, N., Lisberger, S., 2005. Comparison of the spatial limits on direction selectivity in visual areas MT and V1. Journal of Neurophysiology 93, 1235–45.

Corchs, S., Deco, G., 2002. Large-scale neural model for visual attention: integration of experimental single-cell and fMRI data. Cerebral Cortex 12, 339–48.

Deco, G., Rolls, E., 2004. A neurodynamical cortical model of visual attention and invariant object recognition. Vision Research 44, 621–42.

Eckhorn, R., Dicke, P., Arndt, M., Reitboeck, H., 1992. Induced rythms in the brain. Boston/Berlin: Birkhaeuser, Ch. Feature linking of visual features by stimulus-related synchronization of model neurons, pp. 397–416.

Eckhorn, R., Reitboeck, H., Arndt, M., Dicke, P., 1990. Feature linking via synchronization among distributed assemblies: Simulations of results from cat visual cortex. Neural Computation 2, 293–307.

Elder, J., Zucker, S., 1993. The effect of contour closure on the rapid discrimination of two-dimensional shapes. Vision Research 33 (7), 981–91.

Elder, J., Zucker, S., 1994. A measure of closure. Vision Research 34 (24), 3361–9.

Fellemann, D., Van Essen, D., 1991. Distributed hierarchical processing in the primate cerebral cortex. Cerebral Cortex 1, 1–47.

Frien, A., Eckhorn, R., 2000. Functional coupling shows stronger stimulus dependency for fast oscillations than for low-frequency components in striate cortex of awake monkey. European Journal of Neuroscience 12 (4), 1466–78.

Földiak, P., 1991. Learning invariance from transformation sequences. Neural Computation 3, 194–200.

Gerstner, W., Kistler, W., 2002. Spiking neuron models - Single neurons, populations, plasticity. Cambridge University Press, Cambridge, UK.

Gewaltig, M.-O., Körner, U., Körner, E., 2003. A model of surface detection and orientation tuning in primate visual cortex. Neurocomputing 52–54, 519–524.

Girard, P., Hupé, J., Bullier, J., 2001. Feedforward and feedback connections between areas V1 and V2 of the monkey have similar rapid conduction velocities. Journal of Neurophysiology 85 (3), 1328–31.

Goodale, M., Milner, D., 1992. Separate visual pathways for perception and action. Trends in Neuroscience 15, 20,25.

Gove, A., Grossberg, S., Mingolla, E., 1995. Brightness perception, illusory contours, and corticogeniculate feedback. Visual Neuroscience 12, 1027–52.

Green, D., Swets, J., 1988. Signal detection theory and psychophysics. J. Wiley and Sons, New York.

Grossberg, S., 1994. 3-D vision and figure-ground separation by visual cortex. Perception & Psychophysics 55 (1), 48–110.

Grossberg, S., Mingolla, E., Williamson, J., 1995. Synthetic aperture radar processing by a multiple scale neural system for boundary and surface representation. Nature Neuroscience 8 (7), 1005–28.

Hansen, T., Neumann, H., 2004. Neural mechanisms for the robust representation of junctions. Neural Computation 16, 1013–1037.

Hassenstein, B., Reichardt, W., 1956. Systemtheoretische Analyse der Zeit-, Reihenfolgen- und Vorzeichenauswertung bei der Bewegungsperzeption des Rüsselkäfers Chlorophanus. Zeitschrift für Naturforschung 11b, 513–24.

Hebb, D., 1949. The organization of behaviour: A neurophysiological theory. John Wiley, New York.

Hegdé, J., van Essen, D., 2000. Selectivity for complex shapes in primate visual area V2. The Journal of Neuroscience 20 (RC61), 1–6.

Holt, G., Koch, C., 1997. Shunting inhibition does not have a divisive effect on firing rates. Neural Computation 9 (5), 1001–13.

Hubel, D., Wiesel, T., 1962. Receptive fields, binocular interaction and functional architecture in the cat's visual cortex. Journal of Physiology 160, 106–54.

Hubel, D. H., Wiesel, T. N., Mar. 1968. Receptive fields and functional architecture of monkey striate cortex. Journal of Physiology 195 (1), 215–243.

Hupe, J., James, A., Girard, P., Lomber, S., Payne, B., Bullier, J., 2001. Feedback connections act on the early part of the responses in monkey visual cortex. Journal of Neurophysiology 85 (1), 134–45.

Ito, M., Komatsu, H., Mar. 2004. Representation of angles embedded within contour stimuli in area V2 of macaque monkeys. The Journal of Neuroscience 24 (13), 3313–3324.

Itti, L., Koch, C., Braun, J., 2000. Revisiting spatial vision: Towards a unifying model. J. Opt. Soc. Am. 17, 1899–1917.

Jensen, O., Idiart, M., Lisman, J., 1996. Physiologically realistic formation of autoassociative memory in networks with theta/gamma oscillations: Role of fast NMDA channels. Learning and Memory 3 (2-3), 243–56.

Kayser, C., Einhäuser, W., Dümmer, O., König, P., Körding, K., 2001. Extracting slow subspaces from natural video leads to complex cells. ICANN Proceedings LNCS 2130, 1075–80.

Kikuchi, M., Akashi, Y., 2001. A model of border-ownership coding in early vision. ICANN Proceedings LNCS 2130, 1069–74.

Knierim, J., van Essen, D., 1992. Neuronal responses to static texture patterns in area V1 of the alert macaque monkey. Journal of Physiology 67, 961–80.

Kobatake, E., Tanaka, K., 1994. Neuronal selectivities to complex object features in the ventral visual pathway of the macaque cerebral cortex. Journal of Neurophysiology 71 (3), 856–67.

Koch, C., Poggio, T., Torre, V., 1983. Nonlinear interactions in a dendritic tree: Localization, timing, and role in information processing. Proceedings of the National Academy of Sciences of the USA 80 (9), 2799–2802.

Kovács, I., Julesz, B., 1993. A closed curve is much more than an incomplete one: Effect of closure in figure-ground segmentation. Proceedings of the National Academy of Sciences of the USA 90, 7495–97.

Lamme, V., Roelfsema, P., 2000. The distinct modes of vision offered by feedforward and recurrent processing. Trends in Neuroscience 23, 571–79.

Leopold, D., Logothetis, N., 1999. Multistable phenomena: Changing views in perception. Trends in Cognitive Sciences 3 (7), 254–64.

Li, Z., 2005. Border ownership from intracortical interactions in visual area V2. Neuron 47, 143–53.

Markram, H., Tsodyks, M., 1996. Redistribution of synaptic efficacy between neocortical pyramidal neurons. Neuron 382, 807–10.

Mel, B., Fiser, J., 2000. Minimizing binding errors using learned conjunctive features. Neural Computation 12, 247–78.

Mitchell, S., Silver, R., 2003. Shunting inhibition modulates neuronal gain during synaptic excitation. Neuron 38 (3), 433–45.

Molyneaux, B., Hasselmo, M., 2002. GABA B presynaptic inhibition has an in vivo time constant sufficiently rapid to allow modulation at theta frequency 87, 1196–1205.

Necker, L., 1832. Observations on some remarkable optical phaenomena seen in switzerland; and on an optical phaenomenon which occurs on viewing a figure of a crystal or geometical solid. London and Edinburgh Philosophical Magazine and Journal of Science 1, 329–37.

Neumann, H., Sepp, W., 1999. Recurrent V1-V2 interaction in early visual boundary processing. Biological Cybernetics 81, 425–44.

Nishimura, H., Sakai, K., 2004. Determination of border ownership based on the surround context of contrast. Neurocomputing 58-60, 843–48.

Nowak, L., Bullier, J., 1997. The timing of information transfer in the visual system. In: Kaas, J., Rockland, K., Peters, A. (Eds.), Extrastriate Cortex in Primates. Vol. 12 of Cerebral Cortex. Plenum Publishing Corporation, New York, pp. 205–40.

Pasupathy, A., Connor, C., 2002. Population coding of shape in area V4. Nature Neuroscience 5 (12), 1332–8.

Prescott, S., Koninck, Y., 2003. Gain control of firing rate by shunting inhibition: Roles of synaptic noise and dendritic saturation. Proceedings of the National Academy of Sciences of the USA 100 (4), 2076–81.

Prodöhl, C., Würtz, R., von der Malsburg, C., 2003. Learning the gestalt rule of collinearity from object motion. Neural Computation 15, 1865–96.

Riesenhuber, M., Poggio, T., 1999. Hierarchical models of object recognition in cortex. Nature Neuroscience 2 (11), 1019–25.

Roe, A., Ts'o, D., 1995. Visual topography in primate V2: Multiple representation across functional stripes. The Journal of Neuroscience 15 (5), 3689–3715.

Rolls, E., Milward, T., 2000. A model of invariant object recognition in the visual system: Learning rules, activation functions, lateral inhibition, and information based performance measures. Neural Computation 12, 2547–72.

Rossi, D., Hamann, M., 1998. Spillover-mediated transmission at inhibitory synapses promoted by high affinity $\alpha 6$ subunit GABA A receptors and glomerular geometry. Neuron 20 (4), 783–95.

Royer, S., Paré, D., 2003. Conservation of total synaptic weight through balanced synaptic depression and potentiation. Nature 422, 518–22.

Rubin, E., 1921. Visuell wahrgenommene Figuren: Studien in psychologisher Analyse. Gyldendalske Boghandel (Kobenhavn).

Schmolesky, M., Wang, Y., Hanes, D., Thompson, K., Leutgeb, S., Schall, J., Leventhal, A., 1998. Signal timing across the macaque visual system. Journal of Physiology 79, 3272–78.

Siegel, M., Körding, K., König, P., 2000. Integrating top-down and bottom-up sensory processing by somato-dendritic interactions. Journal of Computational Neuroscience 8, 161–173.

Slovin, H., Arieli, A., Hildesheim, R., Grinvald, A., 2002. Long-term voltage-sensitive dye imaging reveals cortical dynamics in behaving monkeys. Journal of Neurophysiology 88, 3421.38.

Spratling, M., 1999. Pre-synaptic lateral inhibition provides a better architecture for self-organizing neural networks. Network: Computation in Neural Systems 10, 285–301.

Stettler, D., Das, A., Bennett, J., Gilbert, C., 2002. Lateral connectivity and contextual interactions in macaque primary visual cortex. Neuron 36 (14), 739–50.

Thorpe, S., Fize, D., Marlot, C., 1996. Speed of processing in the human visual system. Nature 381 (6582), 520–2.

Ts'o, D., Gilbert, C., Wiesel, T., 1986. Relationships between horizontal interactions and functional architecture in cat striate cortex as revealed by cross-correlation analysis. The Journal of Neuroscience 6 (4), 1160–70.

Ungerleider, L., Haxby, J., 1994. "What" and "where" in the human brain. Current Opinion in Neurobiology 4, 157–65.

Vidyasagar, T., 1999. A neuronal model of attentional spotlight: Parietal guiding the temporal. Brain Research Reviews 30 (1), 66–76.

Virsu, V., Hari, R., 1996. Cortical magnification, scale invariance and visual ecology. Vision Research 36 (18), 2971–7.

Wallis, G., Bülthoff, H., 2003. The handbook of brain theory and neural networks, second edition Edition. Bradford Book, Ch. Object Recognition, Neurophysiology.

Weitzel, L., Kopecz, K., Spengler, C., Eckhorn, R., Reitboeck, H., 1997. Computer analysis of images and patterns. CAIP, Ch. Contour segmentation with recurrent neural networks of pulse-coding neurons, pp. 337–44.

Wertheimer, M., 1923. Untersuchungen zur Lehre von der Gestalt II. Psychologische Forschung, 301–50.

Wörgötter, F., Krüger, N., Pugeault, N., Calow, D., Lappe, M., Pauwels, K., Van Hulle, M., Tan, S., Johnston, A., 2004. Early cognitive vision: Using Gestalt-laws for task-dependent, active image-processing. Natural Computing 3 (3), 293–321.

Zhou, H., Friedmann, H., von der Heydt, R., 2000. Coding of border ownership in monkey visual cortex. The Journal of Neuroscience 20 (17), 6594–6611.

Erklärung

Ich versichere, dass ich meine Dissertation "Coding the Presence of Visual Objects in a Recurrent Neural Network of Visual Cortex" selbständig, ohne unerlaubte Hilfe angefertigt und mich dabei keiner anderen als der von mir ausdrücklich bezeichneten Quellen und Hilfen bedient habe. Teile dieser Arbeit sind zur Veröffentlichung im Journal *Biosystems* (2006, special edition "Neural Coding") aktzeptiert worden. Diese Teile entstanden in Zusammenarbeit mit Reinhard Eckhorn und Thomas Wachtler.
Die Dissertation wurde in der jetzigen oder einer ähnlichen Form noch bei keiner anderen Hochschule eingereicht und hat noch keinen sonstigen Prüfungszwecken gedient.

Marburg/Lahn, 19. Juni 2006

Timm Zwickel

Danksagung

Am Ende dieses Projekts angelangt, möchte ich mich bei vielen Menschen bedanken, die mich wissenschaftlich und per moralischer Unterstützung in den letzen Jahren begleitet haben.

Zuallererst möchte ich meinem Betreuer Prof. Reinhard Eckhorn für die Zusammenarbeit bedanken. Ihm verdanke ich viele Ideen, aus seinem Wissensfundus durfte ich schöpfen und unsere Diskussionen brachten meine Dissertation vorran. Prof. Heiko Neumann danke ich, dass er sich bereit erklärt hat, mein Zweitgutachter zu sein.

Danken möchte ich meinen Mitstreitern aus dem Rebellenlabor Basim Al-Shaikhli und Frank Michler für die anregende Arbeit: Nur dank ihrer Hilfe gewann ich so manchen Kampf gegen Hard-, Soft- und Wetware. Meinen Mitarbeitern Tobias Teichert, Markus Wittenberg und Thomas Wachtler danke ich für unsere Diskussionen. Markus und Frank möchte ich zudem für ihre diversen Korrekturen zu diesem Text besonders danken. Meine Simulationen wären ohne NASE, das *Neuron Assembly Simulation Environment*, viel beschwerlicher gewesen und so danke ich stellvertretend Andreas Gabriel, Rüdiger Kupper und Mirko Saam für den Aufbau dieser Simulationsumgebung.

Konzentriert zu arbeiten funkioniert nur, wenn man auch richtig abschalten kann. Dabei unterstützen mich in den vergangenen Jahren aufopferungsvoll Donny, Knuth, Matthias und Sven. Die weltweiten sozialen Bewegungen machten mir zudem immer wieder erneut Mut, nicht den Kopf in den Sand zu stecken. Ohne alle aufzuzählen sei ihr dafür gedankt. Um Leben zu können braucht man Geld. Dank der Promotionsförderung des evangelischen Studienwerks Villigst konnte ich mich in den letzten Jahren geldsorgenfrei auf meine Promotion und mein soziales Engagement konzentrieren. Dafür bin ich sehr dankbar.

Ganz grundlegende Dinge verliert man oft aus den Augen oder tut sie als selbstverständlich ab. Ich möchte diesen Ort zum Anlass nehmen, meinen Eltern für all die Vorraussetzungen, die mir meinen bisherigen Werdegang möglich gemacht haben, zu danken. Dazu gehört u.a. die Sicherheit die sie mir gegeben haben und geben.

Julia danke ich für alles. Dazu gehört auch ihre Geduld während der letzten Monate dieser Arbeit.